DEFENSE DOCUMENTATION CENTER

FOR

SCIENTIFIC AND TECHNICAL INFORMATION

CAMERON STATION, ALEXANDRIA, VIRGINIA

4946

63-4-5

10

414444

CORNELL UNIVERSITY
Center for Radiophysics and Space Research

ITHACA, N. Y.

414444

AUG 2 4 1963

ISIA A

CENTER FOR RADIOPHYSICS AND SPACE RESEARCH
CORNELL UNIVERSITY
ITHACA, NEW YORK

January, 1963

CRSR 120

THE INTERSTELLAR ABUNDANCE OF THE HYDROGEN
MOLECULE

Robert J. Gould

ACKNOWLEDGEMENTS

TABLE OF CONTENTS

LIST OF FIGURES

ix.

x.

xi.

I. INTRODUCTION

A. Interstellar Matter - Brief Review

The combination of observational and theoretical
studies carried out chiefly during the last 25 years leads
to the following picture for the matter between the stars.
The gas, whose relative element abundance is believed to be
essentially the same as that found in stellar atmospheres,
is distributed throughout the galaxy in the "spiral arms"
which form a very flat (thickness $\approx$ 200 pc) subsystem
defining the plane of the galaxy. In the spiral arms the
overall smeared-out density of atomic hydrogen which is the
most easily observable (by 21-cm line studies) component of
the gas is $\bar{n}_H \approx$ 1 atom/cm^3, giving a density $\bar{\rho}_H \approx$ 1 - 2 x
10^{-24} gm/cm^3. Having about the same distribution as the gas
is the interstellar "dust" which is thought to be composed
mainly of ice crystals having dimensions of roughly 10^{-5} -
10^{-4} cm. The smeared-out density of these dust grains is
about $\bar{\rho}_g \approx$ 10^{-26} gm/cm^3. The density of both gas and dust
is much less between the spiral arms and away from the plane
of the galaxy. Actually, there are large variations in
density even within the spiral arms. It is known from
studies of interstellar absorption lines and also from 21-cm
investigations that the gas is distributed in dense clouds
in which the density is $n_H \approx$ 10 atms/cm^3, compared to an

1.

intercloud density of about 0.1 atoms/cm^3. Generally, there is also a corresponding increase in dust density within the dense regions. The clouds fill roughly 10% of the interstellar space and have an average diameter of about 10 pc. In addition to the velocity corresponding to galactic rotation, the clouds have a random motion corresponding to a radial velocity distribution $\frac{1}{2\eta} e^{- \upsilon_r/\eta}$, where $\eta \simeq 10$ km/sec (this is just a rough value for η, later in this work we shall adopt $\eta = 7.5$ km/sec). This so-called "cloud model" of the interstellar medium is an oversimplification but is quite useful as a starting point for theoretical calculations. It should be kept in mind, however, that this picture may change when more complete data on the interstellar medium is available.

About 10% of the interstellar clouds are in the ionized state, the ionized regions (H II regions) being roughly spherical (radius 20-150 pc) and confined to the vicinity of O and B stars or groups of stars. Spitzer[1] has shown that a kinetic temperature in the neighborhood of 10^{4}°K will result in these H II regions from energy balance of electrons between gains from electron capture by protons followed by photoionization and losses by excitation of low-lying states of O^+ ions. It is though that the low density intercloud medium is in the ionized state.

The remaining 90% of the interstellar clouds are neutral (H I regions). Early 21-cm work[2] indicated a

temperature of 125°K for the H I clouds, while more recent investigations[3] of 21-cm line absorption point to a temperature of about 60°K. The processes which control the temperature in H I regions are much more uncertain than those for H II regions and a discussion of these processes will be given later (sections IIID and IVC). One of the cooling processes, namely the radiative de-excitation of rotational levels, involves the hydrogen molecule directly. Generally, a temperature 100°K for the H I clouds will be sufficiently accurate for most calculations performed in this work.

Many of the processes which determine the state of interstllar matter involve the interstellar radiation field. For a typical point in interstellar space this radiation field can be approximated by that of a black body at a temperature $T_o \approx 10^{4\,\circ}$K, but diluted by a factor $W \sim 10^{-14}$. With such a radiation field the relative population of excited states of atoms or molecules is

$$\frac{n_E}{n_o} \sim W\, e^{-E/kT_o}, \tag{1}$$

where n_o is the population in the ground state and E is the excitation energy. This relation holds only if the most important mechanism for excitation and de-excitation is the interaction with the (weak) radiation field and may not hold, for example, for metastable states. The main conclusion to be drawn from (1) is that interstellar atoms and molecules are very predominantly in the ground state.

Since hydrogen atoms are photoionized easily by radiation of wavelength $\lambda < 912$ Å (the Lyman limit), the H I clouds are essentially opaque to radiation beyond the Lyman limit (with a density $n_H = 10$ cm^{-3} and a path length of 1 pc, the optical thickness at the Lyman limit is about 20). In many instances it is a good approximation to use Wien's law instead of Planck's for black body radiation. This allows one to write down a simple expression for the photon flux dJ_ω (number of photons incident per cm^2 per second in the frequency interval $d\omega$):

$$dJ_\omega = J_\omega d\omega = \left(\frac{\omega}{\pi c}\right)^2 W \, e^{-\beta \hbar \omega} \, e^{-\tau_\omega} \, d\omega, \qquad (2)$$

where $\beta = 1/kT_o$, and the optical thickness τ_ω is for H I regions essentially

$$\tau_\omega \longrightarrow \begin{cases} \infty & \omega > \omega_o \\ 0 & \omega < \omega_o \end{cases}$$

ω_o being the frequency corresponding to the edge at 912 Å.

B. Observational Inferences on the H_2 Abundance

1. Spectroscopic Difficulties

Atmospheric absorption limits optical observations to the range 2900 Å - 10,000 Å (1.2 eV - 4.3 eV). Since the first bound excited electronic state of the hydrogen molecule lies more than 11 eV above the ground state, detection of molecular hydrogen thru its absorption

spectrum is impossible from below the atmosphere. Moreover, both the magnetic fine structure and hyperfine structure splittings are zero in first approximation for the hydrogen molecule in the ground $(^1\Sigma_g{}^+)$ state. This situation is similar to that for the helium atom in the ground (^1S) state and arises from the singlet character of the state. It is for this reason that no radio observations analogous to the 21-cm studies for atomic hydrogen can be made for molecular hydrogen (or helium). Another type of energy level splitting, Λ -doubling, is also zero in first approximation, since the ground state of H_2 is a Σ state ($\Lambda = 0$). Radiation between components split by Λ - doubling has been considered by Shklovsky[4] for such inter- stellar molecules as OH.

While direct spectroscopic detection of H_2 seems impossible from below the atmosphere, observations from spectroscope carrying satellites offer a very appealing possibility. The launching of a satellite carrying an ultra-violet stellar spectroscope is tentatively scheduled[5] for 1966. Such a spectroscope would be capable of detecting the interstellar absorption lines of H_2 in the Lyman and Werner bands which correspond to the following transitions (see Fig. 1):

Lyman bands: $\text{X} \longrightarrow \text{B}$ $\nu_{00} = 90196 \text{ cm}^{-1}$ (11.2 eV)

Werner bands: $\text{X} \longrightarrow \text{C}$ $\nu_{00} = 99080 \text{ cm}^{-1}$ (12.3 eV)

$\text{X}:$ $^1\Sigma_g{}^+$ (the ground state)
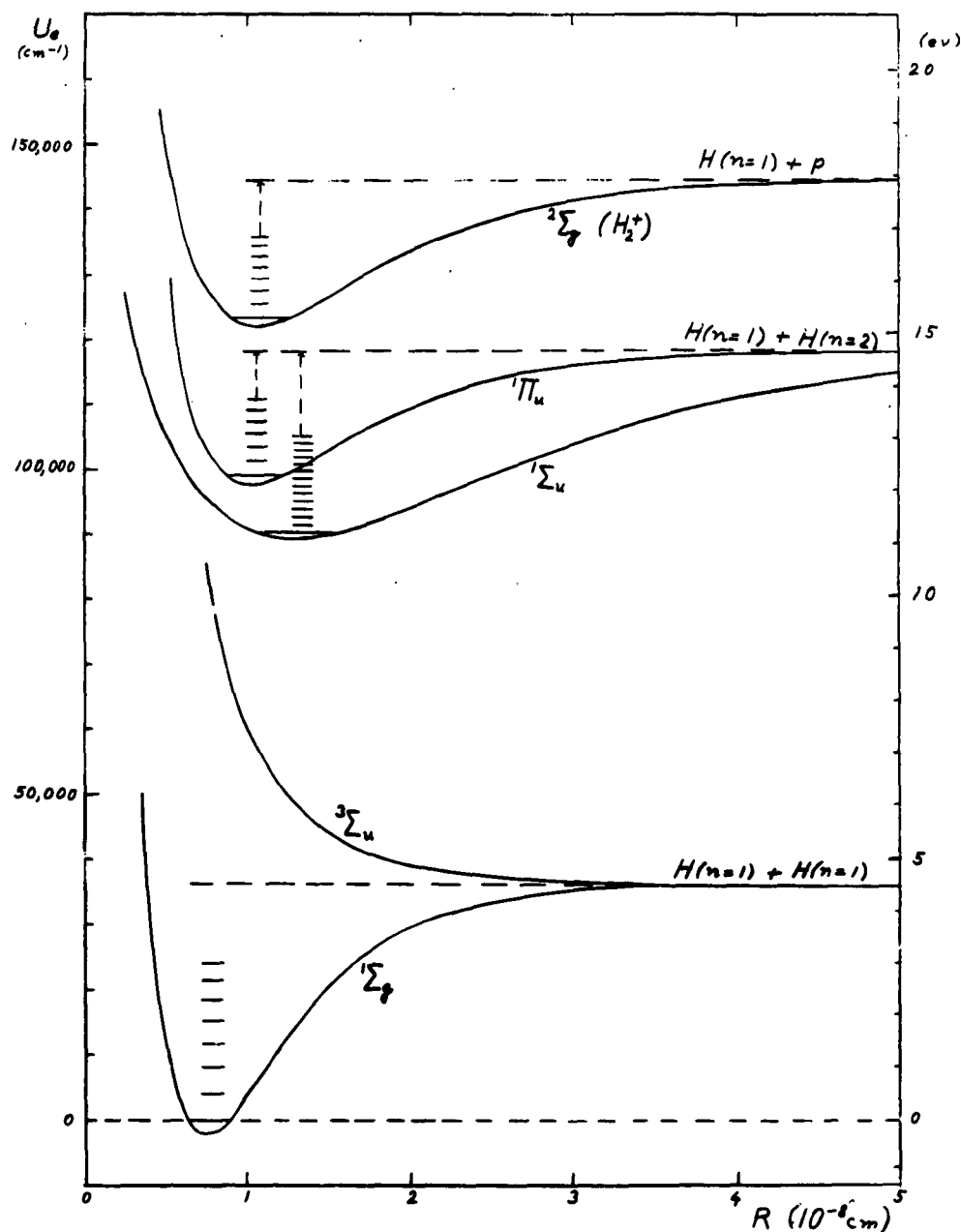
Fig. 1. Potential curves for a few states of H_2 and H_2^+. $U_e(R)$ is the effective potential function for nuclear motion and is essentially $E_e(R) + V_e(R)$ where $E_e(R)$ is the eigenvalue of the electronic energy calculated for a fixed internuclear distance R and $V_e(R)$ is the coulomb repulsion energy for the two nuclei.

B: $\, ^1\Sigma_u^+$

C: $\, ^1\Pi_u$.

These transitions have oscillator strengths of order unity and so even small amounts of molecular hydrogen should be detectable thru the absorption lines.

2. Gas/Dust Correlations

At present, direct evidence for the presence of molecular hydrogen is lacking. However, there is weak indirect evidence for a relatively high abundance in certain regions of the galaxy. It will be shown in part II that recombination on interstellar grains is the only mechanism capable of building up a molecular concentration comparable to the observed atomic densities in a time less than the age of the galaxy. One would expect, then, to find the highest molecular concentration in the regions where the dust density is greatest. Van de Hulst et al[6] did find that the dark regions in Taurus gave only about 30% of the 21-cm line radiation expected from considerations of the amount of dust present. In fact, they suggested that the resulting low atomic density might be because most of the hydrogen had associated to molecular form in these regions. In other 21-cm surveys, Lilley[7] and Heeschen[8] find a general correlation in the amount of gas and dust on the whole, but also find some fluctuations in the gas/dust ratio. Lilley reports a range of 35 - 250 in the density

ratio with a mean value of about 100.

3. Dynamical Astronomy's Limit

An absolute upper limit to the molecular density can be obtained from dynamical astronomy. From studies of the motion of stars normal to the plane of the galaxy a potential curve in the normal (z) direction can be constructed. One finds from these investigations[9,10] that the total mass density (stars + gas + dust) near the sun is $\rho \simeq 0.13 - 0.15$ $M_\odot/pc^3$ (compared with the older figure $0.09 - 0.10$ $M_\odot/pc^3$). Of this figure, about half can be accounted for by observed stars and gas (dust contributes a negligible amount). Oort[11] has attributed the remaining so-called "unaccounted for mass" to faint dwarf stars, while Bok[12] and Gold[13] have suggested that molecular hydrogen may contribute appreciably to this unobserved mass. If we attribute 0.07 $M_\odot/pc^3$ to H_2, we get an upper limit of $\bar{n}_{H_2} \leqslant 1.4$ cm^{-3} for the average molecular abundance (see, however, section B4 of chapter V where an analysis of the z-distribution of the galactic gas points to a higher density).

4. Inferences from Observed H I Cloud Temperatures

Since molecular hydrogen may play an important role in determining the temperature of H I regions, Kahn[14] attempted to determine the H_2 abundance from the observed temperature from 21-cm studies. It turns out, however, that the required molecular concentration necessary to produce a given temperature depends strongly on the value of the

temperature chosen, especially for temperatures below 100°K. This question will be dealt with in more detail later.

In summarizing the observational situation for interstellar H_2, we can say that there is weak evidence for and no evidence against its presence, and that the present observational data will actually tolerate a molecular abundance comparable to and perhaps even greater than the atomic value.

C. Preview

Most of this work is devoted to an analysis of the various processes which determine the abundance of interstellar molecular hydrogen. It will be shown that the principal mechanism for formation of H_2 is that of association on the surface of the interstellar grains. The range of grain temperatures where this reaction is efficient is coincident with the expected range 5-20°K. The most important dissociative process is the ionization (and dissociation) of clouds in random encounters with bright stars. A balance results in which the molecular concentration is (roughly) comparable to the atomic value and in which the molecular hydrogen is spatially distributed in essentially the same manner as the observable atomic hydrogen.

The various implications of a high molecular abundance are discussed. It is shown that molecular hydrogen can account for the unobserved mass of dynamical astronomy. Moreover, it is shown that the observed spatial distribution of the galactic gas implies a high gravitational

attraction near the plane of the galaxy. The mass distri-
bution required to produce this gravitational field is
essentially the same as that of the observed atomic
hydrogen. Roughly ten times as much mass as the atomic
hydrogen is needed to account for this self-gravitation
effect and this mass is attributed to molecular hydrogen.
The integrated mass density above the galactic plane
($\int_0^\infty \rho(z)\, dz$) determined in this manner has about the same
value (2 x 10^{-21} gm-pc/cm^3) as the corresponding quantity
determined from motions of stars perpendicular to the
galactic plane.

II. MECHANISMS FOR THE FORMATION OF MOLECULAR HYDROGEN

A. Radiative Association

Under ordinary laboratory conditions molecules form by three body collisions, the third body being necessary to carry off the (negative) binding energy which results on formation of a stable molecule. The reaction rate for such processes is proportional to the third power of the density. Since interstellar densities are very low, this process is negligible compared to radiative association (rate proportional to the second power of the density) in which the emitted photon does the job of the "third" body. For the formation of H_2, we may write for the number of radiative recombinations $(H + H \longrightarrow H_2 + \gamma)$ per cm^3 per second:

$$(\dot{n}_{H_2})_\gamma = n_H^2 \overline{\sigma v}, \tag{4}$$

where $\overline{\sigma v}$ is the mean value (averaged over the velocity distribution of the hydrogen atoms) of the product of the crossection for the process and the relative velocity of the hydrogen atoms. To estimate σ we write

$$\sigma = \sigma_0 P_\gamma, \tag{5}$$

where σ_0 ($\sim \pi a_0^2$) is the collision crossection and P_γ is the probability per collision of a radiative process leading to a stable molecule. Two types of radiative process can

lead to the formation of a molecule.

The electronic states of the hydrogen molecule which result from bringing two hydrogen atoms in the ground state together adiabatically are the Heitler-London states which are the two lower states shown in the level diagram in Fig. 1. The type of process usually considered in radiative association involves a transition from a repulsive state $(^3\Sigma_u^+)$ to an attractive state $(^1\Sigma_g^+)$. The radiative probability P_γ for this process would be calculated from

$$P_\gamma \cong g \overline{\int A(R) \, dt} \quad , \tag{6}$$

where g is the weight $(3/4)$ of the triplet state and $A(R)$ is the transition probability per unit time for the transition from the repulsive to the attractive state. Again, the bar over the integral means average over the velocity distribution of the hydrogen atoms. The transition $^3\Sigma_u^+ \longrightarrow {}^1\Sigma_g^+$ required for this recombination is forbidden (by the selection rule $\Delta S = 0$) and so $A(R)$ is very small. The quantum mechanical expression for $A(R)$ is[15]

$$A(R) = \frac{4 \, e^2 \, \omega^3(R)}{3 \, \hbar \, c^3} \left| \left\langle {}^1\Sigma_g \left| r \right| {}^3\Sigma_u \right\rangle_R \right|^2 . \tag{7}$$

In terms of the oscillator strength,

$$f(R) = \frac{2 \, m \, \omega(R)}{3 \, \hbar} \left| \left\langle {}^1\Sigma_g \left| r \right| {}^3\Sigma_u \right\rangle_R \right|^2 , \tag{8}$$

$$A(R) = \frac{2 \, e^2 \, \omega^2(R)}{m \, c^3} \, f(R). \tag{9}$$

It will be shown in section III-A that at the equilibrium internuclear distance (R_o = 0.74 $\overset{o}{A}$) for the ground state the f-value for this transition is $\sim 10^{-9}$. It should be noticed that $f \propto \omega$, $A \propto \omega^2 f \propto \omega^3$. At the temperatures of H I clouds (kT $\simeq$ 0.01 eV), few hydrogen atoms will have sufficient kinetic energy before collision to get very far up on the repulsive potential curve. Most of the contribution to (6) will come from the classical turning point, which for the characteristic energies of H I clouds, occurs at large internuclear separations where the energy separation $\hbar\omega$ between the two states is small and so where A is small. It will certainly be true that

$$\overline{\int A(R) \, dt} \ll A(R_o) \, \tau_{coll} \, , \qquad (10)$$

where $A(R_o)$ is the value ($\sim$ 1 sec^{-1}) at the equilibrium R and τ_{coll} is the collision time (approximately equal to the characteristic time for one vibration: $\sim 10^{-14}$ sec). We have then for the crossection for radiative association

$$\sigma \ll \sigma_o \, A(R_o) \, \tau_{coll}. \qquad (11)$$

(It is interesting to note that the quantity $A(R_o) \, \tau_{coll}$ corresponds to the factor $n_3 \, v_A$ for 3-body recombinations, n_3 being the number density of the "third" body and v_A the atomic volume). At 100°K, $\bar{v} \simeq 2 \times 10^5$ cm/sec, so from (4) and (11),

$$(\dot{n}_{H_2})_\gamma \ll n_H^2 \times 10^{-25} \text{ cm}^3 \text{ sec}^{-1}. \tag{12}$$

Clearly, in a galactic age of 10 billion years only a negligible amount of H_2 could form by this process.

As mentioned earlier, there are two types of radiative recombination. The other way in which a stable molecule can be formed is thru a vibrational quadrupole transition. In this process the two atoms collide in the singlet state (g = 1/4) and during the collision the system makes a transition from the vibrational continuum of the $^1\Sigma_g$ state to a bound vibrational state of $^1\Sigma_g$, emitting a quadrupole photon. While this process is fairly independent of energy (temperature) and does not suffer as much from the shall ω's, the characteristic A-value is still quite small. The A's for these vibrational transitions are of the order[16] 10^{-7} sec^{-1}. A summation over transitions to all vibrational states might make the effective A several orders of magnitude larger, but it is clear that this process can produce a reaction rate no larger than the upper limit given by (12).

While radiative association is completely negligible as a mechanism for hydrogen molecule formation, other processes, especially recombination on grains, are much faster. We shall consider these processes in detail in the next sections.

B. Surface Recombination on Interstellar Grains

    1. Basic Ideas of Surface Recombination

        (a) Astronomical time scale for recombination -
The realization that the interstellar grains can serve as
catalysts for the formation of H_2 has existed since the
original suggestion by van de Hulst around 1946. Since that
time, various estimates have been made for the rate of
molecule formation by this process. The simplest assumption
which one can make in order to calculate the reaction rate
is that every hydrogen atom which strikes a grain eventually
leaves as part of a hydrogen molecule or, in the terminology
of Chemical Kinetics, that the recombination coefficient
(γ) is unity. With this assumption the rate of formation
of H_2 can be written as

$$\dot{n}_{H_2} = \frac{1}{2} J A , \tag{13}$$

where J is the flux (number/cm^2/sec) of atoms from the
surrounding gas which hit the surface and A is the total
grain surface area per cm^3 of interstellar space. The flux
J is simply

$$J = \frac{1}{4} n \bar{v} , \tag{14}$$

where

$$\bar{v} = \sqrt{8kT/\pi M} , \tag{15}$$

n being the number of hydrogen atoms per cm^3. The quantity
A was calculated by McCrea and McNally[17] for spherical

grains with a distribution of radii $N(r) = C\, e^{-(r/a)^p}$ based on the work of Oort and van de Hulst.[18] Using a density for the solid grains of 1.1 gm/cm^3 and a temperature of 100°K, the results of McCrea and McNally can be expressed in terms of the (smeared out) density of grains ρ_g as

$$\dot{n}_{H_2} = b\, n\, \rho_g \quad , \tag{16}$$

where $b = 4.0_7 \times 10^9$ gm^{-1} sec^{-1} cm^3. We see that for the densities of H I clouds (n $\sim$ 10 atoms/cm^3, $\rho_g \sim 10^{-25}$ gm/cm^3) a density of 1 molecule/cm^3 can build up in about 10^7 yr (much less than the age of the galaxy!). These figures are for $\gamma = 1$. The right hand side of (16) should really have a factor γ expressing the efficiency of the recombination process. While it has generally been assumed that $\gamma = 1$ for the interstellar conditions, this is by no means obvious. The recombination coefficient has a very strong dependence on the temperature of the solid surface and on the chemical nature of the surface. This is evident from the results of experiments on surface recombination which will be discussed in the following section (section 2). To facilitate an understanding of these experiments we shall spend the rest of this section reviewing the basic principles involved in surface recombination.

(b) <u>Atomic forces in adsorption</u> - As an atom (or molecule) approaches the surface of a solid, it feels a potential of the form shown below.
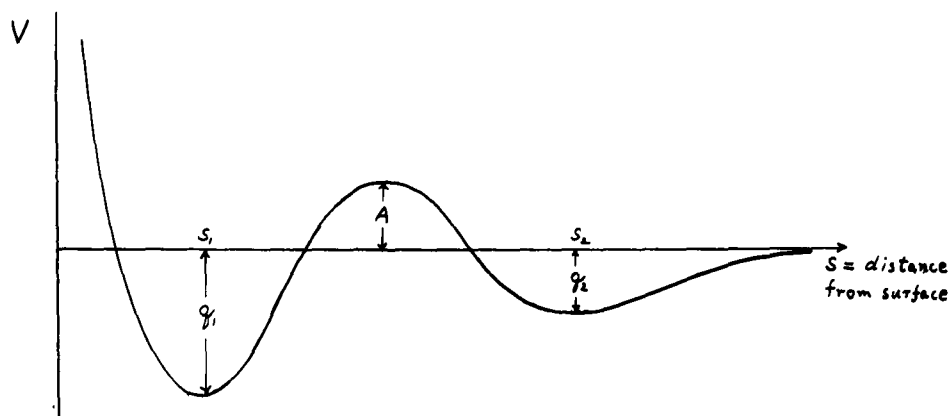
Fig. 2.   Potential energy as a function of distance from
          solid surface — normal case

At large distances, as it approaches the solid, the atom

feels a weak attraction due to London forces (we adopt the

terminology that the specific <u>attractive</u> forces between atoms

and molecules, whose potential goes as r^{-6}, are to be

referred to as <u>London forces</u>; the combination of London

forces and valence repulsion, which would be present at,

for example, s_2, we call <u>van der Waals forces</u>). At shorter

distances, the atom feels a repulsion and most atoms with

kinetic energy less than the "activation energy" A will

not pass over the hump. The activation energy results from

the necessity of breaking a chemical bond in order that the

atom can be adsorbed at the equilibrium position s_1. The

binding energy q_1 is due to valence forces and is quite

large (say, 2 eV), while q_2 is due to the weaker van der

Waals forces and is about an order of magnitude smaller than

q_1. The magnitude of the activation energy A depends

strongly on the nature of the surface and the adsorbing

atom or molecule. In some circumstances the activation
energy is zero or very small, in which case the potential
curve would be of the form shown in Fig. 3.
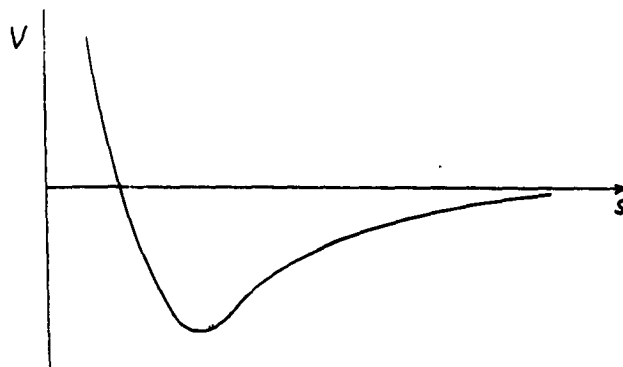
Fig. 3. Potential with no activation energy for
adsorption

There is also the possibility that the electronic state of
the (gas atom) - (solid) system is repulsive, producing a
potential curve as below.
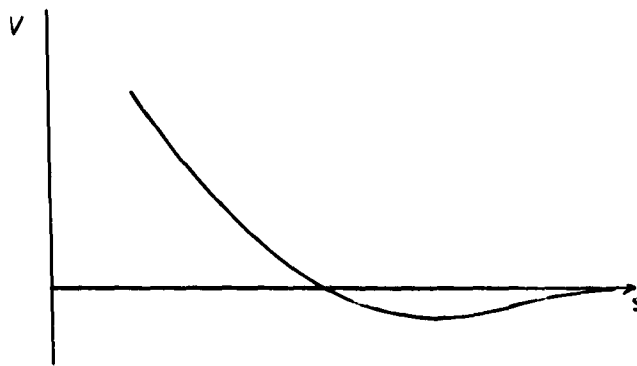
Fig. 4

Potential with an electronic repulsion

(c) <u>Dynamical equilibrium - basic processes</u> -
It is clear that there are two kinds of adsorption - one in
which the atom is held by (strong) valence forces and
another in which the atom is held by (weak) van der Waals
forces. Moreover, a solid surface can exhibit both forms
of adsorption simultaneously. The bare surface could be
attracting the atoms by valence forces, while above the
layer of strongly bound atoms another layer of atoms held
by van der Waals forces could exist. The second layer would
not interact strongly with the first since the chemical
bonds in the first layer would be saturated. The concen-
tration of atoms adsorbed in these two layers results from
a condition of dynamical equilibrium whereby the atoms are
lost from the surface by thermal evaporation and molecule
formation, the surface atoms being replenished by the flux
of atoms from the gas hitting the surface.

Consider the case where there is no activation energy
for an atom of the gas to adsorb by valence forces. We
assume that every atom, whether it strikes the bare or
covered surface, either sticks to the surface or forms a
molecule immediately on striking the surface. Let the total
number of sites per cm^2 on the solid be σ_0. The number of
occupied sites per cm^2 in layers 1 and 2 we denote by σ_1
and σ_2, the corresponding concentrations being $\Theta_1 \equiv
\sigma_1/\sigma_0$ and $\Theta_2 \equiv \sigma_2/\sigma_0$. The equations of dynamical equili-
brium for the two layers will be

layer 1: $J(1-\theta_1) + (1-\theta_1)\theta_2 u_{12} = u_{01}(\theta_1 - \theta_2) +$

$$2u_{12}\theta_1^2 + u_{d1}\theta_1 \qquad\qquad (17)$$

layer 2: $J(\theta_1-\theta_2) = u_{d2}\theta_2 + 2u_{12}\theta_2^2 + (1-\theta_1)\theta_2 u_{12}$

$$+ u_{02}\theta_2 \quad . \qquad\qquad (18)$$

These equations are similar to those of de Boer and van Steenis.[19] The u's (and J) are rate constants for the various processes and have the dimensions $cm^{-2}sec^{-1}$. Many of the rate constants are very difficult to calculate, but rough approximate expressions can usually be written down.

We now explain the origin of the various terms in (17), (18) and enumerate their associated rate constant expressions. For the present we assume both solid and gas to be at the same temperature.

(1) J is simply the flux of atoms hitting the surface. It can be written as

$$J = \frac{1}{4} n \sqrt{8kT/\pi M} = n(kT/h)F_g^{-1/3} , \qquad (19)$$

where

$$F_g \equiv (2\pi MkT)^{3/2}/h^3 . \qquad\qquad (20)$$

(11) u_{12} represents the rate of filling of layer 1 by migrating atoms in layer 2. It is approximately given by

$$u_{12} = \sigma_o \frac{kT}{h} D \quad . \tag{21}$$

Here, kT/h represents a characteristic frequency and D a diffusion factor. If diffusion is by thermal fluctuations, D is given by

$$D_{th} = e^{-\eta q_2/kT} \quad , \tag{22}$$

where ηq_2 is the energy barrier between adjacent equilibrium sites in layer 2. If diffusion is by quantum mechanical barrier penetration, D is given by

$$D_{q.m.} = e^{-\frac{2}{\hbar} \int |p|\, dx} \quad , \tag{23}$$

where the integral in the exponent is over the barrier between two equilibrium sites. This process will be discussed more thoroughly later. Sometimes, (21) is written as

$$u_{12} = \sigma_o \nu_o D \quad , \tag{24}$$

the frequency factor kT/h having been replaced by the characteristic frequency ν_o for vibration in the plane of the surface.

(iii) u_{o1} represents direct molecule formation thru reaction between impinging atoms of the gas and atoms of layer 1. It involves an activation energy A.

$$u_{o1} = n \sigma_o (kT/h) (F_g)^{-1} e^{-A/kT} \tag{25}$$

(the first subscript o means that the reaction is on the

adsorbed layer).

(iv) u_{d1} stands for thermal desorption (evaporation) from layer 1.

$$u_{d1} = \sigma_o (kT/h)\, e^{-q_1/kT} \qquad (26)$$

(v) u_{11} represents molecule formation by reaction between adjacent atoms already adsorbed in layer 1. We treat layer 1 as immobile.

$$u_{11} = \sigma_o\, (kT/h)\, e^{-A'/kT} \qquad (27)$$

(the subscript 1 means that the reaction is $\underline{in}$ the adsorbed layer). Usually A' is rather large and the process is negligible.

(vi) u_{d2} denotes evaporation from layer 2.

$$u_{d2} = \sigma_o\, (kT/h)\, e^{-q_2/kT} \qquad (28)$$

(vii) u_{12} is the rate constant for the reaction of two atoms in layer 2 to form a molecule. It is essentially the rate of encountering atoms and forming a singlet state (probability $\frac{1}{4}$) in diffusing about in layer 2.

$$u_{12} = \tfrac{1}{4}\, \sigma_o\, \frac{kT}{h}\, D \qquad (29)$$

(viii) u_{o2} represents molecule formation thru reaction of atoms of the gas with those of layer 2. An approximate expression for u_{o2} is

$$u_{o2} = \tfrac{1}{4}\, J \qquad , \qquad (30)$$

where once again the factor $\frac{1}{4}$ is simply the probability of forming a singlet state.

Derviations of the basic reaction rate formulae, which we have quoted, may be found in any standard work on Chemical Kinetics such as the book of Glasstone, Laidler and Eyring.[20] Most of the expressions are intuitively obvious. For example, the rate constant for thermal evaporation is a product of a factor representing the number of sites per cm^2 (σ_o), a frequency factor (kT/h or ν_o) which may be taken as a vibrational frequency, and a factor $e^{-q/kT}$ for the probability of getting enough thermal energy from the solid to escape over the barrier q. This probability factor arose from an integral over a Boltzmann distribution with a threshold at q, thus

$$e^{-q/kT} \sim \int_q^\infty f(E) \, e^{-E/kT} \, dE \ . \tag{31}$$

So far, we have assumed that a molecule, once formed, leaves the surface immediately. The validity of this assumption will be analyzed later. Moreover, reactions between the two layers have been neglected. The justification for this is that the activation energy for the reaction is high. We see from Fig. 2 that it is

$$A'' = A + q_2 \ , \tag{32}$$

from which we conclude that a simple evaporation from layer 2 is much more likely than a reaction with atoms of layer 1.

(d) <u>High and Low Temperature Values of the
Recombination Coefficient</u> - We conclude this section with
a brief discussion of the high temperature and low tempera-
ture properties of γ. From the definition of the
recombination coefficient as the fraction of incident atoms
which eventually leave the surface as part of a molecule,
we have

$$\gamma = \frac{2}{J} \left\{ u_{o1}(\Theta_1 - \Theta_2) + u_{11}\Theta_1^2 + u_{o2}\Theta_2 + u_{12}\Theta_2^2 \right\} . \quad (33)$$

At high temperatures evaporation limits Θ_2 to very small
values. As long as the temperature is not too high,
however, Θ_1 is close to unity and γ becomes

$$\gamma_1 \simeq 2u_{o1}/J = 2\sigma_o F_g^{-2/3} e^{-A/kT} . \quad (34)$$

Here, most of the temperature dependence arises from the
exponential factor and we see that γ_1 increases with
temperature. The factor $2\sigma_o F_g^{-2/3}$ is of the order of
unity. At low temperatures, however, processes in layer 1
can be neglected. Setting $\Theta_1 = 1$, the equilibrium equation
(18) simplifies to

$$J(1 - \Theta_2) = u_{d2}\Theta_2 + u_{o2}\Theta_2 + 2 u_{12}\Theta_2^2 . \quad (35)$$

This equation can be solved for Θ_2 to give

$$\Theta_2 = -\frac{U}{4u_1} + \sqrt{\left(\frac{U}{4u_1}\right)^2 + \frac{J}{2u_1}} , \quad (36)$$

where

$$U = u_{d2} + u_{o2} + J \quad . \tag{37}$$

If $u_{12} \gg U, J$,

$$\theta_2 \longrightarrow \sqrt{\frac{J}{2u_{12}}} \left(1 - \frac{U}{2\sqrt{2u_{12}J}} + \ldots\right) \quad , \tag{38}$$

and the recombination coefficient becomes

$$\gamma = 2 \frac{u_{o2}\theta_2 + u_{12}\theta_2^{\,2}}{J} \longrightarrow 1 - \frac{U}{\sqrt{2u_{12}J}} + \ldots, \tag{39}$$

the main contribution coming from u_{12}. This condition produces the limiting value $\gamma \longrightarrow 1$ with an equilibrium value of θ_2 which is small. In this case one can easily show that an adsorbed atom makes $\sim 1/\theta_2$ jumps to adjacent sites before encountering another atom with which it can combine. Such a random walk process may be pictured as resembling a two dimensional gas whose atoms move about with a velocity

$$\bar{v} = a \, \nu_o \, D \quad , \tag{40}$$

a being the distance between adjacent lattice sites. The one-dimensional "cross section" for recombination is

$$\rho \sim \tfrac{1}{4} p \, a \quad , \tag{41}$$

where p is the effective number of sites swept out by the tail of the attractive potential between two hydrogen atoms

We see that this number is of the order of unity since $\ln(\frac{N}{2}) \sim \ln(1/2\theta) \sim 10 - 20$. Thus we shall ignore this effect and take (42) as the correct rate formula.

2. Experiments on Surface Recombination

(a) <u>Older experiments - temperature behavior</u> - An extensive literature exists on the catalytic properties of different surfaces. Unfortunately, most of the work is carried out at high temperatures. The interstellar grains have temperatures around $10^{\circ}K$ and, as shown in the last section, the low temperature mechanism is quite different from that at high temperatures. Nevertheless one finds in the literature on the hydrogen molecule problem several references to experimental work done at high temperatures. To emphasize the different behavior of the recombination coefficient at low and high temperatures we shall analyze the γ vs. T curve for the recombination of H-atoms on glass, paying particular attention to the region of changeover from one mechanism to the other. We shall show, moreover, how one can obtain important information pertaining to low temperatures from the behavior of γ in this region.

The combination of experimental results of several workers leads to the schematic γ vs. T curve shown below (this curve is taken from the paper of Shuler and Laidler)[22].
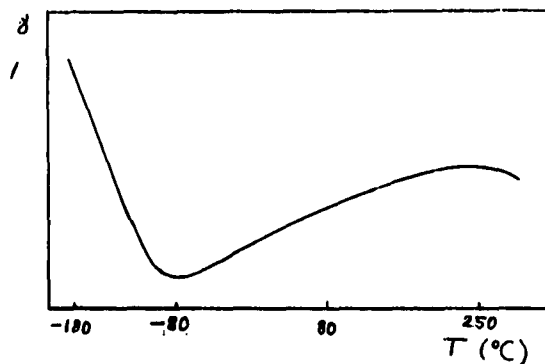
Fig. 5

Recombination Coefficient for Hydrogen Atoms on
a Clean Glass Surface

At high temperatures the recombination occurs on the bare
surface thru the mechanism u_{o1}, while at low temperatures
the recombination occurs in the van der Waals layer by the
mechanism u_{12}. Consider the region around the minimum.
Here, both mechanisms are relatively ineffective. For
layer 1, the temperature is too low for the incoming atoms
to get over the activation energy barrier. For layer 2,
the temperature is too high for the weakly adsorbed atoms
to stay long enough, i.e., they evaporate off before they
have a chance to recombine. Under these conditions, the
equilibrium equations '17) and (18) simplify to

$$J(1-\theta_1) + (1-\theta_1)\theta_2 \, u_{12} = u_{o1}(\theta_1 - \theta_2) \qquad (46)$$

$$J(\theta_1-\theta_2) = u_{d2} \, \theta_2 + 2 \, u_{12} \, \theta_2^2 + (1-\theta_1)\theta_2 \, u_{12}, \qquad (47)$$

with γ given by

$$\gamma = \frac{2}{J} (u_{o1} \Theta_1 + u_{12} \Theta_2^2) . \qquad (48)$$

The approximate solution of (46) and (47) is

$$\Theta_1 \approx 1, \; \Theta_2 \approx \Theta_1 \, J/u_{d2} \approx J/u_{d2} . \qquad (49)$$

We take for the rate constants:

$$J = n \frac{kT}{h} F_g^{-1/3} \qquad (50)$$

$$u_{o1} = n \, \sigma_o \frac{kT}{h} F_g^{-1} \, e^{-A/kT} \qquad (51)$$

$$u_{d2} = \sigma_o \frac{kT}{h} e^{-q_2/kT} \qquad (52)$$

$$u_{12} = \frac{1}{4} \sigma_o \frac{kT}{h} e^{-\eta \, q_2/kT} \quad \text{(thermal walk)}, \qquad (53)$$

which gives for γ:

$$\dot{\gamma} = 2\sigma_o F_g^{-2/3} e^{-A/kT} + \frac{1}{2} n \, \sigma_o^{-1} F_g^{-1/2} e^{-(2-\eta)q_2/kT} \qquad (54)$$

$$= \gamma_{o1} + \gamma_{12} .$$

We can write (54) as

$$\gamma = \alpha \, e^{-a/T} + \beta \, e^{b/T} \qquad (55)$$

where α and β have only a weak temperature dependence. This equation shows clearly how a minimum arises. To the right of the minimum reactions occur predominently on the bare surface (the term $\alpha \, e^{-a/T}$), while to the left of the

minimum recombination takes place in the second layer (the term $\beta\, e^{b/T}$). Actually, one can obtain some important information from equation (55). The process capable of destroying the low temperature limiting value $\gamma \longrightarrow 1$ is evaporation. From (39) we get a condition for γ to be close to unity

$$U \, (2 \, u_{12} \, J)^{-1/2} \ll 1. \tag{56}$$

Substituting for U the expression for u_{d2} and for u_{12} and J their respective rate constant formulas we have the condition

$$e^{q_2 (2 - \gamma)/kT} \gg 2 \, \sigma_o \, n^{-1} \, F_g^{1/3} \,. \tag{57}$$

Clearly, the value of q_2 determines the temperature below which $\gamma \longrightarrow 1$. From a knowledge that the minimum of (55) occurs at $-80^{\circ}C$ ($193^{\circ}K$), we can determine q_2 and hence the temperature T_o below which the recombination coefficient is close to unity. By setting $\frac{d\gamma}{dT}$ in (55) equal to zero at $T = 193^{\circ}K$, we have a relation for the binding energy q_2:

$$x \, e^x = \frac{\alpha}{\beta} \, \frac{a}{T} \, e^{-a/T} \,, \tag{58}$$

where

$$x = b/T = (2 - \gamma)q_2/kT \,. \tag{59}$$

A fairly accurate value of α may be determined from the observed value ($\simeq 0.03$) of γ at $300^{\circ}K$ and the experimental[19] value of A of 0.9 kcal/mol ($= 0.039$ eV). Substituting these

values and using the typical laboratory density of

$n = 10^{15}$ cm^{-3}, we find by solving (58) by iteration

that $x = 12.84$. With $\eta = \frac{1}{2}$ (a typical value for solids),

we get for q_2

$$q_2 = 0.143 \text{ eV}.$$

Substituting this value into (57) we find a T_0 of

$$T_0 = 125^\circ K$$

in rough agreement with experiment.

(b) <u>Recent Experiments</u> - The experimental work

which is by far the most pertinent to the hydrogen molecule

problem is that of Brackmann and Fite.[23] These authors

directed a beam of partially dissociated hydrogen at a

liquid helium cooled copper surface and measured the

reflection probability of atomic and molecular hydrogen.

The beam was a thermal one $(T = 80^\circ K)$ and had a density of

about 10^9 particles per cm^3, while the temperature of the

copper surface was varied from about $80^\circ K$ down to about

$3^\circ K$. The results for the reflection probability P of hydro-

gen atoms can be represented by the schematic curve shown

in Fig. 6 (T_s is the temperature of the surface). In the

region of the minimum $(10^\circ < T_s < 20^\circ)$ it was definitely

established that the low reflectivity was due to molecule

formation on the surface. The character of the surface can

be expected to change as the temperature T_s is lowered. At

different temperatures the different gases present in the
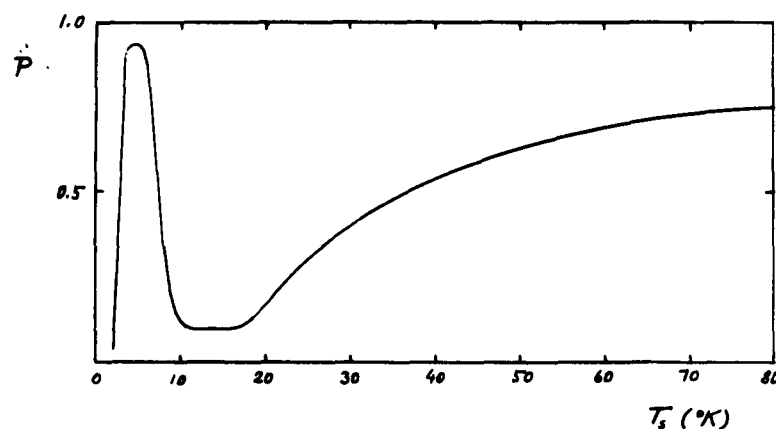
Fig. 6

Reflection probability of a surface at very low temperature

vacuum system will condense on the surface. Brackmann and Fite suggest that in the region of the minimum the surface consists of frozen air with a layer of ice underneath which had condensed at higher temperatures (around $77^\circ K$). They also suggest that the peak at $4^\circ K$ results from a surface of molecular hydrogen which apparently has a high reflectivity. However, they express concern over the fact that this molecular hydrogen surface must begin to form already at $10^\circ K$ while "vapor pressure data" would not allow molecular condensation above about $5^\circ K$. While it is true that solid molecular hydrogen would form only below about $5^\circ K$ at the pressures encountered, one cannot conclude that a monolayer of H_2 would not form for higher temperatures. The surface below this monolayer could give rise to higher (van der Waals) binding forces than would a surface of pure solid H_2. As a matter of fact, stronger binding forces would be

expected, since van der Waals binding energies are proportional to the product of the polarizabilities of the adsorbing molecule (H_2) and the molecular constituent of the solid, and H_2 has a rather low polarizability compared to say, O_2 or N_2.

Clearly, the low temperature behavior of a solid surface is quite complex. The following three sections (3, 4 and 5) are devoted to a more thorough treatment of the properties of solid surfaces and the low temperature behavior of the recombination coefficient.

3. Calculation of the Force Field Above a Solid Surface

(a) <u>Chemical composition and lattice structure of the interstellar grains</u> - Van de Hulst[24] has shown that the most abundant constituent of the interstellar grains is probably ice formed thru the chemical reactions

$$H + O_2 \longrightarrow HO_2 + 40 \text{ kcal} \quad (1 \text{ eV} \simeq 23 \text{ kcal/mol})$$

$$HO_2 + H \longrightarrow \begin{cases} H_2O_2 + 101 \text{ kcal} \\ H_2 + O_2 + 63 \text{ kcal} \end{cases}$$

$$H + H_2O_2 \longrightarrow H_2O + OH + 64 \text{ kcal}.$$
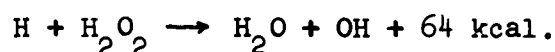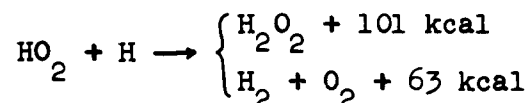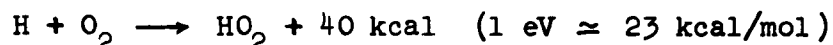
He suggested the following relative composition for the grains

$$100 \text{ molecules } H_2O$$
$$30 \text{ molecules } H_2$$
$$20 \text{ molecules } CH_4$$
$$10 \text{ molecules } NH_3$$

5 molecules MgH, etc.,

the values being very uncertain since it depends strongly on temperature whether the molecules "freeze down". The H_2 concentration is especially uncertain since H_2 will adhere to the surface of the solid only at very low temperatures. As a solid the interstellar grains would be classified somewhere between a hydrogen bonded crystal and a molecular crystal, the former being held together by the quasi-chemical hydrogen bond,[25] the latter by van der Waals forces. The crystal structure of ice is believed to be similar to that of wurtzite[26] with each oxygen atom surrounded tetrahedrally by four other oxygen atoms each at a distance of about 2.8 Å. Because of its geometry, this is a rather difficult structure to deal with and since the surface of the grains probably has a number of adsorbed atoms or molecules on it which further complicates matters, we take the following model for the purposes of making calculations: a body centered cubic lattice with identical force centers situated at the lattice points. With respect to any such force center as origin, this type of lattice has force centers at x_i, y_i, z_i = ip, $(i + \frac{1}{2})p$ with i = 0, 1, 2, 3, ... The density of force centers is then $n = 2\, p^{-3}$. We take the surface of the solid to be uniform, that is, to correspond to atoms at some integer (or half integer) value of, say, z (see Fig. 7).
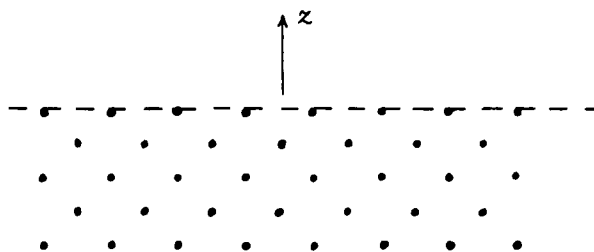
Fig. 7

Idealized solid

Our task is to calculate the potential field above this solid.

    (b) **Binding forces - summation over lattice sites** - Here we are interested in binding caused by van der Waals forces and to calculate the potential as a function of height above the surface we take a Lennard-Jones (6-12) type of potential for the energy of interaction between the adsorbed atom (or molecule) and the lattice sites. This potential is of the form

$$\varphi(r) = 4\epsilon \left[\left(\frac{\sigma}{r}\right)^{12} - \left(\frac{\sigma}{r}\right)^{6} \right] = \varphi_V + \varphi_L , \qquad (60)$$

and represents an attraction due to London forces (φ_L) and a valence repulsion (φ_V). The function has a minimum value of $-\epsilon$ at $r = 2^{1/6}\sigma$. Its chief attribute is that it is characterized by only two parameters: the strength parameter ϵ and the range parameter σ, both of which can be determined by experiment. We assume the potential energy of, say, the hydrogen atom above the surface with the

lattice points to be additive. Then the potential energy
of interaction of the adsorbed atom and the solid as a
function of height above the solid is

$$\varphi(h) = \sum_i \varphi_1(h; r_1) \quad , \tag{61}$$

where the sum is over the lattice sites. To evaluate
$\varphi(h)$, we sum over the nearby atoms in the top layer of
the solid and approximate the contribution from the more
distant lattice sites by smearing them out and replacing
their sum by an integral. Because of the shorter range of
the valence repulsion, these distant atoms will contri-
bute only to φ_L. One can obtain an approximate expression
for $\sum_1 \varphi_{L_1}(h; r_1)$ by smearing out all the atoms of the
solid and replacing the sum by an integral (see Fig. 8).
Such an expression would be valid for large distances from
the surface.
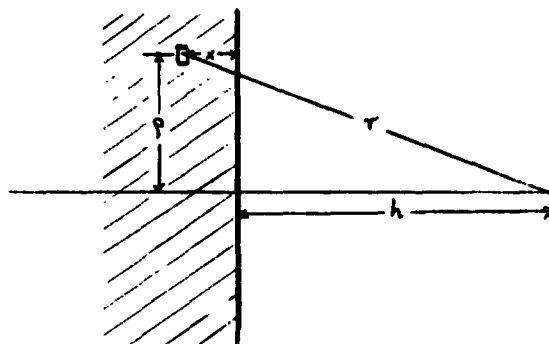
Fig. 8

Uniform solid

$$\sum_i 1/r_i^6 \longrightarrow \int \frac{n\,d\tau}{r^6} = n \int_0^\infty \int_0^\infty \frac{2\pi\rho\,d\rho\,dx}{\left[(x+h)^2 + \rho^2\right]^3}$$

$$= \frac{n\pi}{o}\,\frac{1}{h^3} = \frac{\pi}{3}\,\frac{1}{p^3}\,\frac{1}{h^3}\ .$$

$$\frac{\sum_i \varphi_{L_i}(h;\ r_i)}{4\epsilon} = \frac{\pi}{3}\,\left(\frac{\sigma}{p}\right)^3\left(\frac{\sigma}{h}\right)^3\ . \tag{62}$$

From this expression one also gets the approximate expression for the contribution from the atoms in all the layers below the top to be

$$\sum_i{}' \frac{\varphi_L(h;r_i)}{4\epsilon} \simeq \frac{\pi}{3}\,\left(\frac{\sigma}{p}\right)^3\left(\frac{\sigma}{h + \frac{p}{2}}\right)^3. \tag{63}$$

The sum from the distant atoms in the top layer may be approximated by a similar integral (see Fig. 9).
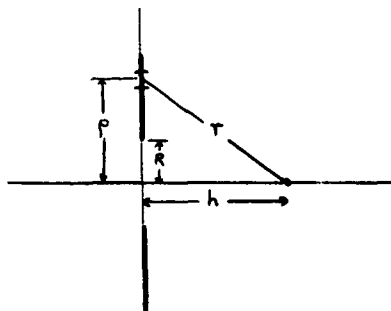
Fig. 9

Uniform surface layer

$$\sum_i r_i^{-6} \longrightarrow \int r^{-6} \, n_\sigma \, 2\pi\rho \, d\alpha \quad (n_\sigma = p^{-2})$$

$$= 2\pi \, p^{-2} \int_R^\infty (\rho^2 + h^2)^{-3} \rho \, d\rho = \tfrac{1}{2} \pi \, p^{-2} (R^2 + h^2)^{-2}$$

$$\frac{\sum_i \varphi_L(h;r_i)}{4\epsilon} \quad \approx \quad \frac{\pi}{2} \left(\frac{\sigma}{p}\right)^2 \times \left(\frac{\sigma^2}{R^2 + h^2}\right)^2. \quad (64)$$

These formulae are useful for computing $\varphi(h)$.

(c) <u>Potential curves</u> - There are three types of locations above the lattice plane which have a symmetry and which therefore could be positions of minimum energy (equilibrium positions). They are shown below ("a" and "b" denote the nearby atoms in the top layer; "o" denotes the position of symmetry in the lattice plane).

Case A: above the midpoint of four surface atoms

4 a-atoms $r_a^2 = h^2 + p^2/2$

8 b-atoms $r_b^2 = h^2 + 5p^2/2$
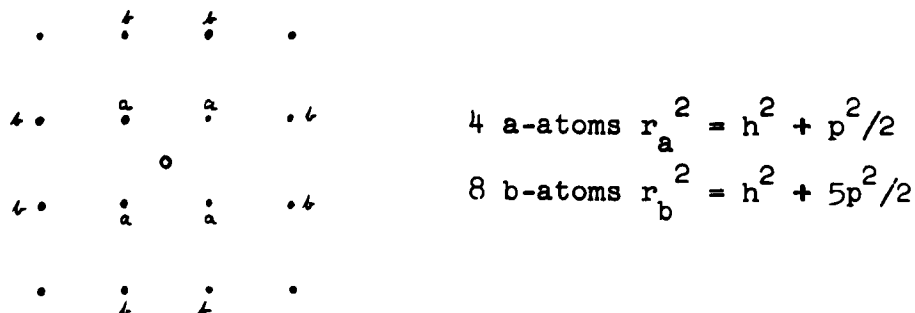
Case B: above a surface atom

1 atom below $r^2 = h^2$

4 a-atoms $r_a^2 = h^2 + p^2$

4 b-atoms $r_b^2 = h^2 + 2p^2$
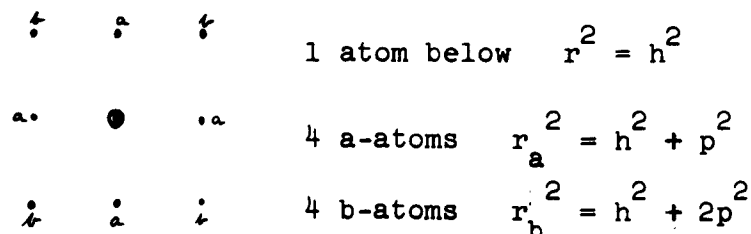
Case C: above the midpoint of two atoms

2 a-atoms $r_a^2 = h^2 + p^2/4$

4 b-atoms $r_b^2 = h^2 + 5p^2/4$
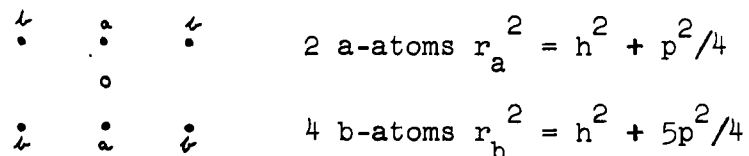
The <u>shape</u> of the resulting potential curves depends only on the ratio σ/p. The range σ of the interaction potential between an adsorbing H-atom and a lattice atom may be expected to be similar to that of the interacting $H-H_2$ system. The interaction potential for this system has been calculated by Margenau and the curve is reproduced in the book of Hirschfelder, Curtiss and Bird.[27] The range of this interaction is roughly 3 Å, and the strength ϵ is between 3×10^{-15} erg and 5×10^{-15} erg, depending on the relative orientation of the hydrogen molecule. Since density considerations for ice suggest a value for p of about 3 Å, we take for our calculations $\sigma/p = 1$. The results of the calculation of $\varphi(h)$ for these conditions is presented in Fig. 10 below.

At large distances from the surface the three curves join and go as h^{-3}. As one might expect, the lowest energy occurs for Case A. It is interesting to note that $(\varphi_{min}/4\epsilon) \simeq -1.5$, while for the interaction of a single pair of particles $(\varphi_{min}/4\epsilon) = -0.25$. The larger binding energy for the atom-solid system results, of course, from the additivity of the London potentials. Generally, the

binding energy to the solid is 5 to 10 times larger than that for a single pair of particles.
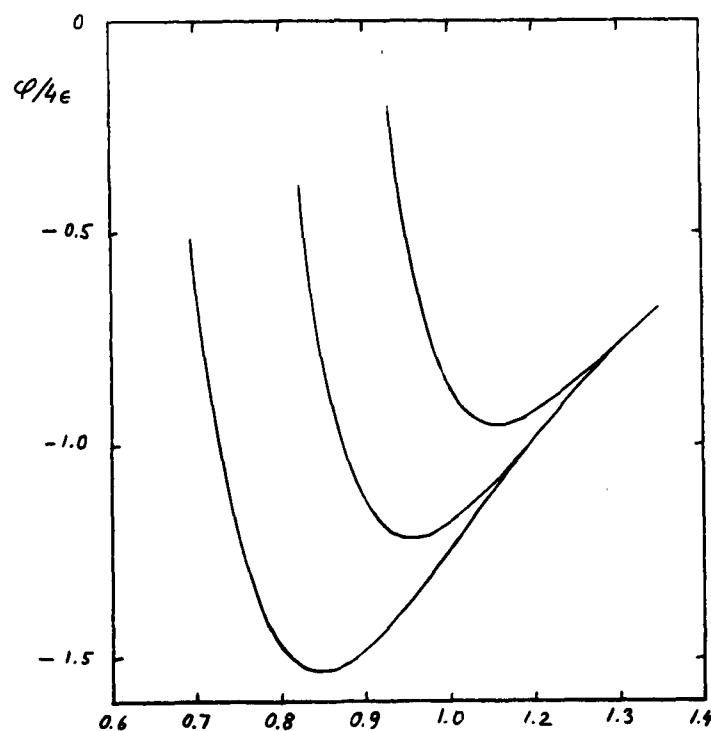
Fig. 10

Potential curves at various points above a bare surface

(d) <u>Surface mobility - quantum mechanical "walk"</u> - The potential <u>across</u> the solid surface is extremely important for the mobility or migration of surface atoms. We distinguish three types of mechanisms for surface migration:

(i) thermal movement (no barrier)

velocity: $V_{th}^o \simeq (kT/M)^{1/2}$ (65-i)

(this type of movement would occur

only for very "smooth" surfaces)

(ii) thermal random walk (with barrier)

velocity: $V_{th}^b \simeq \bigwedge \nu_o \, e^{-E_b/kT}$ (65-ii)

($\bigwedge$: periodicity of the lattice -

usually equal to p; ν_o: frequency of zero point motion

in the lattice plane; E_b: height of barrier)

(iii) quantum mechanical random walk

(barrier penetration)

velocity: $V_{q.m.}^b \simeq \bigwedge \nu_o \, e^{-t}$ (65-iii)

$(t = 2/\hbar \int_a^{a'} |p| \, dx$; no temperature

dependence)

The barrier is, of course, that encountered in going from

one position of minimum energy to an adjacent one. The

path of the atom need not be constrained to a fixed height

above the lattice plane and in fact the quantum mechanically

"easiest" path might correspond to values of h greater than

the equilibrium value since the height V_o of the barrier is

likely to be smaller for larger values of h (see Fig. 11

below).
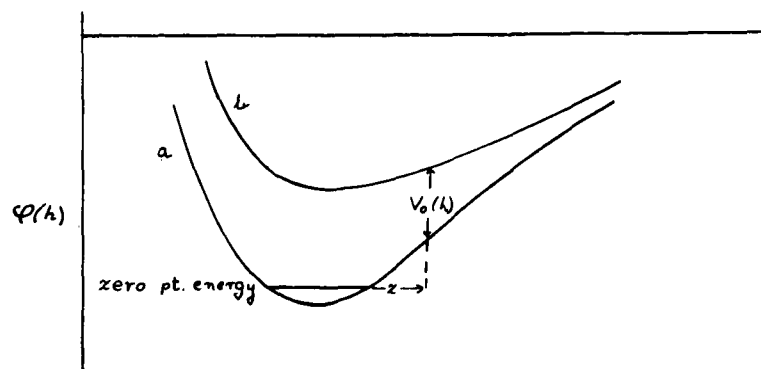
Fig. 11

Energy barrier $V_o(h)$ as a function of height

Curve "a" might correspond to the position above the mid-point of four lattice sites, curve "b" to points above the midpoint of two sites, the path being as below (Fig. 12).
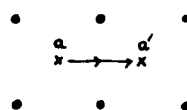
Fig. 12
Path of migrating atom

The quantum mechanical barrier penetration factor $\langle e^{-t} \rangle$ with $t = \frac{2}{\hbar} \int_a^{a'} |p| \, dx$ is a result of the WKB method applied to one dimensional motion. Very little has been done in the application of the WKB method for two and three dimensional barriers. The wave function for vibrational motion perpendicular to the solid has considerable spread and consequently the surface atoms would be found at

various heights above the surface. We make the following
assertion as to the value of the quantum mechanical
average $\langle e^{-t} \rangle$:

$$\langle e^{-t} \rangle \simeq \int e^{-t(h)} \, \psi_0^2(h) \, dh. \qquad (66)$$

Here, $\psi_0(h)$ is the normalized wave function for vibra-
tional motion perpendicular to the surface and $t(h)$ is
the exponent of the one dimensional barrier penetration
factor

$$t(h) = \frac{2}{\hbar} \int_a^{a'} |p(x;h)| \, dx \qquad (67)$$

Actually, since the surface atoms can exist in several
vibrational states v which would be populated according to
a Boltzmann distribution, a more accurate expression than
(66) would be

$$\langle e^{-t} \rangle_T \approx \frac{\sum_v \int_a^{a'} e^{-t_v(h)} e^{-E_v/kT} \psi_v(h) \, dh}{\sum_v e^{-E_v/kT}} \qquad (68)$$

In this case, the barrier penetration factor is tempera-
ture dependent. However, for the low temperatures
encountered in interstellar grains, $E_v/kT \gg 1$ and the
main contribution to the sum in (68) comes from the ground
state. Thus we shall use the simpler expression (66). In
the periodic potential over the solid surface we neglect
the higher Fourier components and take

$$V(x;h) = \frac{1}{2} V_o(h) (1 - \cos 2\pi \frac{x}{\Lambda}) \qquad (69)$$

Expanding (69) for small x, we find for the frequency of zero point motion in the lattice plane:

$$\nu_o = \sqrt{\frac{V_o}{2M \Lambda^2}} . \qquad (70)$$

If in computing the factor t(h), we neglect the zero point energy from (70), we have

$$t(h) = \frac{2}{\hbar} \sqrt{M V_o(h)} \int_0^\Lambda \sqrt{1 - \cos 2\pi \frac{x}{\Lambda}} \, dx$$

$$= \frac{4 \Lambda}{\pi \hbar} \sqrt{2 M V_o(h)} . \qquad (71)$$

The form of ψ_o to be taken depends on which region of h contributes most to the integral in (66). If most of the contribution comes from the region near the equilibrium position h_o, then ψ_o can be taken to be a gaussian

$$\psi_o(h) = (\frac{\alpha}{\pi})^{1/4} e^{-\frac{1}{2} \alpha (h-h_o)^2} \quad (\alpha = M\omega_h/\hbar). \qquad (72)$$

If the main contribution comes from large h, then a WKB wave function would be more appropriate for $\psi_o(h)$:

$$\psi_o(h) = C'(|p|)^{-1/2} \exp(-\hbar^{-1} \int_0^{z(h)} |p(z')| dz'). \qquad (73)$$

In either case we can write formally

$$\psi_o^2(h) \propto e^{-f(h)} , \qquad (74)$$

and can say that except for a numerical factor of order

unity,

$$\langle e^{-t} \rangle \simeq \max \exp \left[-(t(h) + f(h)) \right] \quad . \tag{75}$$

4. <u>Thermal Evaporation and Multilayers</u>

(a) <u>The critical temperature</u> - When a solid surface is in contact with a gas, an equilibrium concentration of adsorbed atoms (or molecules) exists which is determined by evaporation and replenishment from the gas. The equilibrium concentration Θ can be found from the equation

$$J(1 - \Theta) = \Theta \, \nu_o \sigma_o \, e^{-q/kT} \quad , \tag{76}$$

where q is the binding energy to the surface. Solving for Θ, we have

$$\Theta = (1 + \varkappa \, e^{-q/kT})^{-1} \quad , \tag{77}$$

where

$$\varkappa \equiv \nu_o \sigma_o / J \quad . \tag{78}$$

At the densities of interstellar space, $\varkappa \sim 10^{20} \gg 1$, so that Θ has a very sharp dependence on temperature (see Fig. 13 below).
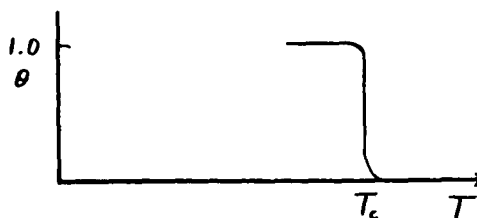
Fig. 13
Surface concentration as a function of temperature

Below a critical temperature T_c the surface becomes covered with adsorbed atoms or molecules. This analysis assumes that atoms from the gas which hit the surface stick to it or, in other words, that the accommodation coefficient α is close to unity. Van de Hulst[24] has argued that it is indeed probable that for interstellar grains α is close to one. The interstellar grains are likely to be at a very low temperature and while it is known that for bare metal surfaces $\alpha \longrightarrow 0$ as $T \longrightarrow 0$, it is also known experimentally that for gas-covered surfaces $\alpha \rightarrow 1$ as $T \rightarrow 0$. As van de Hulst has remarked, the surface condition of the interstellar grains is likely to approximate that of a gas-covered solid. Actually, it is quite reasonable, physically, that such a surface would exhibit efficient kinetic energy exchange properties, since a surface with a layer of adsorbed gas would be "softer" than a bare surface. Landau[28] has shown that at low temperatures and under certain circumstances of energy exchange (which are likely to be appropriate to the interstellar grain problem), the accommodation coefficient is inversely proportional to the cube of the Debye temperature. The adsorbed gases might be thought of as decreasing the effective Debye temperature of the solid. We shall assume, therefore, that the sticking probability for atoms on the interstellar grains is unity. It is clear, then, that the critical temperature T_c is determined only by the binding energy q

and the parameter $\varkappa$ thru the relation

$$e^{q/kT_c} = \varkappa \quad . \tag{79}$$

(b) <u>Adsorption energies</u> - For the interstellar grains it is likely that all interstellar atoms and molecules except He and H_2 are retained indefinitely on the surface. For solid molecular hydrogen to grow in interstellar space the temperature of the grains would have to be less than $2.5^\circ K$. It is quite possible, however, that for temperatures well above $2.5^\circ K$ the interstellar grains may have a monolayer and perhaps even a double layer of H_2 covering the surface. As mentioned earlier, a bare solid surface which is of different constitution than the H_2 is likely to bind the adsorbed H_2 more strongly than if it were solid molecular hydrogen. The reason for the small H_2-H_2 interaction energy is, of course, that the molecule has a relatively small polarizability. Binding is due to the attractive part of the 6-12 potential which represents the London force. The London interaction potential energy of interaction between two atomic systems a and b is roughly given by

$$\varphi_L = -\frac{3}{2} \frac{E_a E_b}{E_a + E_b} \frac{\alpha_a \alpha_b}{r_{ab}^6} \tag{80}$$

where E_a and E_b are characteristic excitation energies of the species (approximately equal to the ionization energies)

and α_a and α_b are the respective polarizabilities. Some molecules which might be candidates for constituents of the interstellar grains are tabulated below along with their respective electronic polarizabilities.[29]

TABLE 1. POLARIZABILITIES OF SOME SPECIES

Molecule	$\alpha \times 10^{25}$ (cm^3)
H_2	7.9
N_2	17.6
O_2	16.0
NH_3	22.6
CH_4	26.0
H_2O	14.9*

*$P = 4\pi N_L \bar{\alpha}/3$ tabulated in L-B.

Bond	Bond Polarizability $\times 10^{25}$ (cm^3)
C-H	6.5
H-N	7.5

In the calculation of binding energies we shall express interaction energies in terms of the parameter ϵ in the $H - H_2$ system which we take as $\epsilon = 4.0 \times 10^{-15}$ erg. The experimental value for $\epsilon_{H_2-H_2}$ is about 5.0×10^{-15} erg. Since the excitation energies for H and H_2 are approximately the same, we shall assume that the interaction of H and H_2 with any atom or molecule (X) will be related by

$$\frac{\epsilon_{H-X}}{\epsilon_{H_2-X}} = 4/5 \quad . \tag{81}$$

It is interesting to note that (80) would predict that the ratio of the interactions would roughly be equal to the ratio of the respective polarizabilities. The ratio of the polarizabilities turns out to be 0.84 which is close to 4/5.

The calculation of potential curves for adsorption was described in the last section (section 3), and the results for a homogeneous solid with a bare surface were presented in Fig. 10. We now consider the case where the surface is covered with hydrogen molecules, the molecules being situated at the equilibrium positions above the midpoint of four surface atoms of the bare solid. Taking these molecules as fixed force centers, the potential curves for the adsorption of H-atoms on this H_2-covered surface can be calculated. We shall assume that the range parameter for the H - H_2 interaction is the same as that for the H - X (H - solid atom) interaction. The results for $\epsilon_{H-X} = \epsilon_0 = 2\epsilon$ are shown in Fig. 14. Here, h is measured from the equilibrium position of the H_2 layer. Fig. 15 shows how the affinity to an H_2-covered surface varies when the strength parameter for the interaction with the bare surface atoms is changed. Clearly, one could go on and consider the field produced by a solid with a double layer of H_2 and
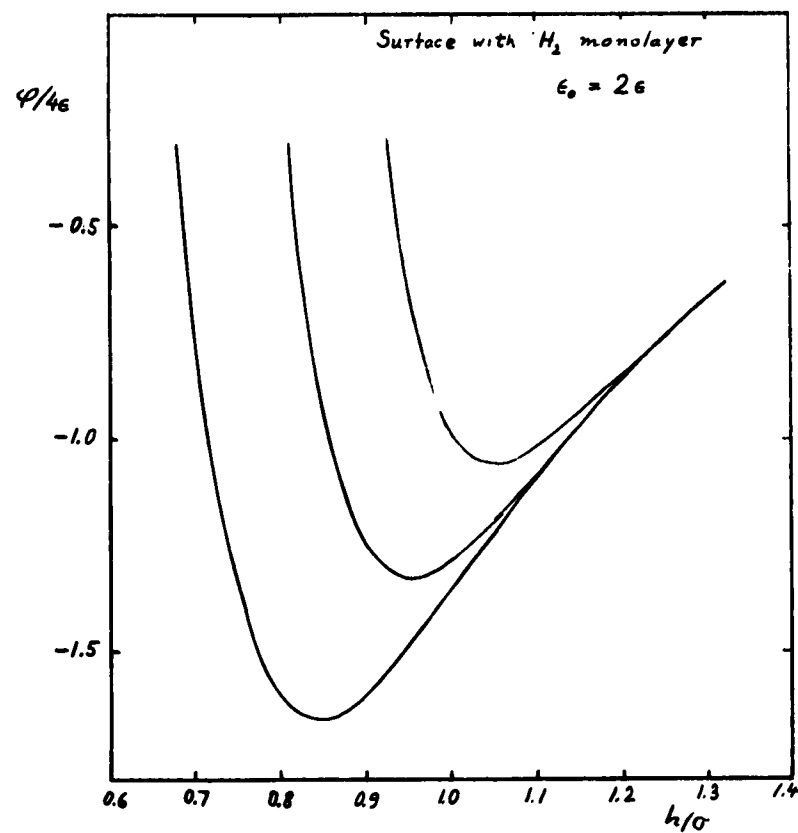
Fig. 14

The potential curves in case a are shown for
Various other values of the parameter ϵ_o
in Fig. 15.

Surface with H_2 monolayer
Case A

$\varphi/4\epsilon$

$\epsilon_0 = 0$
$\epsilon_0 = \epsilon$
$\epsilon_0 = 2\epsilon$
$\epsilon_0 = 3\epsilon$
$\epsilon_0 = 4\epsilon$

h/σ
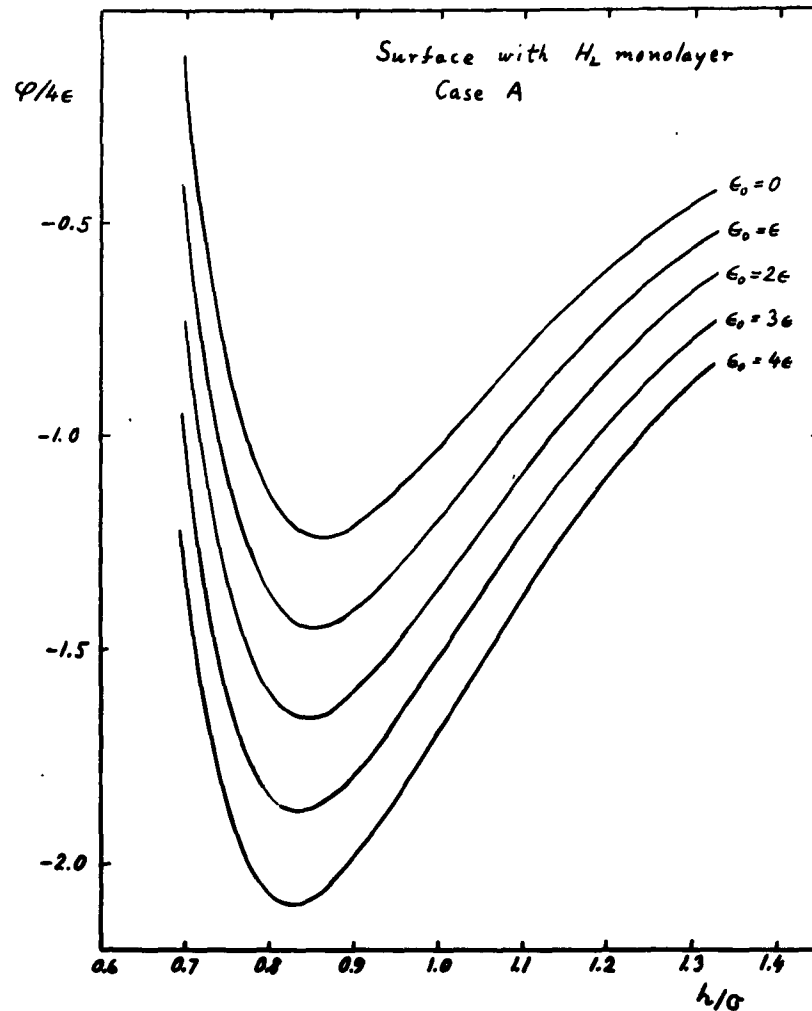
Fig. 15

Potential curves above a surface with an H_2 monolayer-
Case A

so on. However, the surface would then have to resemble
solid H_2 for which there are experimental results (from
vapor pressure data) for the binding energy. The concen-
tration Θ of H_2 on the surface of the interstellar grains
may be expected to vary with temperature in a manner similar

to that shown in Fig. 16 below.
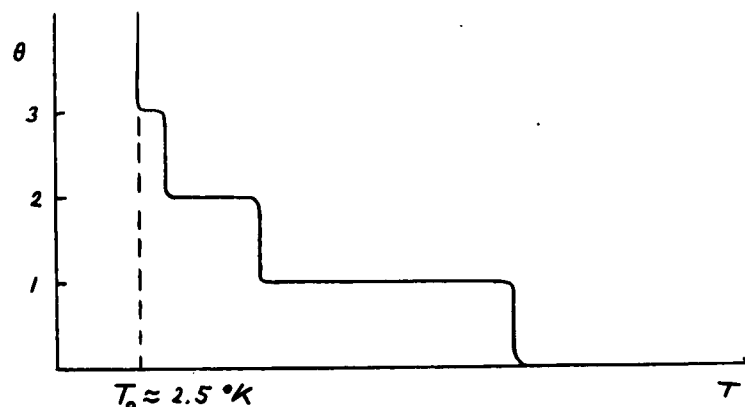
Fig. 16

Surface concentration as a function of temperature-
critical temperatures

Below $2.5^\circ K$, solid H_2 would grow.

(c) <u>Vibrational energy transfer on recombination</u> -
The critical temperatures below which a layer is formed
depend on the H_2 density in the surrounding gas although
not strongly. It will be shown later that one can expect
molecular densities in H I clouds comparable to that
of the atomic densities on the average. If, however, the
molecules which recombine on the surface of the grains do
not leave immediately but come to equilibrium with the
solid, then the density which determines T_c is that of
the <u>atomic</u> hydrogen. In previous papers on the subject,
it has generally been assumed that since on recombination
4.5 eV of excess energy is available, the molecule formed

will immediately leave the surface. This is not
necessarily the case. The 4.5 eV of excess energy is
vibrational energy and for the molecule to escape from
the solid, this internal energy must be transferred to
translational energy. Moreover, this energy transfer
would have to occur in roughly half the period τ_v of
vibration of the molecule. If we denote by M the mass
of the hydrogen atom and by $\overline{F}$ the mean force exerted on
the molecule by the crystal as the molecule vibrates, then
the average kinetic energy of translation which the
molecule acquires is

$$\overline{T} = \overline{p^2}/4M = \frac{\overline{(\int F \, dt)^2}}{4M} \sim \frac{\overline{F}^2 \tau_v^2}{16M} \qquad (82)$$

The mean force $\overline{F}$ can be taken to be (see Fig. 17)

$$\overline{F} \simeq -\overline{\frac{\partial \varphi}{\partial x}} \sim \varphi/\Lambda \quad . \qquad (83)$$
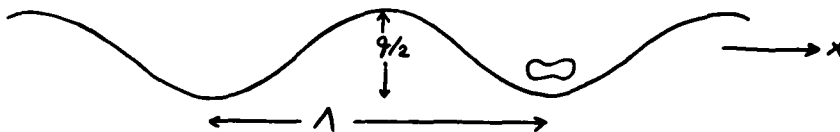
Fig. 17

Potential across a surface

We take the orientation of the molecule to be as shown in Fig. 17 since the recombination is likely to take place thru the mechanism u_1 (recombination between two atoms in the same layer). Clearly, $\overline{T}$ is to be compared with q. We get

$$\frac{\overline{T}}{q} \sim \frac{1}{16M} \left(\frac{\tau_v}{\Lambda}\right)^2 q \quad . \tag{84}$$

With $\tau_v \sim 10^{-15}$ sec, $\Lambda \simeq 3$ Å, $q \simeq 0.02$ eV, we get $\overline{T}/q \sim 10^{-6}$ which would seem to indicate that not enough energy is transferred for the molecule to escape from the solid. This reasoning is perhaps a bit pessimistic. It is conceivable that in the recombination process during which the atoms are attracting themselves by the strong valence force of the singlet state, the energy transfer to the solid (Debye phonon) necessary to form a bound system occurs while the two atoms are situated at, say, the mid-point between two equilibrium sites. As energy is transferred, the vibrational wave function for the molecule shrinks and the two atom system becomes more like a composite particle. Now, during the recombination the molecule is likely to be found at a height above the solid equal to the equilibrium h (for Case A). If the potential curve for Case C (midpoint between the equilibrium sites) is positive at this height, the molecule might then get enough kinetic energy (in sliding down the potential curve) to escape from the surface. However, as both Fig. 10 and

Fig. 14 show, curve C is negative at the equilibrium h
for curve A. For a more irregular surface, however, a
positive value is conceivable. Actually, it is quite
immaterial for the hydrogen molecule problem whether this
happens or not since if the H_2 layer does not form thru
atomic recombination, it will form because of the flux J_{H_2}
of H_2 molecules in the surrounding gas. As long as the
H_2 density is comparable to the atomic density, the value
of T_c can for all practical purposes be calculated using a
J for the atomic density. It may be well to point out
here that the relaxation time for forming a layer of
hydrogen is $\sigma_o/J \sim 100$ yr so that there is plenty of time
for a layer to build up. This time is, however, long
compared to the fraction of a second which an H-atom spends
on a grain before it encounters (on migration) another atom
to combine with.

While for the H_2 problem it does not matter whether
the molecules formed on the surface leave immediately or
not, it is crucial for the suggestion of McNally[30] that CH
can form on the interstellar grains that the CH molecule
should leave the surface immediately - if this molecule
would not evaporate at the particular value of temperature
which the grains have.

    5. The Recombination Coefficient at Low Temperatures -
It appears likely that the most important mechanism for H_2
formation on grains is by u_1 in which the surface atoms

which are held by van der Waals forces migrate about as a
two dimensional gas and occasionally encounter one another
to form a molecule. For the binding forces which were
calculated in the last section, it also appears that the
principle mechanism for this random walk process is that of
quantum mechanical barrier penetration. For values of the
periodicity Λ of about 3 Å and for barrier heights which
one would expect for van der Waals forces, one finds by
employing (75) that $\langle e^{-t} \rangle \equiv D_0 \sim 10^{-2}$. The inequality
(56), which is to be satisfied if γ is close to unity,
becomes, when $U \to u_d$,

$$\sqrt{\frac{2\sigma_0 \, \nu_0^{(a)}}{J \, D_0}} \; e^{-q^{(a)}/kT} \ll 1 \quad , \tag{85}$$

where the superscript (a) means that the parameters for
hydrogen <u>atoms</u> are to be used. On the other hand, (77)
gives a condition to be satisfied if a molecular layer is
not to form (that is, if the molecules formed are to be
able to evaporate from the surface). This condition is

$$\frac{\sigma_0 \, \nu_0^{(m)}}{J} \; e^{-q^{(m)}/kT} \gg 1 \tag{86}$$

where the superscript (m) stands for <u>molecule</u>. For inter-
stellar densities, $J \sim 3 \times 10^5$ cm^{-2} sec^{-1}, and substituting
$\nu_0^{(a)} \approx \nu_0^{(m)} \approx 10^{13}$ sec^{-1}, $\sigma_0 \approx 10^{15}$ cm^{-2}, (85) and (86)
give essentially

$$e^{2q^{(a)}/kT} \gg \varkappa/D_o \sim 10^{24} \tag{87}$$

$$e^{q^{(m)}/kT} \ll \varkappa \sim 10^{22} \quad , \tag{88}$$

where as defined earlier,

$$\varkappa \equiv \sigma_o \, \nu_o/J \quad . \tag{89}$$

These inequalities put limits on the value which the temperature T of the interstellar grains can have if the recombination coefficient is to be close to one, the limits being

$$T_c < T < T_m \quad , \tag{90}$$

where

$$T_m \simeq \frac{q^{(a)}}{2.3 \times 12 \ k} \quad , \tag{91}$$

$$T_c \simeq \frac{q^{(m)}}{2.3 \times 22 \ k} \quad . \tag{92}$$

Physically, what the inequality (90) means is that the grains must be hot enough so that an additional layer of H_2 must not form (in other words, that the H_2 will evaporate off) and cold enough so that the atoms which stick momentarily to the grain surface find another atom to recombine with before they, the atoms, evaporate off. An inequality like (90) must hold for each layer of adsorbed H_2. That is, at higher temperatures where there is a bare

58.

surface there will be a particular range of temperature in
which $\gamma \longrightarrow 1$, and also at lower temperatures where there
will be a monolayer of H_2 on the surface, a different
(because of the different binding energies involved) range
of temperature will exist where $\gamma \longrightarrow 1$. The results of the
calculation of T_c and T_m and hence of the recombination
coefficient are presented in Fig. 18 which shows the
temperature dependence of γ for various values of ϵ_o (ϵ_o
and ϵ were defined earlier).
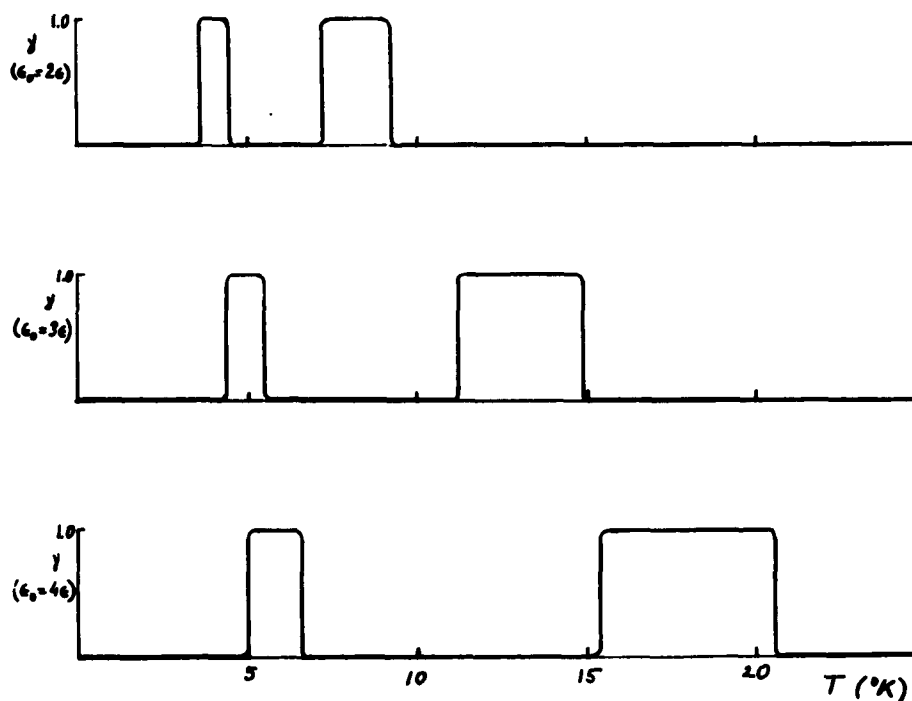
Fig. 18

Recombination coefficient as a function of surface
temperature

We see that at high grain temperatures, where recombination would occur on the bare surface, the range of temperature where $\gamma \rightarrow 1$ is quite strongly dependent on the interaction parameter ϵ_0. However, at lower temperatures where there is an H_2 layer upon which recombination takes place, the range of temperature where $\gamma \rightarrow 1$ is rather weakly dependent on ϵ_0. This is to be expected, since the binding energies (which determine T_c and T_m are due mostly to the interaction with the top layer. It might be mentioned that the recombination on a _second_ layer of H_2 at even lower temperatures can be neglected, since such a surface would be very similar to that of solid H_2 and the molecules formed would remain on the surface as succeeding layers formed.

It is significant that the recombination coefficient for the idealized case of a uniform surface has maxima within the expected temperature range of the grains of $5-20^{\circ}K$. Since the grains are likely to have a distribution of sizes and so a distribution of temperatures, the width of the maxima will be increased. Moreover, irregularities in the surfaces of the grains will smear out the regions where $\gamma \rightarrow 1$ so that the effective recombination coefficient will probably not be reduced to very low values anywhere within the temperature range $5-20^{\circ}K$.

6. Effects of Radiation

So far we have neglected the effects of photo-detachment of atoms (and molecules) from the surface of the grains by the interstellar radiation field. We shall see that the radiation field can produce quite different results depending on the surface condition of the grains. The effects of radiation on the atoms which are momentarily bound on the surface (or on the H_2 monolayer) are negligible. These atoms migrate about and quickly recombine and escape from the surface in a time short compared with the characteristic time for interaction with the interstellar radiation field. Consider, however, the effects of the photon flux on the surface atoms of the grains. If the grains do not have an H_2 monolayer, these atoms (which are held by valence forces) can escape from the surface if the photons induce a transition from a bonding to an anti-bonding orbital of the atom-solid system. This is the most efficient mechanism for photodetachment, since the "vibrational overlap factor" is unity. The number of photodetached atoms per cm^2 per sec is then given by

$$u_p = \sigma_0 \tau_\gamma^{-1} , \qquad (93)$$

where τ_γ^{-1} is the rate constant (in sec^{-1}) for the photo-detachment of a single hydrogen atom (we assume that the surface bond is to an H-atom). It can be estimated from equation (136) of section IIIA with an additional factor

1/2 due to the fact that the atoms on the surface of the
grains can receive galactic radiation only from a solid
angle 2π instead of 4π. Thus, we estimate τ_γ^{-1} from

$$\tau_\gamma^{-1} = \frac{\alpha \lambda^3 e_\lambda f}{4 \ mc} \ .$$ (94)

If $u_p < J$, the atoms which strike the surface will,
on migration, fill the vacant sites. If the recombination
coefficient is unity in the absence of the interstellar
radiation field, it will then be, clearly,

$$\gamma = 1 - u_p/J \ .$$ (95)

If $u_p > J$, all the atoms which strike the surface will be
used in filling the vacated (by photodetachment) sites and
the recombination coefficient will go to zero.

If the surface has a monolayer of (van der Waals)
adsorbed H_2 molecules on top of which recombination occurs,
the mechanism for photodetachment is slightly different.
Here the _molecules_ can be ejected if they make a transition
to a state in which the van der Waals forces between the
molecule and surface atoms are repulsive so that the mole-
cules are repelled from the surface. Here, however, the
radiation field has an effect on the recombination
coefficient only if the temperature of the grains is such
that $\gamma \rightarrow 0$ in the absence of the radiation field (in other
words, the region between the maxima in Fig. 18). The
interesting result is that the radiation flux _increases_ the

recombination coefficient. It does so by ejecting molecules
which would otherwise stay on the surface because the grains
are too cold to evaporate them. The recombination
coefficient in this region is, instead of zero,

$$\gamma = \begin{cases} 2u_p'/J & 2u_p' < J \\ 1 & 2u_p' > J \end{cases} \qquad (96)$$

The rate constant u_p' would be calculated from the same
expression (94).

The overall effect of radiation can be summarized in
Figs. 19a, 19b, and 19c below. γ_0 denotes the value of the
recombination coefficient in the absence of the radiation
field.
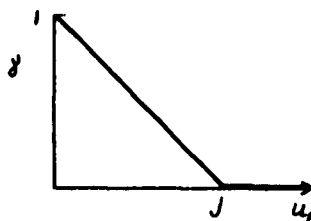
Fig. 19a

Recombination coefficient as a function of
photodetachment rate: (a) Bare surface,
$\gamma_0 = 1$
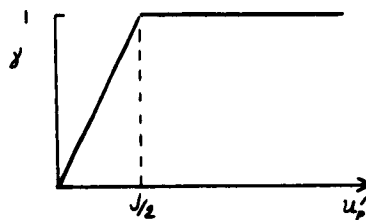
Fig. 19b

H_2 covered surface, $\gamma_o = 0$
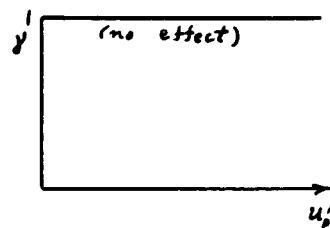
Fig. 19c

H_2 covered surface, $\gamma_o = 1$

It is difficult to estimate u_p (or u_p') for the grains without knowing the chemical properties of their surface. If we take a wavelength of 1000 Å and an oscillator strength of 0.1, we find, using a spectral energy density factor e_λ from the work of Lambrecht,[31] $u_p \sim 5 \times 10^4$ cm^{-2} sec^{-1}. This rate is still smaller than J ($\simeq 3 \times 10^5$ cm^{-2} sec^{-1}) but not much smaller, and it is conceivable that in regions of the galaxy where the radiation field is strong the effects of radiation are important. Moreover, if the predominant temperature of the grains lies where $\gamma_o = 0$, the radiation field can produce a finite recombination coefficient.

For the case of a bare surface which exists for high grain temperatures, perhaps if the hydrogen atoms are adsorbed thru a bond involving a carbon atom or ion the calculations of the photodissociation rate of CH and CH$^+$ by Bates and Spitzer[32] are pertinent. They find the rate constants for photodissociation by galactic radiation to be:

Process	Rate constant (τ_γ^{-1})
CH $+\ \gamma \rightarrow$ C + H	1.5×10^{-11} sec^{-1}
CH$^+ + \gamma \rightarrow$ C$^+$ + H	5×10^{-13} sec^{-1}.

These rate constants for the case of an atom adsorbed on the surface of the grains should be halved for the reason previously discussed (solid angle 2π). The resulting u_p's are:

$$(u_p)_{CH} \simeq 7 \times 10^3 \text{ cm}^{-2} \text{ sec}^{-1}$$

$$(u_p)_{CH+} \simeq 2.5 \times 10^2 \text{ cm}^{-2} \text{ sec}^{-1}$$

which are smaller than J by almost two orders of magnitude.

C.   Alternate Mechanisms

Here we consider a number of other mechanisms for molecule formation. We shall see that these mechanisms are only capable of producing molecular densities which are much smaller than that resulting from the catalytic reaction on grain surfaces. Nevertheless, these alternate mechanisms can usually be understood better than the grain recombination reaction and it is important to consider them, especially if the grains should turn out to be of a vastly different nature than presently thought.

1.   Chemical Exchange Reactions

Herzberg[33] has enumerated a number of exothermic reactions of the form AB + C $\longrightarrow$ AC + B which produce H_2. The activation energies for these reactions may be estimated from the semi-emperical relation

$$A = 0.055 \ D_{AB} \tag{97}$$

due to Hirschfelder (D_{AB} is the dissociation energy of the molecule AB). Four such reactions are given below along with their associated activation energies calculated from (97).

Reaction				A
(i)	$CH + H$	$\rightarrow$	$C + H_2$	0.19 eV
(ii)	$CH^+ + H$	$\rightarrow$	$C^+ + H_2$	0.20 eV
(iii)	$NH + H$	$\rightarrow$	$N + H_2$	0.21 eV
(iv)	$OH + H$	$\rightarrow$	$O + H_2$	0.24 eV

The reaction rate of, say, (i) would be roughly given by

$$\dot{n}_{H_2} \simeq n_{CH}\, n_H\, \sigma_{coll}\, \bar{v}\, e^{-A/kT} \quad , \tag{98}$$

where σ_{coll} is the collision cross section and $\bar{v}$ is the mean velocity of the H-atoms. With $T = 100°K$, $A/kT \simeq 22$, and the factor $e^{-A/kT}$ makes the reaction rate extremely small. With $T = 1000°K$, however, we get, using $n_{CH} = 10^{-7}$, $n_H = 10$ cm^{-3}, $\sigma_{coll} = 10^{-16}$ cm^2, and $\bar{v} = 3 \times 10^5$ cm/sec,

$$\dot{n}_{H_2} \simeq 3 \times 10^{-19} \text{ cm}^{-3} \text{ sec}^{-1}.$$

Such high temperatures can be produced in inelastic cloud-cloud collisions and while there is some question as to whether magnetic fields might prevent the inelastic collisions (and high temperatures), we shall consider the case where the clouds are heated. The clouds, after being heated to about $3000°K$, quickly cool down. The rate of cooling is proportional to the H_2 concentration in the cloud and the time to cool to, say, $500°K$ (see Fig. 33 of section IVC2) is about $2 \times 10^{9+p}$ sec, where $p = \log(n_H/n_{H_2})$. In this section we shall be dealing with moderate H_2

concentrations and shall take p = 4 and so a time

$\tau_h = 2 \times 10^{13}$ sec during which the cloud stays heated.

This time is so long that essentially all of the CH would

undergo the chemical reaction to produce H_2. If n_{CH} is

the CH density before the cloud collision (roughly equal

to the observed density 10^{-7} cm^{-3}) and Z ($\sim 10^{-14}$ sec^{-1})

is the collision frequency of the clouds, the rate of H_2

formation thru this mechanism would be

$$\dot{n}_{H_2} = Z\, n_{CH} \simeq 10^{-21} \text{ cm}^{-3} \text{ sec}^{-1} \quad . \tag{99}$$

Consideration of reactions (ii), (iii), and (iv) leads to

similar results.

2. **Reactions Involving H_2^+**

  (a) $\underline{H_2^+ + H \quad H_2 + p}$ - This reaction might also

be classified as a chemical exchange reaction. It is

exothermic by almost 2 eV and could conceivably be very fast

if the activation energy is small ((97) gives A = 0.15 eV).

The rate of formation of H_2 in this manner can be written as

$$\dot{n}_{H_2} = \alpha_e\, n_H\, n_{H_2^+} \tag{100}$$

The problem is that of the formation of H_2^+ which can be

formed either by ionization of H_2 by cosmic rays (p + $H_2 \longrightarrow$

H_2^+ + p + e) or by radiative association of a proton and

a hydrogen atom (p + H $\longrightarrow H_2^+ + \gamma$). The H_2^+ is very likely

to be destroyed by dissociative recombination ($H_2^+ + e \longrightarrow 2H$).

The rate of destruction of H_2^+ in this manner can be written as

$$\dot{n}_{H_2^+} = -\alpha_{dr}\, n_e\, n_{H_2^+} \quad , \tag{101}$$

where the rate constant α_{dr} is likely to be quite large[34] $(\sim 10^{-7}\ cm^3\ sec^{-1})$ since the process does not involve the emission of a photon. The coulomb attraction between the electron and molecular ion also makes the cross section very large. If H_2^+ is formed principally by ionization of H_2 by cosmic rays and suprathermal particles (rate constant τ_{si}^{-1}, see section IIIC3), the equilibrium concentration will be

$$n_{H_2^+} = \frac{n_{H_2}}{n_e} \frac{\tau_{si}^{-1}}{\alpha_{dr}} \quad . \tag{102}$$

If the molecular ion is formed by the recombination $H + p \rightarrow H_2^+ + \gamma$, the equilibrium concentration would be

$$n_{H_2^+} = \frac{n_H\, n_p}{n_e} \frac{\gamma_5}{\alpha_{dr}} \tag{103}$$

Here γ_5 is the rate constant for the radiative association of H_2^+ and has been calculated by Bates[35] (who used the notation γ_5) for temperatures from $500^\circ K$ to $64,000^\circ K$. Several values are listed below

T	γ_5
$500^\circ K$	1.3×10^{-18} cm^3 sec^{-1}
1000	5.2×10^{-18}
2000	1.9×10^{-17}
4000	6.2×10^{-16}

The recombination involves a downward transition between the two states of H_2^+ shown in Fig. 20.
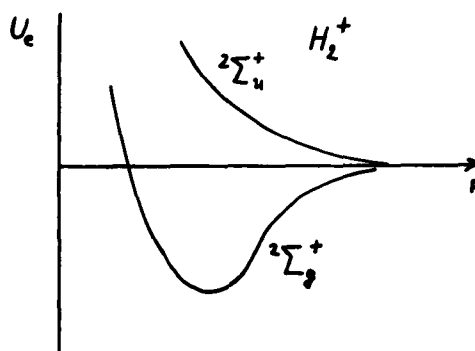
Fig. 20

Potential curves for lowest states of H_2^+

At low temperatures most of the transitions occur at large R where the transition probability is small. This is the main reason for the strong decrease in γ_5 with decreasing temperature.

In calculating the rate of formation of H_2 by (100) one should use the expression (103) for the H_2^+ concentration since, although the $n_{H_2^+}$ given by (102) may be larger, it arises from the destruction of a hydrogen molecule, and we

are concerned with the effective rate of <u>formation</u> of H_2.
Thus we get by substituting (103) into (100):

$$\dot{n}_{H_2} = \frac{n_H^2 \, n_p}{n_e} \, \alpha_e \, \frac{\gamma_5}{\alpha_{dr}} \quad . \tag{104}$$

The proton concentration n_p arises from the ionization of
hydrogen atoms by cosmic rays (and suprathermal particles)
and from electron captures in excited states (rate constant
$\overline{\sigma_p v}$, see section IVA2) and is given by

$$n_p = \frac{n_H}{n_e} \, \frac{\tau_{si}^{-1}}{\overline{\sigma_p v}} \quad . \tag{105}$$

Inserting this into (104) we have

$$\dot{n}_{H_2} = \frac{n_H^3}{n_e^2} \, \alpha_e \, \frac{\gamma_5}{\alpha_{dr}} \, \frac{\tau_{si}^{-1}}{\overline{\sigma_p v}} \quad . \tag{106}$$

Since γ_5 is very small at low temperature, H_2 can form thru
this chain of processes only if the clouds are heated. We
can estimate the effective rate by setting γ_5 equal to its
value $\overline{\gamma}_5$ at, say, $1000^\circ K$ and by multiplying (106) by $Z \, \tau_h$
(essentially the fraction of the time that the cloud is
heated). Thus we have, finally,

$$\dot{n}_{H_2} = \frac{n_H^3}{n_e^2} \, \alpha_e \frac{\gamma_5}{\alpha_{dr}} \, \frac{\tau_{si}^{-1}}{\overline{\sigma_p v}} \, Z\tau_h \quad . \tag{107}$$

The value of the rate constant τ_{si}^{-1} is very uncertain although upper and lower limits can be established. It will be shown later on in this work that these limits are

$$5 \times 10^{-19} \ \text{sec}^{-1} < \ \tau_{si}^{-1} < 10^{-15} \ \text{sec}^{-1} \quad .$$

If the cosmic ray flux is anywhere near the upper limit given above, the electron (and proton) densities in H I clouds will be very high and will be given by

$$n_e = \sqrt{n_H \frac{\tau_{si}^{-1}}{\overline{\sigma_p v}}} \tag{108}$$

instead of by the usually quoted value of $2 \times 10^{-4} \ n_H$ corresponding to the cosmic abundance of atoms capable of being ionized by photons of energy < 13.6 eV. If (108) is substituted into (107), we get

$$\dot{n}_{H_2} = n_H^2 \ \alpha_e \ \frac{\gamma_5}{\alpha_{dr}} \ Z \ \tau_h \tag{107'}$$

which is independent of the value of the cosmic ray flux. Substituting the values $n_H = 10 \ \text{cm}^{-3}$, $\alpha_e/\alpha_{dr} \sim 10^{-3}$ (a rough estimate), $\overline{\gamma}_5 = 5 \times 10^{-18} \ \text{cm}^3 \ \text{sec}^{-1}$, and $Z \ \tau_h = 0.2$ we obtain a rate

$$\dot{n}_{H_2} \sim 10^{-19} \ \text{cm}^{-3} \ \text{sec}^{-1} \quad .$$

On the other hand, if we take the lower limit $\tau_{si}^{-1} = 5 \times 10^{-19} \ \text{sec}^{-1}$, $n_e = 2 \times 10^{-3} \ \text{cm}^{-3}$, $\overline{\sigma_p v} = 10^{-12} \ \text{cm}^3 \ \text{sec}^{-1}$ (the approximate value at 1000°K), and the values just

given for the other parameters, we get from (107) the same rate $\dot{n}_{H_2} \sim 10^{-19}$ cm^{-3} sec^{-1}! This results because the electron density produced by cosmic rays, even for their minimum flux, is approximately the same as the figure 10^{-4} n_H which arises from the atoms with ionization potential less than 13.6 eV.

(b) <u>Radiative capture</u> - The rate constant for the recombination reaction (first suggested as a mechanism for H_2 formation by Herzberg[33])

$$H_2^+ + e \rightarrow H_2 + \gamma$$
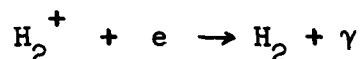
can be estimated to within a factor of about 2. It is given by

$$\overline{\sigma v} = \sum_{n'} \sum_{v'} \int \sigma_{n'v'}(v) \, v \, f(v) \, dv \quad , \qquad (109)$$

where the summation is over all electronic (n') and vibrational (v') states of the H_2 molecule and the integration is over the velocity distribution of the electrons. We neglect rotational fine structure. The cross section $\sigma_{n'v'}$ has been neither calculated nor measured. The cross section for the reverse reaction, that is, the photo-ionization reaction

$$\gamma + H_2 \longrightarrow H_2^+ + e$$

has been measured by Lee and Weissler.[36] The measurements are not very accurate, however, since it is difficult to

separate the absorption continuum due to ionization form

that due to dissociation. The experimental cross section

is sketched below (see also Appendix A).
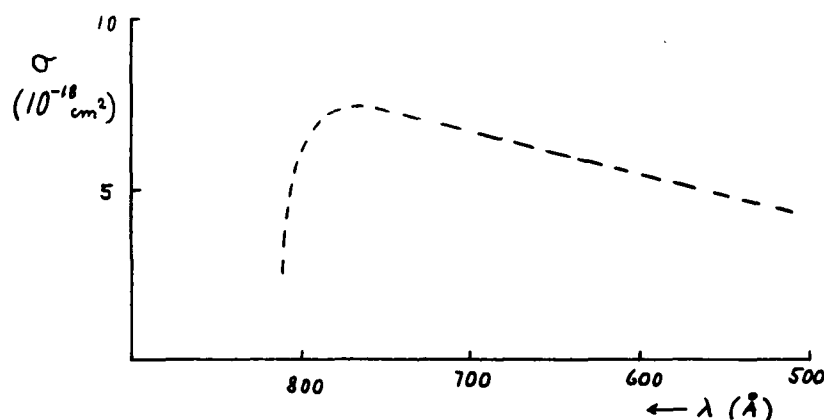
Fig. 21

Photoionization cross section of H_2

The edge at $\hbar\omega = 15.4$ eV corresponding to photoionization

from the ground electronic and vibrational state of H_2 to

the ground electronic and vibrational state of H_2^+. If we

denote the cross section for photoionization by σ_{AB} and

the cross section for radiative capture between the same

energy states by σ_{BA}, we have a straightforward application

of the principle of detailed balance

$$\frac{\sigma_{AB}}{\sigma_{BA}} = \frac{1}{2} \left(\frac{mcv}{\hbar\omega}\right)^2 . \tag{110}$$

We have omitted the ratio of the degeneracies which is unity.

The relation between ω and v is

$$\hbar\omega = E_{e''} - E_{e'} + E_{v'';e''} - E_{v';e'} + \tfrac{1}{2}mv^2 \quad , \quad (111)$$

where E_e denotes electronic energy and $E_{v;e}$ vibrational
energy of the respective molecules. The experimental cross
section σ_{BA} is, of course, that for the ground electronic
state E_{e_0} of H_2. We can obtain an approximate expression
for the rate constant (109) by considering only recombina-
tions to this ground electronic state. Since we are con-
sidering low temperatures where $\tfrac{1}{2}mv^2 \ll E_{e''} - E_{e'}$, and since
the vibrational energies are much smaller than the
electronic energies, we can set ω in (111) equal to ω_0 (the
threshold frequency). Substituting σ_{BA} ($= \sigma_{n'v'}(v)$) from
(110) into (109), we have

$$\overline{\sigma\, v} = 2 \sum_{v'} \int \sigma_{AB} \left(\frac{\hbar\,\omega_0}{m\ cv}\right)^2 v\ f(v)\ dv \quad . \quad (112)$$

We now make use of the Franck-Condon principle (see Appendix
A) which tells us that the cross section for radiative
processes like the one we are considering is proportional
to an electronic factor and a vibrational overlap factor
$|\langle v'|v''\rangle|^2$. We can then make use of the vibrational sum
rule

$$\sum_{v'} |\langle v'|v''\rangle|^2 = \sum_{v''} |\langle v''|v'\rangle|^2 = 1 \quad (113)$$

by employing this in (112). We then choose a value of the
cross section σ_{AB} where the photon energy is large enough
that transitions can occur to essentially all vibrational

states v' so that (113) can be applied. Such photon energies occur already around 700 $\overset{\text{o}}{\text{A}}$ where the cross section from Fig. 20 is $\sum_{AB} \simeq 6 \times 10^{-18}$ cm^2. Substituting this cross section into (112) and carrying out the integration over v using

$$f(v) = 4\pi \ (m/2\pi \ kT)^{3/2} \ v^2 \ e^{-mv^2/2kT} \quad , \quad (114)$$

we find

$$\overline{\sigma \ v} \simeq (\frac{\hbar \ \omega_0}{m \ c})^2 \ \sqrt{\frac{8 \ m}{\pi kT}} \ \sum_{AB} \quad (115)$$

To calculate the rate of formation of H_2 by radiative capture we again determine the "effective" H_2^+ concentration by (103) and (105) so that we have

$$\hat{n}_{H_2} = \frac{n_H^2}{n_e} \ \frac{\tau_{si}^{-1}}{\overline{\sigma_p' \ v}} \ \frac{\gamma_5}{\alpha_{dr}} \ \overline{\sigma \ v} \quad (116)$$

Once again, because of the strong temperature dependence of γ_5, we require the clouds to be heated and replace γ_5 by its value at 1000°K and introduce a factor $Z \ \tau_h$ as in (107). Thus,

$$\dot{n}_{H_2} = \frac{n_H^2}{n_e} \ \frac{\tau_{si}^{-1}}{\overline{\sigma_p' \ v}} \ \frac{\overline{\gamma_5}}{\alpha_{dr}} \ \overline{\sigma \ v} \ Z\tau_h \quad . \quad (117)$$

Here one gets the largest rate with a high cosmic ray rate constant. Taking the upper limit $\tau_{si}^{-1} = 10^{-15}$ sec^{-1} we find

$$\dot{n}_{H_2} \leq 5 \times 10^{-22} \ \text{cm}^{-3} \ \text{sec}^{-1} \quad ,$$

states v' so that (113) can be applied. Such photon energies occur already around 700 $\overset{o}{A}$ where the cross section from Fig. 20 is $\sum_{AB} \simeq 6 \times 10^{-18}$ cm^2. Substituting this cross section into (112) and carrying out the integration over v using

$$f(v) = 4\pi \ (m/2\pi \ kT)^{3/2} \ v^2 \ e^{-mv^2/2kT} \quad , \qquad (114)$$

we find

$$\overline{\sigma \ v} \ \simeq \ (\frac{\hslash \ \omega_o}{m \ c})^2 \ \sqrt{\frac{8 \ m}{\pi kT}} \ \sum_{AB} \qquad (115)$$

To calculate the rate of formation of H$_2$ by radiative capture we again determine the "effective" H$_2{}^+$ concentration by (103) and (105) so that we have

$$n_{H_2} \ = \ \frac{n_H^2}{n_e} \ \frac{\tau_{si}^{-1}}{\overline{\sigma_p' \ v}} \ \frac{\gamma_5}{\alpha_{dr}} \ \overline{\sigma \ v} \qquad (116)$$

Once again, because of the strong temperature dependence of γ_5, we require the clouds to be heated and replace γ_5 by its value at 1000°K and introduce a factor Z τ_h as in (107). Thus,

$$\dot{n}_{H_2} \ = \ \frac{n_H^2}{n_e} \ \frac{\tau_{si}^{-1}}{\overline{\sigma_p' \ v}} \ \frac{\overline{\gamma_5}}{\alpha_{dr}} \ \overline{\sigma \ v} \ Z\tau_h \quad . \qquad (117)$$

Here one gets the largest rate with a high cosmic ray rate constant. Taking the upper limit $\tau_{si}^{-1} = 10^{-15}$ sec^{-1} we find

$$\dot{n}_{H_2} \ \leq \ 5 \times 10^{-22} \ cm^{-3} \ sec^{-1} \quad ,$$

while the lower limit $\tau_{si}^{-1} = 5 \times 10^{-19}$ sec^{-1} gives

$$\dot{n}_{H_2} \simeq 5 \times 10^{-24} \text{ cm}^{-3} \text{ sec}^{-1} .$$

3. Associative Detachment

The reaction

$$H^- + H \longrightarrow H_2 + e \quad ,$$
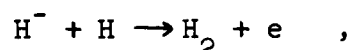
called "associative detachment", has been considered by Pagel for its role in the solar atmosphere and more recently by McDowell[37] for the interstellar H I clouds. The rate of formation of H_2 by this mechanism would be given by

$$n_{H_2} = \alpha_{ad} \, n_H \, n_{H^-} \quad , \tag{118}$$

where α_{ad} is the rate constant. The H$^-$ concentration is determined by photodetachment (rate constant $\tau_{\gamma d}^{-1}$) and radiative association (rate constant $\alpha_{a\gamma}$) and is given by

$$n_{H^-} = \frac{\alpha_{a\gamma}}{\tau_{\gamma d}^{-1}} \, n_H \, n_e \quad . \tag{119}$$

Substitution of this expression into (118) gives

$$\dot{n}_{H_2} = \frac{\alpha_{ad} \, \alpha_{a\gamma}}{\tau_{\gamma d}^{-1}} \, n_H^{\,2} \, n_e \quad . \tag{120}$$

McDowell estimates the rate constants α_{ad} and $\alpha_{a\gamma}$ to be

$$\alpha_{ad} = 1.2 \times 10^{-11} \, T^{1/2} \text{ cm}^3 \text{ sec}^{-1} \quad , \tag{121}$$

and

$$\alpha_{a\gamma} = 1.5 \times 10^{-17} \, T^{1/2} \, cm^3 \, sec^{-1} \quad , \qquad (122)$$

where T is the kinetic temperature. The rate constant $\tau_{\gamma d}^{-1}$ is more uncertain since it involves the interstellar radiation field. McDowell suggests a value $2 \times 10^{-7} \, sec^{-1}$. If we take the usual densities $n_H = 10 \, cm^{-3}$, $n_e = 2 \times 10^{-3} \, cm^{-3}$ and a temperature of $100^{\circ}K$, we have from (120), (121), and (122)

$$\dot{n}_{H_2} \simeq 2 \times 10^{-20} \, cm^{-3} \, sec^{-1} \quad .$$

If, however, we take a higher electron density of $6 \times 10^{-2} \, cm^{-3}$ which one obtains from (108) using the upper limit $(10^{-15} \, sec^{-1})$ to the cosmic ray ionization rate constant we have

$$\dot{n}_{H_2} \simeq 6 \times 10^{-19} \, cm^{-3} \, sec^{-1} \quad .$$

D. Summary of Mechanisms

The expected rates for formation of H_2 under "normal" conditions $(n_H = 10 \, cm^{-3}, \, T = 100^{\circ}K)$ are summarized in Table 2 below.

Table 2

Mechanism	Rate $(\dot{n}_{H_2})$
$CH + H \longrightarrow H_2 + C$	10^{-21} cm^{-3} sec^{-1}
$H_2^+ + H \longrightarrow H_2 + p$	10^{-19}
$H_2^+ + e \longrightarrow H_2 + \gamma$	5×10^{-24} to 5×10^{-22}[*]
$H^- + H \longrightarrow H_2 + e$	2×10^{-20} to 6×10^{-19}[*]
$H + H\text{-}S \longrightarrow H_2 + S$ (surf. rec.)	4×10^{-15} $(\gamma = 1)$

[*] Depending on cosmic ray flux (or electron density)

We see that the rate of formation through the catalytic reaction on the surface of the interstellar grains can be much larger (by a factor $\gtrsim 10^4$) than that of any of the other mechanisms considered. However, we know really very little about the interstellar grains, especially their chemical composition. Moreover, the recombination coefficient for the grains is apparently strongly dependent on their temperature as was shown for the idealized case of a uniform surface. In spite of these uncertainties, it is the opinion of the writer that unless the grains have a structure vastly different from what we now believe them to have, the recombination coefficient is very likely to be between 0.1 and 1. For it was shown that for the idealized

case the recombination coefficient has maxima in the
expected temperature range of the grains of $5\text{-}20^{\circ}K$.
Irregularities in the surface of the grains are likely to
smear out considerably the interval of grain temperature
where $\gamma \longrightarrow 1$. Also, as was shown, the galactic radiation
field may help form molecules by ejecting them from the
surface of the grains when otherwise they would be held
indefinitely.

Some have suggested that the grains may have so-called
"active sites" on their surface which would gather up
hydrogen atoms easily and hold them strongly, but which
would readily give them up to other hydrogen atoms to form
molecules. This may well be the case if there are free
radicals on the surface. It is extremely difficult, however,
to estimate quantitatively such an effect. One can only
guess what fraction of the surface has such "active sites".
It is clear, though, that such an effect can only increase
the recombination coefficient.

While our lack of knowledge of the grains forces us to
make qualified predictions of the recombination rate of grain
surfaces, this is not so for all of the other reactions
listed in Table 2. The rates for the first three reactions
listed are esimtated on the assumption that the clouds are
heated periodically (in cloud-cloud collisions). However,
the associative detachment reaction $H^- + H \longrightarrow H_2 + e$ does
not require high temperatures but only that there are free

electrons around (which can attach themselves to hydrogen atoms). There is <u>certain</u> to be enough electrons to form H^-, even if the electrons must come from the ionization of hydrogen atoms by cosmic rays. Hence the associative detachment mechanism is completely understood and will produce H_2 if all other processes fail. Thus, while the catalytic reaction on grain surfaces provides us with an estimate of the <u>upper</u> limit to the rate of molecule formation, the rate calculated from the associative detachment process gives us a <u>lower</u> limit.

III. DISSOCIATIVE PROCESSES FOR A STATIC INTERSTELLAR MEDIUM

A. Photodissociation Through the Forbidden Transition
$${}^1\Sigma_g^+ \rightarrow {}^3\Sigma_u^+$$
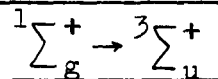
As a result of the high opacity of atomic hydrogen for photon energies beyond the Lyman limit (13.6 eV), the galactic radiation field in the interior of H I clouds suffers a sharp cutoff at 912 $\overset{o}{A}$. Because of this cutoff, one is led to consider processes involving radiation of wavelength $\lambda > 912$ $\overset{o}{A}$. The simplest of such processes is that of photodissociation thru the transition ${}^1\Sigma_g^+ \rightarrow {}^3\Sigma_u^+$ (see Fig. 1) which requires photon energies of only 8-10 eV. Kahn[38] and McCrea and McNally[17] considered this mechanism to be the main cause of the dissociation of H_2. The rate of dissociation can be written in terms of the photo-dissociation crossection $\sigma(\omega)$ and the photon flux dJ_ω as

$$(\dot{n}_{H_2})_{\gamma d} = n_{H_2} \int \sigma(\omega) \, dJ_\omega \tag{123}$$

$$= n_{H_2} \int \sigma(\omega) \, J_\omega \, d\omega \quad . \tag{124}$$

Since the crossection is peaked around a frequency ω_0, we can take J_ω out of the integral (124) and set it equal to

the value J_{ω_0} corresponding to the frequency ω_0 where $\sigma(\omega)$ is a maximum. Then we employ (A21) from Appendix A which gives the result

$$(\dot{n}_{H_2})_{\gamma d} = \tau_{\gamma d}^{-1}\, n_{H_2} \quad , \tag{125}$$

with

$$\tau_{\gamma d}^{-1} = J_{\omega_0}\, \frac{2\pi^2 e^2}{m\, c}\, \bar{f}_e \quad . \tag{126}$$

Denoting the ground state $(^1\Sigma_g^+)'$ by $|m'\rangle$ and the repulsive state $(^3\Sigma_u^+)'$ by $|n'\rangle$, the oscillator strength $\bar{f}_e$ would be given by

$$\bar{f}_e = \frac{2m}{3\hbar}\, \omega(R_0)\, \left|\langle n'|\, r\, |m'\rangle\right|^2 \quad , \tag{127}$$

where the wave functions are to be calculated at the equilibrium internuclear separation (R_0) of the ground state. The dipole operator is simply $r_1 + r_2$, where r_1 and r_2 are the (vector) position operators of the two electrons. The matrix element $\langle n'\,|\, r_1 + r_2|m'\rangle$ involves an integral over the position space of both electrons and a sum over spins. If $|m'\rangle$ were purely singlet and $|n'\rangle$ purely triplet, this matrix element would vanish because of the orthogonality of the spin wave functions. A similar result would be obtained for the matrix elements involved in magnetic dipole and quadrupole radiation. The vanishing of the matrix element results only from the assumption that the complete wave function can be written as a product of a

part describing the space properties of the state and a part describing the spin. It does not depend on the validity of the Born-Oppenheimer approximation (see Appendix A). That the total wave function can be written as a product of space and spin wave functions follows exactly if the Hamiltonian for the molecule contains no terms coupling the space and spin coordinates. Actually, there are such terms although they are small. Both the spin-spin and spin-orbit interaction terms are of this nature. Because of their presence, the ground state is not purely singlet but has a small triplet part. Similarly, the repulsive state is partly singlet. If we write the Hamiltonian for the molecule as

$$H = H_o + H' \quad , \tag{128}$$

where H_o contains all the terms not involving spin and H' is the part due to spin-spin and spin-orbit interactions $(H' = H'_{ss} + H'_{so})$, then we can estimate the amount of mixing of the wave functions. From simple perturbation theory,

$$|m'\rangle = |m\rangle + \sideset{}{'}\sum_{k} \frac{\langle k|H'|m\rangle}{E_m^{(o)} - E_k^{(o)}} |k\rangle + \ldots$$

$$\langle n'| = \langle n| + \sideset{}{'}\sum_{\ell} \frac{\langle n|H'|\ell\rangle}{E_n^{(o)} - E_\ell^{(o)}} \langle \ell| + \ldots \tag{129}$$

The states without the primes are the unperturbed states and the $E^{(o)}$'s are the unperturbed energies $(H_o|k\rangle = E_k^{(o)}|k\rangle)$.

The primes on the summation signs mean that the term $k = m$ in the first sum and $\ell = n$ in the second sum are omitted. Employing the expansions (129), we have for the dipole matrix element :

$$\langle n' \mid \mathbf{r}_1 + \mathbf{r}_2 \mid m' \rangle = \sum_k {}' \frac{\langle k \mid H' \mid m \rangle}{E_m^{(o)} - E_k^{(o)}} \langle n \mid \mathbf{r}_1 + \mathbf{r}_2 \mid k \rangle$$

$$\text{(130)}$$

$$+ \sum_\ell {}' \frac{\langle n \mid H' \mid \ell \rangle}{E_n^{(o)} - E_\ell^{(o)}} \langle \ell \mid \mathbf{r}_1 + \mathbf{r}_2 \mid m \rangle + \ldots .$$

The operators H'_{ss} and H'_{so} are similar to those for the helium atom[39] and their matrix elements are both of the order of magnitude $\alpha^2 \frac{e^2}{a_o}$, α being the fine structure constant. Since the energy denominators are of the order of e^2/a_o and the dipole matrix elements are of the order of a_o, we can expect a value of $\langle n' \mid \mathbf{r}_1 + \mathbf{r}_2 \mid m' \rangle$ of the order of $\alpha^2 a_o$. This gives an oscillator strength $\overline{f}_e \sim \frac{2 m \omega}{3 \hbar} (\alpha^2 a_o)^2$.

Setting $\hbar \omega \sim e^2/a_o$, we have, since $a_o = \hbar^2/m e^2$,

$$\overline{f}_e \sim \alpha^4 . \qquad \text{(131)}$$

This estimate is perhaps a little too high since we have assumed large matrix elements throughout. The correct value is probably between 10^{-10} and 10^{-8} but in any case it is considerably smaller than the value 10^{-5} used by Kahn and by McCrea and McNally. The associated rate constant $\tau_{\gamma d}^{-1}$ calculated from (126) will also be reduced accordingly.

The value of the interstellar spectral flux J_ω can be found from the work of Lambrecht[31] who gives the spectral distribution of the energy density as

$$\frac{de}{d\lambda} \equiv e_\lambda \quad .$$ (132)

The relation between e_λ and J_ω may be found from

$$dJ_\omega = c \frac{de}{\hbar\omega} = J_\omega \, d_\omega \quad ,$$ (133)

giving J_ω in terms of e_λ :

$$J_\omega = 2\pi \frac{\bar{\lambda}^3}{\hbar c} e_\lambda \quad ,$$

where

$$\bar{\lambda} \equiv \frac{\lambda}{2\pi} \quad .$$ (135)

Substituting (134) into (136) we have, since $\alpha = e^2/\hbar c$,

$$\tau_{\gamma d}^{-1} = \frac{\alpha \lambda^3 e_\lambda \bar{F}_e}{2 mc}$$ (136)

For the $^1\Sigma_g$ - $^3\Sigma_u$ transition, $\lambda \simeq 1500 \, \overset{\circ}{A}$, and using a corresponding e_λ from Lambrecht of $e_\lambda \simeq 7 \times 10^{-9}$ erg cm^{-4}, and an $\bar{F}_e$ of 10^{-9} we find

$$\tau_{\gamma d}^{-1} \simeq 3 \times 10^{-18} \text{ sec}^{-1}.$$

This rate constant is four orders of magnitude smaller than the value calculated by Kahn. We shall see that there are other processes which are much more effective in dissociating the molecule so that the $^1\Sigma_g$ - $^3\Sigma_u$ dissociative

transition can be neglected altogether.

B. **Resonance-Fluorescence and Raman Excitation**

   1. **Resonance-fluorescence**

   The edge for the photodissociation of H_2 thru an allowed transition occurs at 14.5 eV, that is, beyond the Lyman limit. This edge corresponds to a dissociation in which one of the H-atoms goes off in the first excited state (see Appendix A). The energy 14.5 eV is needed if the molecule is initially in the ground vibrational state. Since the energy difference between vibrational states is about 0.53 eV, a molecule in the second vibrational state would require photon energies less than 13.5 eV for photodissociation. This photon energy is below the Lyman limit and so should be present in the energy spectrum of the galactic radiation field. Thus, if there were some way in which the molecule could get into the second (or third, fourth, etc.) excited vibrational state, it could be dissociated by the galactic radiation field. The population of excited states by thermal means is negligible, since the excitation energy is much greater than kT ($\simeq$ 0.01 eV). However, there are two other mechanisms for the population of excited vibrational states which might be important and which are very interesting in themselves.

   The first such mechanism that we shall consider is that of resonance-fluorescence which can populate excited vibrational states in the following manner. The molecule

in the ground state absorbs a photon which causes a transition to an excited electronic state (e.g., the B or C state). After a time of the order of 10^{-8} seconds the molecule drops down to the ground electronic state. In this process any of the vibrational levels of the ground electronic state can be excited. (Actually, the vibrational continuum of the ground state can be excited in this manner although it is a very unlikely process, the vibrational overlap factors involved being very small.) The relative probability of a certain level v being excited depends only on the vibrational overlap factors involved. The vibrational levels are predominantly de-excited by quadrupole transitions which have a probability per unit time for spontaneous emission of about[16] $A \simeq 2 \times 10^{-7}$ sec^{-1}. If the rate constant (in sec^{-1}) for the excitation of the resonance lines is denoted by B, the relative population of the excited vibrational states would be

$$n_v/n_o \sim B/A \quad . \qquad\qquad (137)$$

If oscillator strengths of unity are taken for the resonance lines, we find by employing (136) with $\lambda \simeq 1000$ $\overset{o}{A}$ that $B \sim 10^{-9}$ sec^{-1}. This would produce a population of excited vibrational states of $n_v/n_o \sim 10^{-2}$ which would seem to imply that the process is extremely important as a dissociation mechanism (the rate constant for dissociation would then be roughly $B n_v/n_o \sim B^2/A \sim 10^{-11}$ sec^{-1}). However, the mechanism fails for the following reason. Because the

absorption coefficient is so high for the resonance lines, essentially all the H_2 in a cloud is shielded by self absorption from these lines. For example, with a density of $n_{H_2} \sim 1$ cm^{-3} and a path length of 1 pc, the optical depth in the resonance lines is of the order of 10^6. Thus, the molecular hydrogen is in a sense prevented from being photodissociated by its own self absorption.

One might wonder whether these resonance lines would eat their way thru the H_2 and thus dissociate the whole cloud. Actually, the time required for a resonance line to do this is likely to be very long, with roughly one characteristic time for dissociation needed for each optical thickness of H_2 which is dissociated. Moreover, one can treat the problem as a steady state one and calculate the radius of the sphere of dissociated hydrogen in a manner similar to that used to calculate the radii of ionized regions (see section IVA). When this is done one finds that in the steady state the resonance line penetrates only a very short distance into the cloud, even if the rates of formation of H_2 is much slower.

2. Raman scattering

Vibrational levels can also be excited by Raman scattering. However, the selection rule for the vibrational quantum number v in Raman scattering is $\Delta v = \pm 1$, so that a Raman population of the second excited vibrational state would involve a two step process. If we again denote the

spontaneous radiation transition probability per unit time for excited states by A and the transition probability per unit time for excitation by Raman scattering by B, we will have for the steady state population of excited states (n_o = density in ground state, n_1 = density in first excited state, etc.) :

$$n_1 = n_o \frac{B}{A}$$

$$n_2 = n_o \left(\frac{B}{A}\right)^2$$

. . (138)

. .

The rate constant B would be calculated from the (Stokes) Raman cross section σ_ω^{SR} by

$$B = \int J_\omega \, \sigma_\omega^{SR} \, d\omega \quad . \tag{139}$$

Since Raman scattering is a process whereby a photon is absorbed and re-emitted ("second order" process), its cross section is very small ($\sim 10^{-25}$ cm^2) except where there is a resonance at which the cross section is very large. However, since resonance Raman scattering occurs at the same frequencies as that of the resonance absorption lines which are optically thick, the contribution from resonance Raman scattering can be neglected.

We now consider the effects of <u>non-resonance</u> Raman scattering. Here the cross section can be written for practical purposes as

$$\sigma_\omega^{SR} \simeq \frac{8\pi}{3} \frac{\omega^4}{c^4} |\alpha'|^2 \quad . \tag{140}$$

α' is the so-called "derived polarizability" and is essentially given by $(\frac{\partial \alpha}{\partial R})_{R_0} \langle v| R - R_0 | v' \rangle$, that is, the product of the derivative of the polarizability with respect to the internuclear separation and the matrix element of the variation from the equilibrium distance. The order of magnitude of α' is roughly 0.1α where $\alpha \ (\sim a_0^3)$ is the polarizability.

To calculate B from (139), we shall take the interstellar radiation field to be that of a black body at $T_0 = 10^4 \, ^\circ K$ diluted by a factor $W \sim 10^{-14}$. Since the integrand in (139) is proportional to ω^6, we take the Wien approximation to the radiation formula. Further, since the maximum of the integral occurs around $\hbar \omega \sim 6 \, kT_0 \sim 6 \, eV$, we shall take the integration over ω to be from 0 to ∞, thus

$$B \simeq \frac{8\pi}{3} \frac{|\alpha'|^2}{\pi^2 c^6} W \cdot \int_0^\infty \omega^6 e^{-\hbar\omega/kT_0} d\omega$$

$$= \frac{1920}{\pi} W \frac{|\alpha'|^2}{c^6} (kT_0/\hbar)^7 \quad . \tag{141}$$

With $W = 10^{-14}$, $\alpha' \sim 10^{-25}$ cm^3, $T_o = 10^{4}$ °K, we get

$$B \sim 6 \times 10^{-19} \text{ sec}^{-1} \quad .$$

Thus, $B/A \sim 3 \times 10^{-12}$ and the fraction of molecules in the second excited vibrational state will be $\sim 10^{-23}$. This fraction is so small that the process can be completely neglected. It might be argued that near bright stars the radiation field will be much more intense and consequently the Raman process will be enhanced. However, it is difficult to conceive of an increase in B of more than about 3 orders of magnitude and it seems safe to say that the Raman process can be neglected altogether.

C. Cosmic Rays and Suprathermal Particles

1. Energy spectrum and low energy cut-off

Cosmic ray protons cause ionization (formation of H_2^+) of hydrogen molecules. Since these H_2^+ molecules are quickly dissociated either by photodissociation or by dissociative recombination (see section II-C), formation of H_2^+ can be considered equivalent to dissociation. Most of the data available on the cosmic ray flux is for energies > 10 BeV where the flux follows a power law spectrum[40] :

$$J(E) = \frac{dJ}{dE} = 0.46 \, E^{-2.15} \text{ particles/cm}^2/\text{sec/ster/BeV}$$
$$\text{interval.}$$

Here $E = T + Mc^2$ is the _total_ energy in BeV. At these high energies the ionization cross section is very small and so

the process $p + H_2 \longrightarrow H_2^+ + p + e$ can be neglected.
However, the cross section increases as the incident proton
energy is lowered, thus making the low energy cosmic rays
of prime importance. Magnetic fields in the solar system
prevent the observation of low energy cosmic rays, so that
considerations of the low energy flux must involve unverified
theory.

A Fermi-I type mechanism[41] for the acceleration of
protons predicts a power law spectrum $n(E) = K\ E^{-(\gamma + 1)}$
in the total energy E extending into the non-relativistic
region. In this mechanism the protons, in encountering
random "magnetic clouds", increase their energy at a rate

$$\frac{dE}{dt} = \alpha\ E \quad . \tag{142}$$

α is proportional to the velocity of the protons and we
write it as

$$\alpha = \alpha_o \frac{v}{c} \quad . \tag{143}$$

If the protons are lost by proton-proton collisions which
have a cross section independent of velocity, it may easily
be shown that a power law spectrum in the total energy results
for the non-relativistic region as well as for the
relativistic region. Thus, if the protons are accelerated
by this type of mechanism we should expect the non-
relativistic spectrum $n(E \simeq Mc^2)$ to be flat. However, the
energy spectrum of the flux should not be flat since it is

essentially v n(E) where v is the particle velocity. We should thus expect an energy distribution in the flux to go as $T^{1/2}$, the spectrum being as below (Fig. 22).
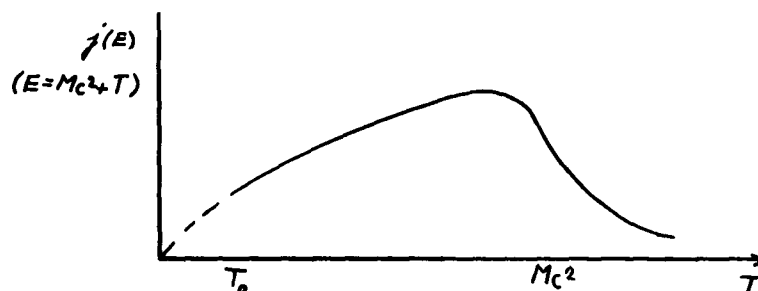
Fig. 22

Cosmic ray flux predicted by a fermi-type acceleration process

There should be a low energy cut-off to the spectrum at an energy T_o where the rate of energy gain thru acceleration by the Fermi mechanism equals the rate of energy loss thru ionization. The ionization loss for protons traversing atomic hydrogen regions of various degrees of ionization has been calculated by Hayakawa and Kitao.[42] They present curves for $dT/d(\rho x)$, where ρ is the density and x the path length. The cut-off energy T_o would occur where

$$- \left(dT/d(\rho x)\right)_{ioniz.} = \left(dE/d(\rho x)\right)_{Fermi} = \frac{1}{\rho} \frac{v}{v} \frac{v}{c} \alpha_o Mc^2 = \frac{\alpha_o Mc}{\rho}.$$

(144)

Taking the value $\alpha_o = 10^{-17}$ sec^{-1} recommended by Ginzburg[43] and a density $\rho \sim 10^{-26}$ gm/cm^3 corresponding to the galactic

halo, we find $(dE/d(\rho x))_{Fermi} \approx 30$ MeV/gm-cm^{-2}. One finds using curve C (50% dissociated hydrogen) of Hayakawa and Kitao's Fig. 1, that a cut-off would occur at $T_o \approx 100$ MeV.

2. Ionization rate constant

The cross section for ionization of a hydrogen molecule by a high energy non-relativistic proton of kinetic energy T is of the form[44]

$$Q = \frac{A}{T} \ln \frac{T}{B} \quad . \tag{145}$$

For a flat energy density spectrum $n(E) = n(Mc^2) =$ constant, the rate constant for ionization would be

$$\tau_{ci}^{-1} \simeq C \int_{T_o}^{Mc^2} \frac{v}{c} Q(T) \, dT \simeq 2^{3/2} C A \ln \frac{Mc^2}{B} \cdot$$

$$\left(1 - \left(\frac{T_o}{M c^2} \right)^{1/2} \frac{\ln \frac{T_o}{B}}{\ln \frac{Mc^2}{B}} \right) , \tag{146}$$

where $C = 4\pi \, j(Mc^2)$ is computed from the high energy data quoted earlier. Using $T_o = 100$ MeV and values of A and B similar to those for atomic hydrogen, we find $\tau_{ci}^{-1} \simeq 5 \times 10^{-19}$ sec^{-1}. This number may be taken to be a reasonable lower limit to the actual rate constant. If the flux is extended all the way to $T_o = 0$, we get $\tau_{ci}^{-1} \simeq 7 \times 10^{-19}$ sec^{-1}. While these numbers are indeed small, they are based on the Fermi model for cosmic ray acceleration which, although widely used, is of questionable validity.

3. Suprathermal particles

Hayakawa et al[45] favor the existence of so-called "suprathermal" particles whose energy spectrum extends below the injection energy for the Fermi mechanism. These particles are supposed to have a much larger low energy flux than the ordinary cosmic ray protons and, in fact, Hayakawa et al take a $j(E)$ spectrum with a peak at 10 MeV. There is, of course, no direct observational evidence for the existence of these suprathermal particles and no accepted theory of their origin. The main reason for believing in their existence is that, since they contribute to the heating of the gas, they can explain the observed temperature of H I regions. From a consideration of the heating of the interstellar gas one can put an upper limit on the rate constant $\tau_{si}^{-1} = \int j_s(E) \, \sigma_1(E) \, dE$ for the ionization of hydrogen atoms by suprathermal protons. Since the cross section for the ionization of H_2 can be expected to be approximately equal to the ionization cross section for H, the rate constant determined from temperature considerations can be taken to be also the rate constant for dissociation of H_2. We shall come back to this point at the end of the next section.

D. Temperature Considerations

In this section we shall review some of the basic processes involved in establishing the temperature of H I regions. We consider here only processes which are

important for a <u>static</u> interstellar medium. Heating effects of cloud-cloud collisions will be treated later (section IV-c).

1. Cooling processes

While the mechanism for heating in H I clouds is very uncertain, at least two known processes are capable of cooling the clouds efficiently. These two are: (1) excitation of low lying states of C^+, Si^+ and Fe^+ ions by electron impact, and (2) excitation of rotational states of H_2 molecules thru collisions with hydrogen atoms. In both processes the energy is lost by radiative de-excitation of the excited levels.

If we assume the relative abundances

$$n_H : n_{C^+} : n_{Si^+} : n_{Fe^+} = 10^6 : 91 : 34 : 16 \qquad (147)$$

the cooling rate (in erg cm^{-3} sec^{-1}) for electron excitation of ions is, according to Seaton's calculations,[46]

$$\Lambda_{ei} = 10^{-23} T^{-1/2} (0.64 \ e^{-92/T} + 6.4 \ e^{-413/T}$$

$$+ 1.7 \ e^{-554/T} + 2.2 \ e^{-961/T}) \ n_H \ n_e \quad . \qquad (148)$$

We assume the electron temperature to be the same as that of the heavy particles. The presence of ions also gives rise to heating since the ions capture electrons which are then ejected thru photoionization by the galactic radiation field. This leads to an energy <u>gain</u> Γ_{ei} and an effective

cooling rate Λ_{ei} - Γ_{ei} due to the interaction of electrons with ions. The graph of $(\Lambda_{ei}$ - $\Gamma_{ei})/n_H n_e$ as a function of temperature is shown in Fig. 23. This curve is plotted from Table 3 of the useful review of Takayanagi and Nishimura[47] (hereafter referred to as TN).

In their paper TN calculated the cross sections for the excitation of rotational levels of H_2 thru collisions with H-atoms in order to compute the cooling rate Λ_{HH_2}. To calculate the population of excited rotational levels they assumed a steady state to arise from collisional excitation and de-excitation and radiative de-excitation. For radiative de-excitation TN used spontaneous transition probabilities calculated from the formula for quadrupole transitions given by Spitzer[16]. Osterbrock[48] has pointed out that the transition probability for the $J = 2 \rightarrow J = 1$ transition is roughly two orders of magnitude larger than that for the $J = 2 \rightarrow J = 0$ transition. The latter is a quadrupole transition and has a transition probability per unit time $A_{20} = 2.4 \times 10^{-11}$ sec^{-1}. Osterbrock estimates the ortho-para rates to be $A_{10} \sim 10^{-10}$ sec^{-1}, $A_{21} \sim 2 \times 10^{-9}$ sec^{-1}. With such high rates of radiative de-excitation collisions can be neglected in depopulating the levels. Moreover, since the higher J levels have much larger A-values, we can assume that they are unpopulated and calculate Λ_{HH_2} by considering only the excitation of the $J = 2$ level. Thus
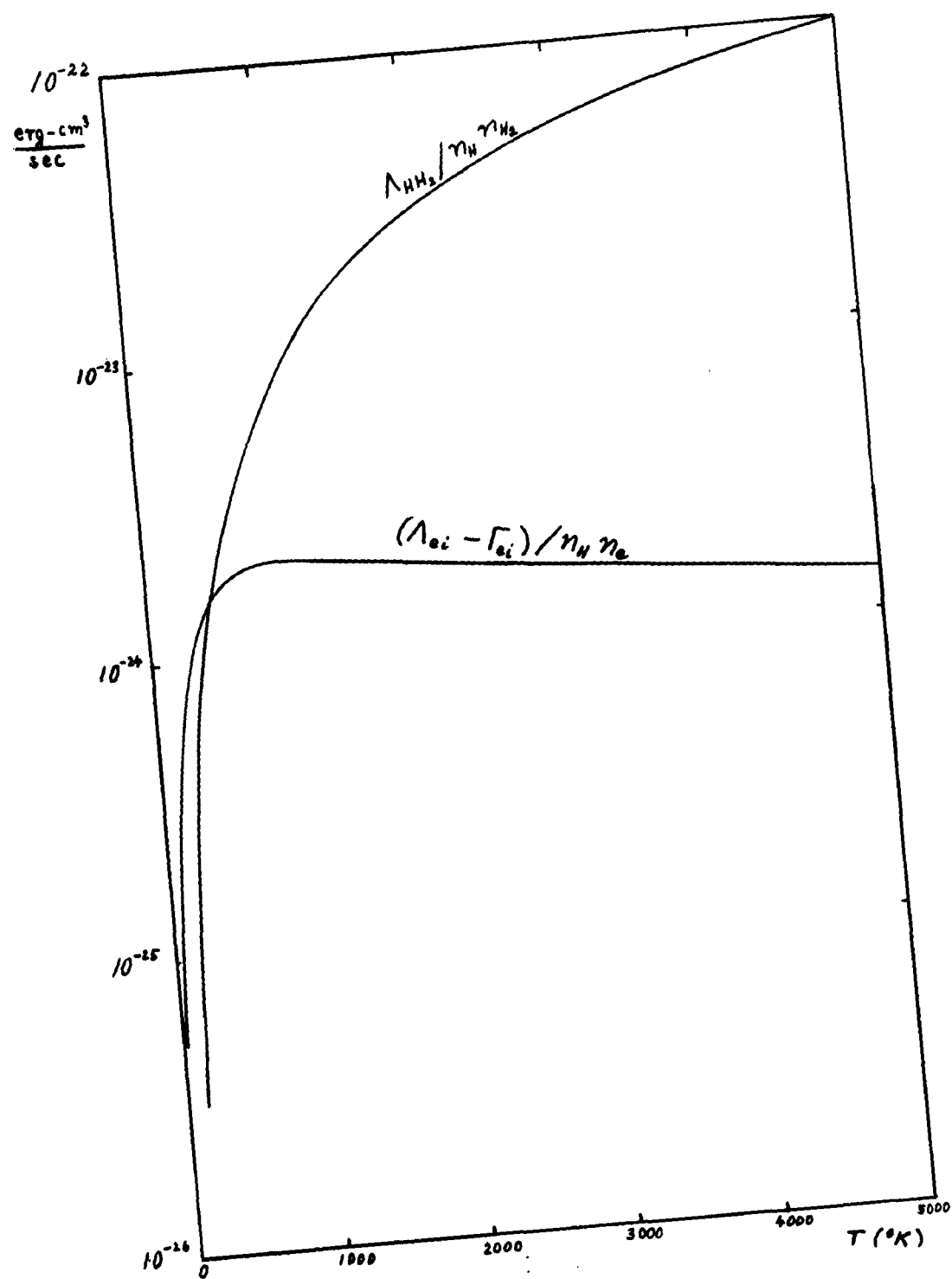
Fig. 23

Cooling rates as a function of temperature

$$\bigwedge_{HH_2} \simeq n_H \, n_{H_2} \left\langle v \, Q_{0 \to 2} \right\rangle \Delta E \qquad (149)$$

where ΔE is the excitation energy of the $J = 2$ state and $\left\langle v \, Q_{0 \to 2} \right\rangle$ is the mean value (averaged over the velocity distributions) of the product of the relative velocity and the cross section. Taking $\left\langle v \, Q_{0 \to 2} \right\rangle$ from Table 1 of TN, $\bigwedge_{HH_2}$ can be calculated from (149). The results are plotted in **Fig. 23**. We see that at high temperatures the hydrogen molecule is very effective as a cooling agent.

The low temperature dependence of $\bigwedge_{HH_2}$ and $\bigwedge_{el} - \Gamma_{el}$ is exhibited in **Fig. 24** for the molecular and electron densities shown. For these densities cooling by $\bigwedge_{el}$ dominates below about $50^{\circ}K$. This is due to the low value ($\Delta E/k = 92^{\circ}K$) of the excitation energy of C^{+}.

One might wonder whether the hydrogen-deutarium molecule HD might be an effective cooling agent since for this molecule both even and odd J levels are possible and the excitation energy of the $J = 1$ level of HD is only about $1/4$ that of the $J = 2$ level of para-hydrogen. Taking a D/H abundance ratio of 10^{-4} and assuming that the excitation cross sections are comparable one finds that the critical temperature below which HD is more effective than H_2 is about $36^{\circ}K$. At such low temperatures cooling by electron excitation of low lying states of ions ($\bigwedge_{el}$) would be more effective.
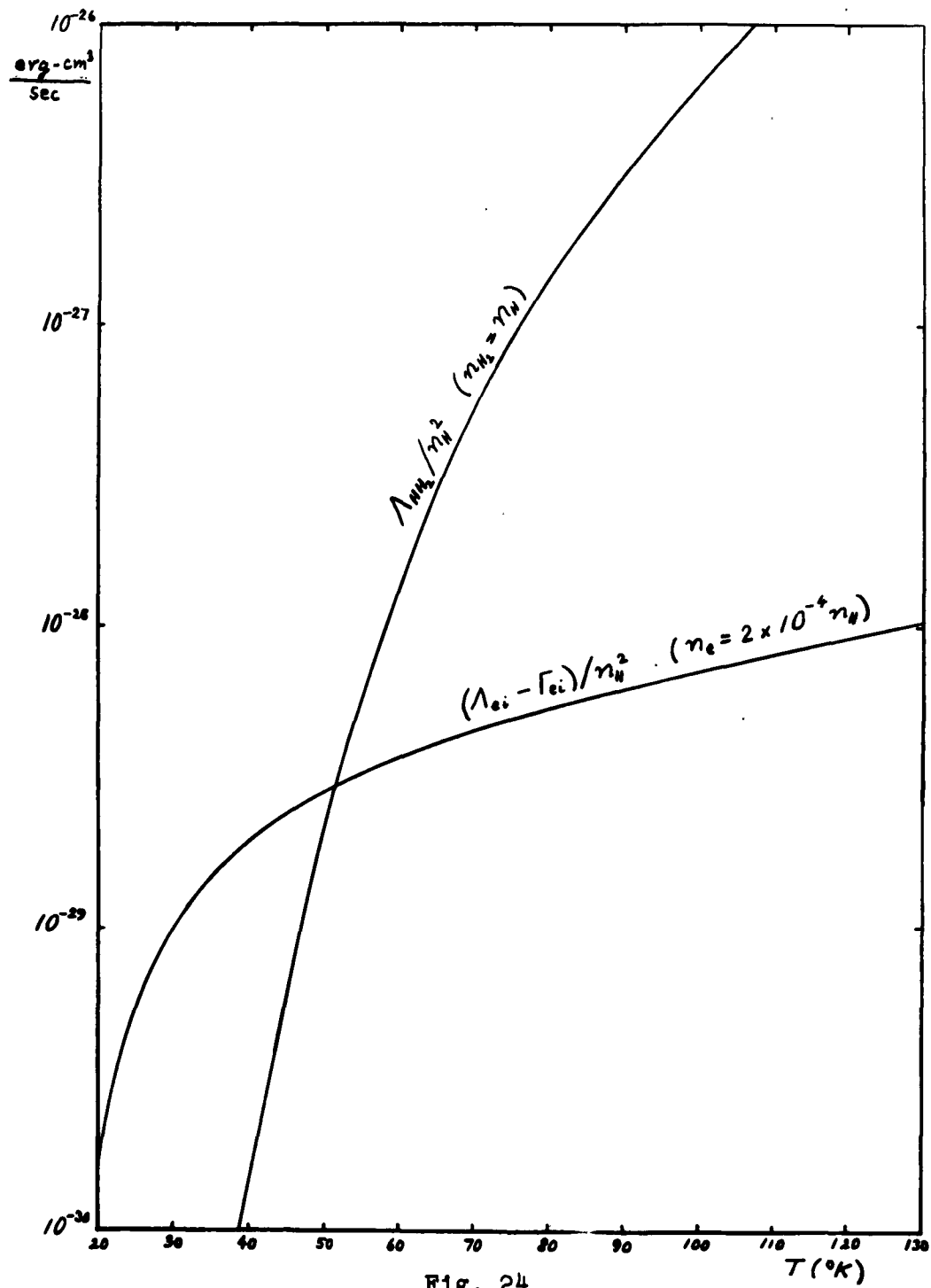
Fig. 24

Low temperature behavior of cooling rates

2. Suprathermal particle flux and the equilibrium temperature

Thus far we have considered only cooling processes. To explain the observed temperature of H I clouds a heating mechanism is needed. Hayakawa, Nishimura, and Takayanagi[45] have considered the role of the suprathermal particles in heating the clouds. The flux needed to produce the observed temperature ($\simeq 100^\circ K$) is so high that the electron density results mainly from the ionized (by the suprathermal protons) H-atoms and is of the order of $0.01 - 0.03$ cm^{-3}. With such a high electron density, the main source of cooling is Λ_{ei}. Setting the rate of heating thru ionization by suprathermal particles Γ_{si} equal to the effective cooling rate $\Lambda_{ei} - \Gamma_{ei}$ one can relate the equilibrium temperature to the rate constant τ_{si}^{-1} for ionization by suprathermal particles. This was done by HNT. From their Fig. 2 one finds that for a temperature $125^\circ K$ corresponding to the older[2] 21-cm observations and for a cloud density of $n_H = 10$ cm^{-3} the required rate constant for ionization by suprathermal particles is $\tau_{si}^{-1} \simeq 10^{-15}$ sec^{-1}. For a temperature of $60^\circ K$ as found by recent investigators[3] a value $\tau_{si}^{-1} \simeq 10^{-16}$ sec^{-1} is required for the same n_H.

IV. DISSOCIATIVE EFFECTS OF CLOUD MOTIONS

A. Ionization of H I Clouds

The following four sections concern the problem of determining the rate at which H I clouds become ionized thru their passage near bright stars. One is led to consider the effect of relative motion of gas and star on the shape of the H II region surrounding the star and this problem is treated in the second section. The methods developed in this section are employed to calculate the Strömgren radii of main sequence O and B stars and the mean free path for ionization of the clouds.

1. Mean time between ionizations - basic physical assumptions

The interstellar gas is in a state of turbulent motion, the average cloud velocity being $\bar{v} = 2\eta \simeq 20$ km/sec (see Appendix B). Thru this random motion the clouds often pass near bright stars which are capable of ionizing (and dissociating the clouds. Thus we speak of a cloud "encountering an H II region". The mean time between encountering H II regions would be $\tau_1 = \lambda_1/\bar{v}$, where λ_1 is the mean free path for ionization. Actually, in the galactic disk λ_1 turns out to be much larger than the thickness of the gas layer so that a cloud meanders thru

essentially all values of z, the height above the plane of the galaxy between ionizations. λ_1 is a function of z and it will be shown rigorously in the last chapter that the appropriately averated λ_1 is the harmonic mean whereby $\lambda_1^{-1}(z)$ is averaged over z according to the amount of time a cloud spends at the particular z. Hence the effective rate constant for ionization is

$$\bar{\gamma}_1 = \bar{v} \left\langle \lambda_1^{-1} \right\rangle \quad . \tag{150}$$

We shall see that $\bar{\gamma}_1$ has the value $\sim 3 \times 10^{-16}$ sec^{-1}, giving a mean time between ionizations of $\sim 10^8$ yr. The rate constant is quite large indicating that this process may well constitute the most important mechanism for dissociation of molecular hydrogen in H I clouds.

We now treat this problem in detail, that is, we consider the problem of determining the ionization produced in a moving cloud when it passes near a bright star. In a large cloud there will not be complete ionization; only that fraction of the cloud which is carved out by the Strömgren sphere will be ionized. It might be objected that as soon as the cloud would come near the star and its outer edges became ionized, the resulting pressure difference caused by the ionized gas would lead to dynamical motion of the unionized gas away from the star. In this case the gas in the cloud would flow around the star as indicated in Fig. 25 below. The effective cross section for
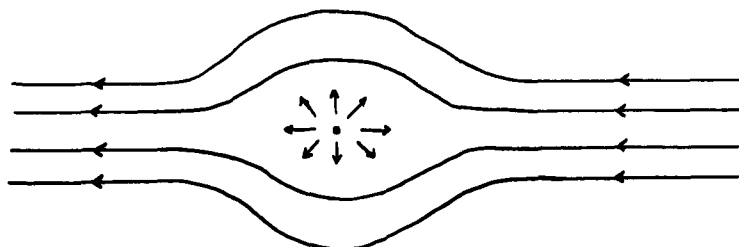
Fig. 25
Possible dynamical motion of gas near star

ionization that the star would present to the cloud would then be smaller than if there were no dynamical motion. However, simple considerations of the motion of the gas at the boundary of the H II region suggest that these dynamical effects can be neglected if

$$\bar{v}^2 \gtrsim kT_1/M \simeq v_s^2 \quad , \tag{151}$$

where T_1 is the temperature ($10^{4\,\circ}K$) of the H II region, M is the proton mass, and v_s is the velocity of sound in the H II region. The inequality (151) means simply that if the relative velocity of the medium with respect to the star is greater than the sound velocity in the ionized medium, then dynamical motions can be neglected. Physically, this results because the gas moves by the star so fast that the pressures, which result from the temperature difference between the ionized and non-ionized regions, do not have sufficient time to act and cause motion of the gas. Since

$v_s \simeq 10$ km/sec and $\overline{v} \simeq 20$ km/sec, we shall assume (151)
satisfied for the encounters of H I clouds with H II regions
and consider the problem of determining the shape of an H
II region which results when the star and cloud have
relative motion.

2. **H II regions for a moving medium - the ionization equation**

We take the reference frame in which the star is
at rest at the origin, and in which the medium moves past
the star with velocity $\overline{v}$ to the left (see Fig. 26). We use
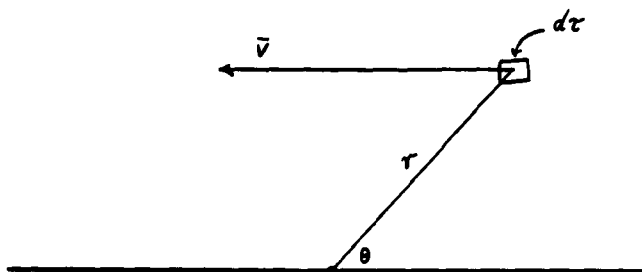
Fig. 26

Polar coordinates

spherical polar coordinates (r, θ, φ). Obviously, the
problem has **axial** symmetry (no φ dependences). The
velocity of the medium with respect to the star will be,
in spherical polar coordinates, $v = (v_r, v_\theta, v_\varphi) =$
$(-\overline{v} \cos \theta, \overline{v} \sin \theta, 0)$. The rate of change of concentration
of species i in the element of volume $d\tau$ will be determined
by the equation

$$\dot{n}_1 \; = \; \frac{\partial n_1}{\partial t} \; + \; \mathbf{v} \cdot \nabla n_1 \quad . \tag{152}$$

We consider the case where a steady state exists, so that $\frac{\partial n_1}{\partial t} = 0$. Taking 1 to correspond to hydrogen atoms, $\dot{n}_H$ would be given by

$$\dot{n}_H \; = \; - \; \tau_\gamma^{-1} n_H \; + \; \overline{\sigma_p v} \; n_e n_p \quad , \tag{153}$$

where the first term represents photoionization and the second term recombination. We neglect the effect of molecules which for the <u>unionized</u> cloud can be expected to have a concentration $n_{H_2} \sim n_H$. This neglect of molecules can be considered to be justified by the results in Appendix C in which it is shown that the "molecular Strömgren sphere" extends beyond the ordinary sphere of ionization. That is, the molecular concentration is appreciable only at distances from the star where the gas is almost completely neutral, so that the ionization problem can be considered separate from the dissociation problem.

In calculating $\dot{n}_H$ it will be justifiable to assume that all the hydrogen atoms are in the ground state, since the hydrogen atoms formed from electron captures in excited states will quickly drop down to the ground state. Thus, in computing τ_γ^{-1} we can consider only photoionizations from the ground state. The ionizing photons come from two sources: (1) from the central star, and (2) from electron-proton radiative recombinations to the ground state. We

shall avoid considering the latter photons by using the following procedure: We consider $\dot{n}_H$ to be due to photo-ionization only by radiation from the central star and recombinations to only _excited_ states. A little reflection shows that this is a very reasonable procedure. When an electron is captured into the ground state, the resulting photon emitted can be considered (roughly) equivalent to the photon which initially ejected the electron from another nearby atom. The process involves essentially the exchange of an electron between two protons (see Fig. 27 below).
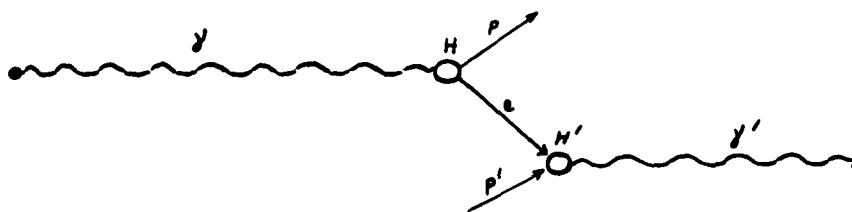
Fig. 27

Photoionization-recombination process

The final photon will, of course, be emitted in an arbitrary direction so that the assumption is made that this recombination radiation intensity varies with distance from the star in the same manner as the stellar radiation. This is a very reasonable assumption since in a steady state the recombination rate is proportional to the intensity of the stellar radiation field. Hence, if we denote by $\tau_{\gamma o}^{-1}$ the

rate constant for photoionization by the stellar radiation field, and by $\overline{\sigma_p' v}$ the product of the capture cross section and electron velocity summed over principle quantum numbers $n = 2, 3, 4, \ldots$ and integrated over the velocity distribution of the electrons, we have

$$\dot{n}_H = - \tau_{\gamma o}^{-1} n_H + \overline{\sigma_p' v} \, n_e n_p. \tag{154}$$

In spherical polar coordinates, the "flow" term $\mathbf{v} \cdot \nabla n_H$ in (155) is

$$\mathbf{v} \cdot \nabla n_H = - \bar{v} \left(\cos \Theta \frac{\partial n_H}{\partial r} - \frac{\sin \Theta}{r} \frac{\partial n_H}{\partial \Theta} \right) . \tag{155}$$

We now introduce the degree of ionization x and the total heavy particle density n_o.

$$
\left.
\begin{aligned}
x &= n_e/(n_e + n_H) \\
n_e &= n_p \quad \text{(neutrality)} \\
n_o &= n_p + n_H = n_e + n_H
\end{aligned}
\right\} \tag{156}
$$

For a constant n_o (152) becomes an equation for the degree of ionization $x(r,\Theta)$. In the case of a steady state $\left(\frac{\partial x}{\partial t} = 0 \right)$ we have

$$- \tau_{\gamma o}^{-1} n_o (1 - x) + \overline{\sigma_p' v} \, n_o^2 x^2 - \bar{v} n_o \left(\cos \Theta \frac{\partial x}{\partial r} - \frac{\sin \Theta}{r} \frac{\partial x}{\partial \Theta} \right) = 0. \tag{157}$$

This equation differs from the ordinary equation for a static medium by the addition of the third term with the coefficient $\bar{v}$.

We shall take the radiation field of the star to be
that of a black body of temperature T_o, diluted by a factor
$W = R^2/4r^2$, and reduced thru absorption by a factor $e^{-\tau\omega}$.
Thus,

$$\tau_{\gamma o}^{-1} = (R^2/4r^2) \int_{\omega_t}^{\infty} J_\omega \, \sigma_\omega \, e^{-\tau\omega} \, d\omega \quad , \qquad (158)$$

where

$$J_\omega = \left(\frac{\omega}{\pi c}\right)^2 e^{-\hbar\omega/kT_o} \quad , \qquad (159)$$

$$\sigma_\omega = \sigma_t \left(\frac{\omega_t}{\omega}\right)^3 \text{(approximately)}, \qquad (160)$$

$$\tau_\omega(r,\theta) = n_o \int_o^r (1 - x(r',\theta)) \, \sigma_\omega \, dr' \quad . \qquad (161)$$

The subscript t in σ_t and ω_t stands for <u>threshold</u>. In the
calculation of $\overline{\sigma_p' v}$ we assume the electron temperature T_e
to be uniform, thus making $\overline{\sigma_p' v}$ simply a constant. This
is probably a good approximation even at the boundary of
the H II region since the electrons involved in recapture
have been photoejected from H-atoms and are likely to
correspond to the temperature of the H II region rather than
to the temperature of the neutral region. Moreover, $\overline{\sigma_p' v}$
goes roughly as $T_e^{-1/2}$ and so is not strongly dependent on
temperature. It is given by

$$\overline{\sigma' v} = \frac{2 A}{(\pi L)^{1/2}} \beta \, \phi'(\beta) \quad , \qquad (162)$$

where[49]

$$\beta = \hbar\omega_t/kT_e, \quad L = m_e/2kT_e \quad , \qquad (163)$$

$$A = 2^5 \, 3^{-3/2} \alpha^3 \pi a_o^2 = 2.11 \times 10^{-22} \, cm^2 \quad (164)$$

$$\alpha = e^2/\hbar c, \quad a_o = \hbar^2/m_e e^2 \quad , \quad (165)$$

$$\phi'(\beta) = \sum_{n=1}^{\infty} \frac{\beta}{n^2} \, e^{\beta/n^2} \, K(\beta/n^2) = \phi(\beta) - \beta e^\beta \, K(\beta), \quad (166)$$

and

$$K(\beta) = \int_\beta^\infty \frac{e^{-u}}{u} \, du. \quad (167)$$

The function $\phi(\beta)$ has been taulated by Spitzer and is of the order of unity. It is interesting to compare (164) with (11). The factor πa_o^2 is roughly the collision cross section and it may be shown that α^3 is approximately $A_\gamma \tau$ where A_γ is the characteristic spontaneous electric dipole transition probability per unit time and τ is the characteristic time for electronic motion in atoms.

Returning now to (157), we have for the equation to be solved for $x(r,\theta)$:

$$- \frac{R^2}{4r^2} \, n_o (1 - x) \int_{\omega_t}^\infty J_\omega \sigma_\omega \, e^{-\tau_\omega} \, d\omega + \overline{\sigma_p v} \, n_o^2 x^2$$

$$- n_o \overline{v} (\cos\theta \, \frac{\partial x}{\partial r} - \frac{\sin\theta}{r} \, \frac{\partial x}{\partial \theta}) = 0. \quad (168)$$

This integro-differential equation can only be solved numerically. In Appendix C methods are developed for its solution and results are given for a particular case of the parameters R, T_o, n_o, T_e, and $\overline{v}$. While a detailed solution of (168) is very difficult, the solution for the general

shape of the H II region can be found with comparative ease. To accomplish this we first multiply both sides of (168) by $r^2 dr$ and integrate over r from 0 to some radius r_o. We get

$$- \frac{1}{4} R^2 n_o \int_o^{r_o} (1 - x(r,\theta))r^2 dr \int_{\omega_t}^\infty J_\omega \sigma_\omega e^{-\tau\omega} d\omega$$

$$+ \int_o^{r_o} \overline{\sigma_p v} \, n_o^2 x^2 r^2 dr - n_o \bar{v} \int_o^{r_o} r^2 (\cos\theta \frac{\partial x}{\partial r} -$$

$$\frac{\sin\theta}{r} \frac{\partial x}{\partial\theta})dr = 0 \quad . \tag{169}$$

From (160) we have the identity

$$- n_o (1 - x(r,\theta))\sigma_\omega e^{-\tau\omega} = \frac{\partial}{\partial r} e^{-\tau\omega} \quad . \tag{170}$$

Substituting (170) into (169) and carrying out the r integration in the first term, we have

$$\frac{1}{4} R^2 \int_{\omega_t}^\infty J_\omega \left[e^{-\tau\omega}\right]_o^{r_o} d\omega + \int_o^{r_o} \overline{\sigma_p v} \, n_o^2 x^2 r^2 dr$$

$$- n_o \bar{v} \int_o^{r_o} r^2 (\cos\theta \frac{\partial x}{\partial r} - \frac{\sin\theta}{r} \frac{\partial x}{\partial\theta})dr = 0. \tag{171}$$

We choose a value of r_o much larger than the H II region boundary so that $\tau_\omega(r_o) \gg 1$, and $\left[e^{-\tau\omega}\right]_r^{r_o} \longrightarrow -1$. The first term in (170) is then

$$- \frac{1}{4} R^2 \int_{\omega_t}^\infty J_\omega d\omega = - \frac{1}{4} (\frac{R}{\pi c})^2 \alpha_o^{-3} (\beta_o^2 + 2\beta_o + 2)e^{-\beta_o}, \tag{172}$$

where

$$\alpha_o = \hbar/kT_o, \quad \beta_o = \hbar\omega_t/kT_o \quad . \tag{173}$$

This term is independent of Θ.

Now, the variation of x with r is of the form shown below (Fig. 28).
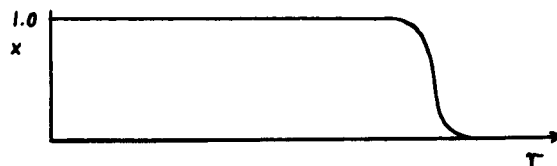
Fig. 28

Ionization as a function of distance from star

One is thus lead to define a quantity

$$r_s^3(\Theta;\bar{v}) = 3 \int_{\bullet}^{r_0 \to \infty} x^2(r,\Theta;\bar{v})r^2 dr \quad . \qquad (174)$$

For an infinitely sharp ionization boundary, $r_s(\Theta;\bar{v})$ would be identical to the radius of the boundary. Clearly, $r_s(\Theta;\bar{v})$ with $\bar{v} = 0$ is to be identified with the radius r_s of the classical Strömgren sphere which by (171), (172), and (174) is equal to

$$r_s^3 = \frac{3}{4} \left(\frac{R}{\pi c}\right)^2 \frac{\beta_\bullet^2 + 2\beta_\bullet + 2}{a_o^3 \, n_o^2 \, \overline{\sigma_p v}} \, e^{-\beta_\bullet} \qquad (175)$$

Thus, from eq. (171) thru (175) we have

$$r_s^3(\Theta;\bar{v}) = r_s^3 + \frac{3 \, \bar{v}}{n_o \, \overline{\sigma_p v}} \int_{o}^{r_0 \to \infty} r^2 \left(\cos\Theta \, \frac{\partial x}{\partial r}\right.$$

$$\left. - \frac{\sin\Theta}{r} \, \frac{\partial x}{\partial \Theta}\right) dr \quad . \qquad (176)$$

Since the ionization x varies only near the boundary, $\partial x/\partial r$ will vary as below (Fig. 29).
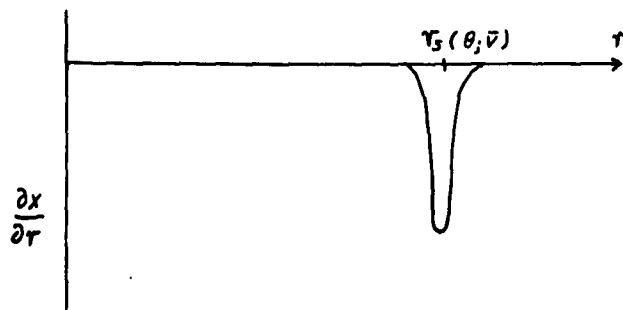
Fig. 29

$\partial x/\partial r$ as a function of distance from star

For an infinitely sharp boundary

$$\frac{\partial x}{\partial r} \longrightarrow \delta(r - r_s(\theta;\overline{v})) \quad . \tag{177}$$

Moreover, for moderate asymmetries in the (distorted) Strömgren sphere it can be assumed in first approximation that

$$\cos \theta \frac{\partial x}{\partial r} \gg \frac{\sin \theta}{r} \frac{\partial x}{\partial \theta} \tag{178}$$

Because of (178), we neglect the second term in the integrand of (176) and also make use of the approximate limiting case (177) to get

$$r_s^{\,3}(\theta;\overline{v}) = r_s^{\,3} - \frac{3\,\overline{v}}{n_o\,\overline{\sigma_p'v}}\, r_s^{\,2}(\theta;\overline{v})\cos \theta \quad . \tag{179}$$

If the second term on the right in (179) is small, we can

replace $r_s^2(\theta;\bar{v})$ in it by r_s^2 and get the following simple relation for $r_s(\theta;\bar{v})$:

$$r_s(\theta;\bar{v}) = r_s(1 - \epsilon \cos \theta) \qquad (180)$$

where the asymmetry parameter ϵ is

$$\epsilon = \frac{\bar{v}}{n_o \overline{\sigma_p' v}\, r_s} \qquad . \qquad (181)$$

It is interesting to note that ϵ can also be written as

$$\epsilon = \tau_{rec}/\tau_{\bar{v}} \qquad (182)$$

where τ_{rec} $(= (n_o \overline{\sigma_p' v})^{-1})$ is the characteristic time for recombination and $\tau_{\bar{v}}(= r_s/\bar{v})$ is the time for medium to tranverse a distance equal to the Strömgren radius. Since $r_s \propto n_o^{-2/3}$,

$$\epsilon \propto \frac{\bar{v}}{n_o^{1/3}\, r_{so}} \qquad , \qquad (183)$$

where r_{so} is the Strömgren radius for $n_o = 1$ cm^{-3}. A typical value of ϵ would be that corresponding to $r_s = 10$ pc, $n_o = 10$ cm^{-3}, and $\bar{v} = 20$ km/sec. For these conditions we get $\epsilon \simeq 0.02$. The function $1 - \epsilon \cos \theta$ is shown for several values of the asymmetry parameter ϵ in Fig. 30. The general shapes exhibited in Fig. 30 are as one might expect, that is, there is an ionization front which is closer to the star in the direction of the oncoming medium and farther away in the opposite direction.
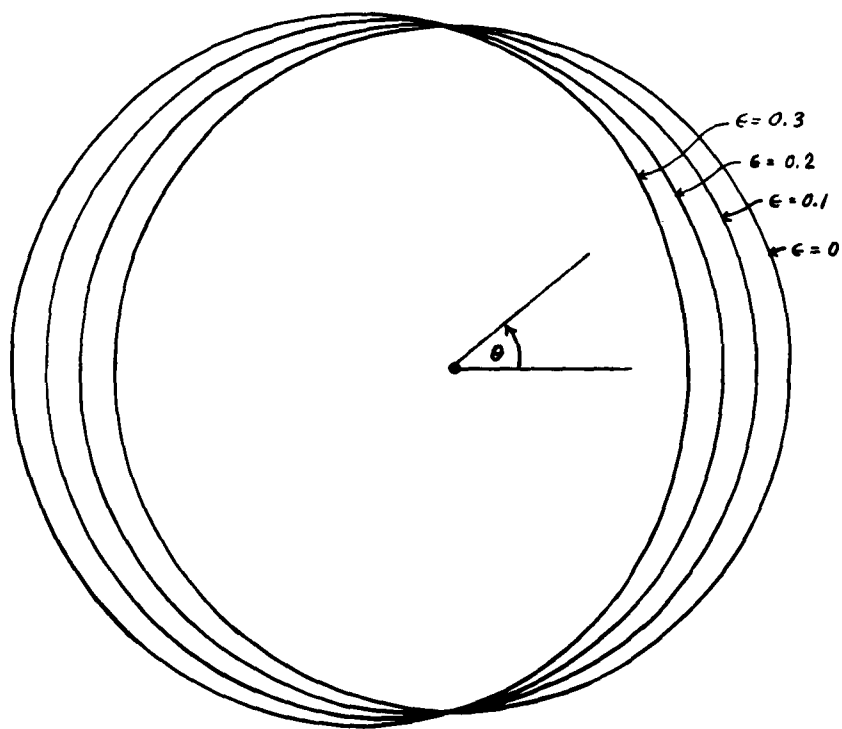
Fig. 30

Polar plot of $1 - \epsilon \cos \theta$ for various values of ϵ. The
medium moves to the left past the star denoted
by a dot.

The result obtained for the shape of the H II region
assumes that a steady state exists since earlier we had set
the partial derivatives of the particle densities with
respect to time equal to zero. For this condition to exist
for most of the star-cloud collision the condition

$$\tau_S \ll \tau_c \tag{184}$$

would have to be satisfied, where τ_S is the characteristic time for formation of a Strömgren sphere and $\tau_c = r_c/\bar{v}$ is the time that the star spends in or near the cloud, r_c being the cloud radius. The time τ_S is essentially the time required to carve out a Strömgren sphere if a star was suddenly placed inside of a cloud and this time is roughly equal to the characteristic time for electron-proton recombination $\tau_{rec.}$. For consider the development of the ionization front as it progresses away from the star. The velocity of the ionization front will be proportional to the ultraviolet flux behind the front and this flux is the same as the flux at this value of r for the final steady state Strömgren sphere. One can show from direct calculations for the static Strömgren sphere that this flux drops sharply near the boundary of the sphere. Hence, the time to form the whole Strömgren sphere is essentially the time to ionize the last optical thickness at the edge which in turn is equal to the characteristic time for recombination. Thus,

$$\tau_S \sim \tau_{rec.} \tag{185}$$

and

$$\tau_S/\tau_c \sim \tau_{rec.}/(r_c/\bar{v}) \equiv \epsilon' \quad . \tag{186}$$

It should be realized that τ_s (and ϵ') are independent of the properties of the central star. One finds that for typical cloud velocities, densities, and radii that $\epsilon' \sim 10^{-2}$ so that the steady state is likely to be closely approached.

To observe such a "distorted Strömgren sphere" one should look for H II regions whose exciting star does not lie at the center of the region. The off-center star would probably be easier to detect that the distorted H II region since as Fig. 30 shows, the ionized regions retain their spherical shape for moderate values of the asymmetry parameter ϵ. The exciting star, however, is displaced from the center of the H II region by an amount ϵr_s, a quantity of first order in ϵ.

3. Strömgren radii

It is of interest to compare the Strömgren radii r_{so} (density = 1 cm^{-3}) calculated from (175) with the radii s_o calculated according to the original Strömgren theory. The latter radii are conveniently calculated from the expression given in Aller's book.[50] The data on the stellar radius (R) and black body surface temperature (T_o) needed to calculate the Strömgren radii were taken from two sources: (1) for $M_v > -2$ (B stars) from the compilation given by Schwarzschild,[51] and (2) for $M_v < -2$ (O stars) from the results of the theoretical model calculations of Haselgrove and Hoyle.[52] The T_o vs. M_v and R vs M_v curves from these two sources were made to join smoothly at

M_v = -2. Some of the resulting stellar radii and tempera-
tures are given in Table 3 below. For the calculation of
r_{so} and s_o and electron temperature T_e = $10^{4}{}^{o}$K was assumed
in all cases (giving $\overline{\sigma_p' v}$ = 2.73 x 10^{-13} cm^3 sec^{-1}). The
calculated Strömgren radii are shown in the table. The
absolute visual magnitude M_v was related to the bolometric
magnitude M_b by means of Kuiper's[53] bolometric corrections
for different surface temperatures. Also tabulated is the
main sequence luminosity function ϕ for the solar neighbor-
hood as given by Sandage[54] and the calculated fraction q_1
of the photon flux that is on the short wavelength side
of the Lyman limit. To a good approximation q_1 is given by

$$q_1 = \frac{\int_{\beta_o}^{\infty} x^2 e^{-x} dx}{\int_o^{\infty} \frac{x^2 dx}{e^x - 1}} = \frac{\beta_o^2 + 2\beta_o + 2}{2 \, \zeta(3)} e^{-\beta_o} , \quad (187)$$

where $\zeta(3)$ is the Riemann zeta-function of argument 3 and
equals 1.202. The quantity d shown in the last column of
the table in the linear distance travelled by a cloud moving
at 10 km/sec during the main sequence burning time of the
star characterized be the particular value of M_v. This
distance may be of some use in considerations of the
spatial correlation of bright stars and gas clouds.

The close agreement between r_{so} and s_o exhibited in
Table 3 is surprising. In his treatment of the problem
Strömgren neglected (1) the variation of the absorption

Table 3. <u>Strömgren Radii and Other Data for Main Sequence Stars</u>

M_v	M_b	$\log\phi+10$	R (10^{11} cm)	T_o (°K)	q_i	r_{so} (pc)	s_o (pc)	d (pc)
-6	-10.53	1.39	8.20	55,250	0.380	135	129	27
-5	-9.27	2.43	5.74	49,250	0.315	89.0	87.4	41
-4	-7.93	3.18	4.18	42,400	0.234	56.2	56.6	67
-3	-6.52	3.82	3.09	35,500	0.150	33.2	34.3	120
-2	-4.98	4.42	2.42	28,200	0.069	17.3	18.4	160
-1	-3.18	5.04	2.14_8	19,950	0.0122	6.49	6.98	380
0	-1.59	5.60	1.70_5	15,490	0.0020	2.30	2.58	1300
+1	-0.04	6.17	1.29_4	12,310	0.0002	0.725	0.824	3900
+2	+1.55	6.60	1.00_5	9,330	6×10^{-6}	0.141	0.162	10^4

cross section with frequency (this does not affect the
Strömgren radius, however), (2) captures to excited states,
(3) the effect of the recombination radiation, and (4) the
specific character of the spectrum of the photon flux from
the central star. Since all of these were taken into
account in the calculation of r_{so}, the very close agreement
with s_o must be considered somewhat accidental.

4. Calculation of λ_1 - the "small cloud approximation"

As we have seen, the asymmetry in H II regions due
to the relative motion of gas and star can be expected to
be small in most cases so that the cross section for
ionization that a star presents to a cloud is πr_s^2. With a
distribution of stars as given by the luminosity function ϕ
(number of stars per cubic parsec per interval of absolute
visual magnitude M_v) the mean free path for ionization
would be given by

$$\lambda_1 = (\pi \int_{-\infty}^{\infty} r_s^2 \phi \, dM_v)^{-1} \quad . \tag{188}$$

With the stellar radii and temperatures and the main sequence
luminosity function taken from the same sources that pro-
duced the results in Table 3 one calculates the $r_{so}^2 \phi$ vs.
M_v and $r_{so}^3 \phi$ vs. M_v curves shown in Fig. 31. The curves
shown in Fig. 31 will no doubt need considerable revision
when better data on stellar temperatures and radii are
available. The Strömgren radii produced by the relatively
cool stars are especially strongly dependent on temperature.
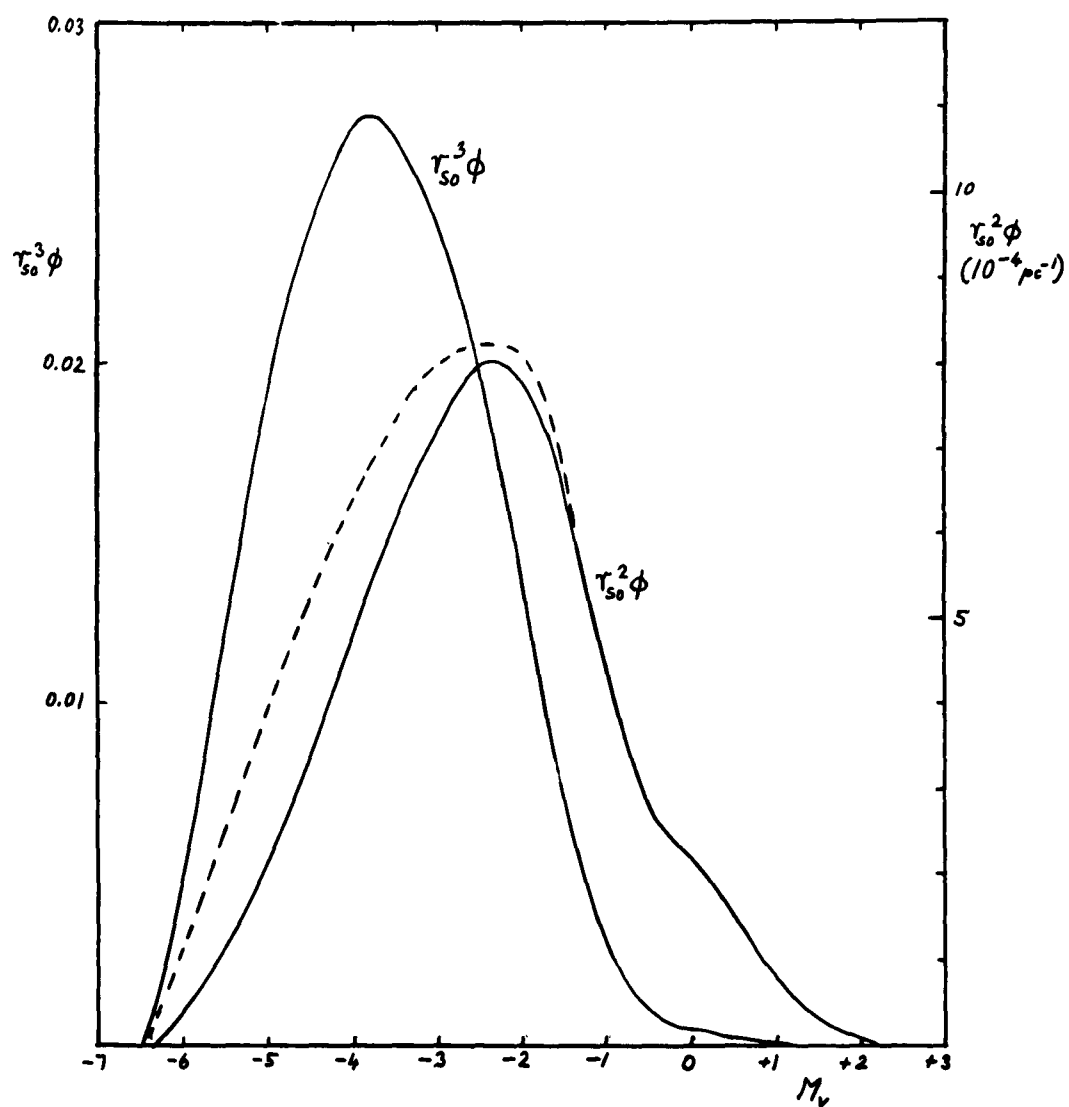
Fig. 31

$r_{so}^2 \phi$ and $r_{so}^3 \phi$ as a function of M_v. The ionization is seen to be due essentially to the O and B stars.

For example, if the temperature of a star is raised from 20,000°K to 25,000°K, the Strömgren radius is increased by a factor of two.

The curve $r_{so}^3 \phi$ indicates that the main contribution to the ionization of the interstellar clouds comes from the main sequence stars around $M_V \approx -4$. These stars are so hot that they ionize a <u>number</u> of clouds surrounding them. Hence, it is best to adopt the picture where the clouds (radii $\sim$ 5 pc) are <u>small</u> compared with the radius of the ionized region. The Strömgren radius used to calculate λ_1 in (188) will then be different from the radius of the ionized region for a uniform medium. We denote the radius (in the small cloud picture) of the ionized region surrounding the star by $\bar{r}_s$. All clouds within $\bar{r}_s$ of a star will be ionized. We consider the intercloud medium to have a negligible density and denote the fraction of the volume occupied by the clouds by f_c, the cloud (total heavy particle) density by n_o (assumed the same for all clouds), and the mean (smeared out) density by $\bar{n}_o$.

$$f_c = \bar{n}_o/n_o \quad . \tag{189}$$

Moreover, we denote the Strömgren radius for a <u>uniform</u> medium (density n) by $r_s(M_V, n)$ which is proportional to $n^{-2/3}$. The radius of an ionized region of uniform density $\bar{n}_o$ (no discrete clouds) would then be $r_s(M_V, \bar{n}_o)$. To

calculate λ_1 one needs the radius $\bar{r}_s$ of the ionized region surrounding the star. The relation between $\bar{r}_s$ and $r_s(M_v, \bar{n}_o)$, the Strömgren radius which would result if the medium were of uniform density $\bar{n}_o$, is easily obtained since for any region of ionization surrounding a star of given radius and surface temperature

$$(\text{density})^2 \times (\text{volume where recombination occurs}) = \text{constant}.$$

Hence,

$$\bar{n}_o^2 \, r_s^3(M_v, \bar{n}_o) = n_o^2 \, f_c \, \bar{r}_s^3 = n_o \, \bar{n}_o \, \bar{r}_s^3 , \qquad (190)$$

so that the relation between $\bar{r}_s$ and $r_s(M_v, \bar{n}_o)$ is

$$\bar{r}_s^3 = \bar{r}_s^3(M_v, \bar{n}_o, n_o) = \frac{\bar{n}_o}{n_o} \, r_s^3(M_v, \bar{n}_o) . \qquad (191)$$

Since $r_s(M_v, \bar{n}_o) \propto \bar{n}_o^{-4/3}$, $\bar{r}_s^3 \propto \bar{n}_o^{-1}$ if n_o is fixed.

The mean free path for ionization of a cloud is then given by

$$\lambda_1^{-1} = \pi \int \phi(M_v) \, \bar{r}_s^2(M_v, \bar{n}_o, n_o) \, dM_v$$

$$= \pi(\bar{n}_o/n_o)^{2/3} \int \phi(M_v) \, r_s^2(M_v, \bar{n}_o) dM_v \propto (n_o \bar{n}_o)^{-2/3} .$$

$$(192)$$

Since $r_s^2(M_v, \bar{n}_o) \propto \bar{n}_o^{-4/3}$, $\lambda_1^{-1} \propto \bar{n}_o^{-2/3}$. Now, the density to be used in the calculation of λ_1^{-1} should be the <u>total</u> density (atomic + molecular: $n_o = n_1 + 2n_2$, n_1 = atomic density, n_2 = molecular density). The molecular density is, of course, unknown. We are attempting to calculate it. It

will be shown that one can expect an amount comparable to the atomic density to be in molecular form. The observed atomic densities are (roughly): $\bar{n}_1 = 1$ cm^{-3}, $n_1 = 10$ cm^{-3}. For the present we shall assume that half the hydrogen is in molecular form so that $\bar{n}_o = 2$ cm^{-3}, $n_o = 20$ cm^{-3}. The end result of our analysis predicting the molecular abundance should, of course, be consistent with this assumption which we make here to __estimate__ the effect of ionization. With these assumed densities one calculates $\lambda_1^{-1} = 0.800 \times 10^{-3}$ pc^{-1} from (192).

One can also calculate the fraction f_1 of the inter-stellar clouds that are ionized. This fraction is given by

$$f_1 = \frac{4\pi}{3} \int \phi(M_V)\, \bar{r}_s^3(M_V, \bar{n}_o, n_o)\, dM_V$$

$$= \frac{4\pi}{3}\, (\bar{n}_o/n_o) \int \phi(M_V)\, r_s^3(M_V, \bar{n}_o)\, dM_V \quad \propto \quad (n_o \bar{n}_o)^{-1}.$$

$$\tag{193}$$

Substituting $\bar{n}_o = 2$ cm^{-3} and $n_o = 20$ cm^{-3}, one calculates $f_1 \approx 0.01$. If, however, one substitutes instead the observed (rough) values for the densities of __atomic__ hydrogen $(\bar{n}_o = 1$ cm^{-3}, $n_o = 10$ cm$^{-3})$, one obtains roughly 0.04 for the fraction. The observed fraction is about 0.1 so that it would seem that the agreement with observation is better when we do not allow for the molecules. If the ratio $\bar{n}_o/n_o = 1/10$ is retained, the calculated fraction is 10% for $\bar{n}_o \approx 0.6$ cm^{-3} which is fairly close to the best value

of 0.8 cm^{-3} as determined from the 21-cm investigations.
However, as mentioned earlier, the calculated Strömgren
radii may be in serious error because of the uncertainties
in the adopted temperatures. It might be mentioned that
the observed fraction ionized of 10% corresponds essentially
to the ratio of total ionized hydrogen (atomic + molecular)
to unionized atomic hydrogen. This observed fraction is
related to f_i by $(f_i)_{obs} = f_i/(1 - \langle F \rangle)$, where $\langle F \rangle$ is the
mean fraction of the hydrogen which is in molecular form.
The dependence of $(f_i)_{obs}$ on the molecular density is some-
what complicated, since as $\langle F \rangle \longrightarrow 1$ the factor $(1 - \langle F \rangle)^{-1}$
tends to increase $(f_i)_{obs}$.

Because of the nonuniformity of the medium (discrete
clouds of high density) the actual regions of ionization will
not be perfect spheres. The fluctuations in the radius of
the ionized medium will be of the order of the mean free path
distance to another cloud $\overline{\lambda} \sim 50$ pc. The radius $(\overline{r}_s)_m$ where
$\overline{r}_s^3 \phi$ is a maximum is roughly 15 pc (for $\overline{n}_o = 2$ cm^{-3}, $n_o =$
20 cm^{-3}), indicating a sizeable deviation from spherical
symmetry. However, since there is an observed tendency of
clustering of gas clouds around O and B stars, these figures,
which correspond to the condition $\overline{n}_o/n_o \approx 0.1$, can be expected
to be different for the typical ionization region. $\overline{\lambda} \propto$
$\overline{n}_o^{-1}$, while $(\overline{r}_s)_m \propto \overline{n}_o^{-1/3}$, so that the effect of clustering
of clouds around the stars would decrease the ratio $\overline{\lambda}/(\overline{r}_s)_m$
and thus decrease the asymmetry effect. However, the

resulting overall error in the calculated value of λ_1 may amount to a factor of about 2.

One might wonder how the clustering clouds around the stars would affect the calculation of f_1 and λ_1^{-1}. The apparent clustering around stars probably results because there is a higher probability for say, an O star to be born if the medium is more dense. The O star and cloud aggregate have a rather small gravitational attraction for another cloud. The presence of the O star would then be interpreted as a result of a density fluctuation in the interstellar gas. In this picture the phenomenon of ionization of clouds would correspond to a chance occurance of the cloud in a region of high density where a star has formed. With the clustering, however, the _same_ amount of ionization is produced. This can also be seen thru the following reasoning. The number of cloud ionizations produced in a given region would be proportional to the probability of a cloud being within the ionization distance of an O star and also to the number density of clouds ionized within the region. The probability of being within the ionization distance of the O star is proportional to the _volume_ ($\propto \bar{r}_s^3$) of the ionized region, since this is purely a statistical phenomenon. If the region of high density where the O star has formed has a cloud density $\bar{n}_0'$, this latter probability is proportional to $(\bar{n}_0')^{-1}$ (since $\bar{r}_s^3 \propto (\bar{n}_0')^{-1}$). But the number density of clouds ionized within the region

is proportional to $\overline{n}_o'$, so that when one takes the product of the two factors the dependence on density cancels. Thus, the calculation of f_1 is not affected by the clustering of the clouds. It should be mentioned however, that if in the clustering the _internal_ density of the clouds (n_o) is increased, the value of f_1 (and λ_1) _will_ be affected.

The _rate_ of ionization of clouds is affected by the clustering although only slightly. The rate of ionization in the region around the star is proportional to the product of density $(\overline{n}_o')$ and cross section for ionization ($\propto \overline{r}_s^2 \propto \overline{n}_o'^{-2/3}$) so that the ionization rate is proportional to $\overline{n}_o'^{1/3}$. The dependence on density is thus rather weak. Since the actual degree of clustering is not known very accurately, the correction for this effect will not be carried out here. It might be remarked that Gold[13] has suggested that the apparent clustering of gas around young stars could be an effect of the greater probability of a cloud recently being ionized when it is near the star, giving a higher atom to molecule ratio for these clouds.

The effect of clustering of stars has been neglected here since a separate Strömgren sphere was assumed for each individual star of absolute visual magnitude M_v. Actually, O and B stars tend to be formed in numbers, several stars being formed in a small "nest". This clustering has an effect on the mean free path for ionization of the clouds. For the radius of the ionized region surrounding N identical

hot stars will be larger than the radius produced by a single star by a factor $N^{1/3}$. The total amount of ionization produced is, of course, independent of clustering. The contribution to λ_1^{-1} from these N stars is reduced by a factor $N^{1/3}$ below the contribution that the N separate stars would produce, however. The effect of the clustering is essentially to produce larger H II regions, the number of H II regions being decreased. Again, because of the relatively weak dependence ($\propto N^{-1/3}$) of λ_1^{-1} on the clustering we shall not try to correct for it. It should be mentioned that due to the larger radii of the ionized regions, the asymmetry of the regions resulting from the nonuniformity of the interstellar medium would be reduced.

We have also neglected the effects of a velocity correlation between the stars and the gas clouds which they ionize. It may be that O and B stars tend to form more readily when a group of gas clouds has small relative motions. In this case the newly formed star would (for a while) "carry" its surrounding cloud and the cloud ionization rate would be decreased. The magnitude of this effect is larger for the more luminous stars which burn on the main sequence for a shorter time and which, therefore, have less time to escape from their surrounding cloud. The short main sequence burning time for the O stars has an additional effect on the calculated λ_1 when the burning time is short compared with the time for a cloud to traverse the

Strömgren sphere. Here one should view the process of cloud
ionization as being due to a certain star formation rate.
For the luminous stars this rate is essentially given by
ϕ/τ_{ms} where ϕ is the (observed) main sequence luminosity
function and τ_{ms} is the main sequence burning time. One may
readily show that due to this effect the integrand of λ_1^{-1}
in (192) must be multiplied by $1 + 4\bar{r}_s/3d$, where d is the
distance travelled by a cloud during the time τ_{ms}. Using
the d-values from Table 3 and the $\bar{r}_s$ calculated for the
conditions $\bar{n}_o = 2$ cm^{-3}, $n_o = 20$ cm^{-3} one obtains the
"effective" $r_{so}^2 \phi$ curve given by the dotted line in **Fig. 31**.
It appears this effect tends to cancel somewhat the velocity
correlation effect previously mentioned.

The calculated value for λ_1 corresponds to the solar
neighborhood which is essentially at z = 0, the plane of
the galaxy. It will be shown in the last chapter of this
work, when the z-distribution of molecular hydrogen is
discussed, that λ_1 increases rapidly with z and that the
quantity which determines the effective rate constant for
ionization is the harmonic mean of λ_1 averaged over all z
with a weight factor which is essentially the observed
distribution of atomic hydrogen. The resulting effective
mean free path for ionization is about twice the local value
at z = 0 or roughly 2 kpc, giving an effective rate constant
for ionization of about 3×10^{-16} sec^{-1}.

B. Cloud-Cloud Collisions

While the temperatures ($\sim 3000^{\circ}K$) produced[14] in completely inelastic cloud collisions are not high enough to cause appreciable dissociation of the H_2 present in the clouds, the initial violent collisions between the atoms and molecules of the cloud can be more effective in causing dissociation. We consider the most violent type of cloud-cloud collision, namely a head-on collision. On collision, the clouds, which we denote by A and B, penetrate each other (see Fig. 32).
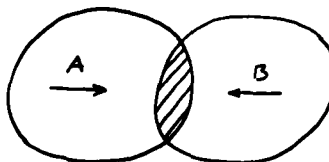
Fig. 32
A cloud-cloud collision

The shaded (hot) region is essentially at rest relative to the remainder of the clouds since the mean free path for collisions is only a very small fraction of the radius of a cloud. Thus, the situation to consider would be that of a collision between a molecule of, say, cloud A moving with a velocity v and a hydrogen atom at rest. The minimum velocity v needed to dissociate the molecule would corres- pond to a dissociation in which all three particles are moving with the same velocity in the direction of the initial

velocity of the molecule. Solving the momentum and energy
conservation equations we find for this threshold velocity:

$$v_t = (3D_o/M)^{1/2} , \qquad (194)$$

where D_o is the dissociation energy (≈ 4.5 eV) of the
hydrogen molecule and M is the mass of the hydrogen <u>atom</u>.
We obtain a value $v_t = 36$ km/sec for the threshold velocity.
Since the clouds have a velocity distribution characterized
by an exponential factor $e^{-v/\eta}$ with $\eta \approx 10$ km/sec, only
a fraction $\sim e^{-v_t/\eta} \approx 0.03$ of the clouds would have
sufficiently high velocities to produce direct dissociation.
Moreover, the rate constant for the overall process would
have factors < 1 which arise because most cloud-cloud
collisions are not head-on and most $H-H_2$ collisions will
not produce the most favorable (threshold) kinematic
results. As a rough estimate for the rate constant for this
dissociative process we take 10^{-3} Z where Z is the collision
frequency of the clouds and is of the order of 10^{-14} sec^{-1}.
The resulting rate constant for the process is then of the
order of 10^{-17} sec^{-1} which is smaller by almost two orders
of magnitude than the figure corresponding to collisions
between the clouds and H II regions. Of course, if
magnetic fields happen to prevent the penetration of the
clouds, the effective dissociation rate would be consider-
ably smaller.

C. Cooling Curves and the Harmonic Mean Temperature

1. Heating by cloud-cloud collisions - the cooling equation

Some attempts have been made to interpret the observed temperature of H I regions as a statistical average over many clouds at different temperatures. The different temperatures arise because the clouds are observed in different stages of cooling after having been heated to about $3000^{\circ}K$ in cloud-cloud collisions. In cooling, the temperature of the cloud is determined by the cooling rate $L(T) = \Lambda_{HH_2} + \Lambda_{ei} - \Gamma_{ei}$ (we neglect other sources of cooling such as interaction with grains). The temperature as a function of time can be found by solving the equation

$$dE/dt = - L(T) \quad , \tag{195}$$

where

$$E = \frac{3}{2} nkT \quad , \tag{196}$$

n being the total particle density. The cooling equation (195) can be integrated numerically to give $T(t)$, the temperature as a function of time after heating. From this "cooling curve" the mean temperature (averated over time) can be determined. As Figs. 23 and 24 show, most of the cooling at high temperatures is due to hydrogen molecules, while the low temperature cooling is due predominantly to excitation of ions by electrons. The temperature where the two cooling rates are equal depends, of course, on the

concentrations of the molecules, ion, and electrons. For
the abundances used in calculating the curves in Fig. 24,
the temperature where $\Lambda_{HH_2} = \Lambda_{ei} - \Gamma_{ei}$ is about $50^\circ K$.
Our knowledge of the abundances is based highly on theory
and is subject to change. For example, the C^+ ions which
are responsible for the cooling at low temperatures may well
be locked up in the interstellar grains. Fig. 33 shows the
low temperature dependence of $L(T)$ for different values of
n_{H_2} with n_e fixed at 2×10^{-3} cm^{-3} and with the ionic
concentration given by (147). Fig. 34 shows the cooling
curves corresponding to these same concentrations under the
assumption that the initial temperature of the cloud is
$3000^\circ K$. We see that at **high temperatures** the temperature
after heating is strongly dependent on the molecular con-
centration. This illustrates how efficient H_2 is in cooling
a cloud down to a temperature of, say, $100^\circ K$.

2. The harmonic mean temperature

Kahn[14] has shown that the temperature determined
from 21-cm studies is to be interpreted as a harmonic mean
$(\bar{T} = (\langle 1/T \rangle)^{-1})$ averaged over many clouds. However, van
de Hulst[55] has questioned this interpretation since it
assumes that the clouds are optically thin. He suggests
rather that the temperature of the nearer clouds would be
impressed more on the observational value. To obtain a
calculated harmonic mean temperature, one must integrate
T^{-1} over t with a weight factor e^{-Zt} where Z is the
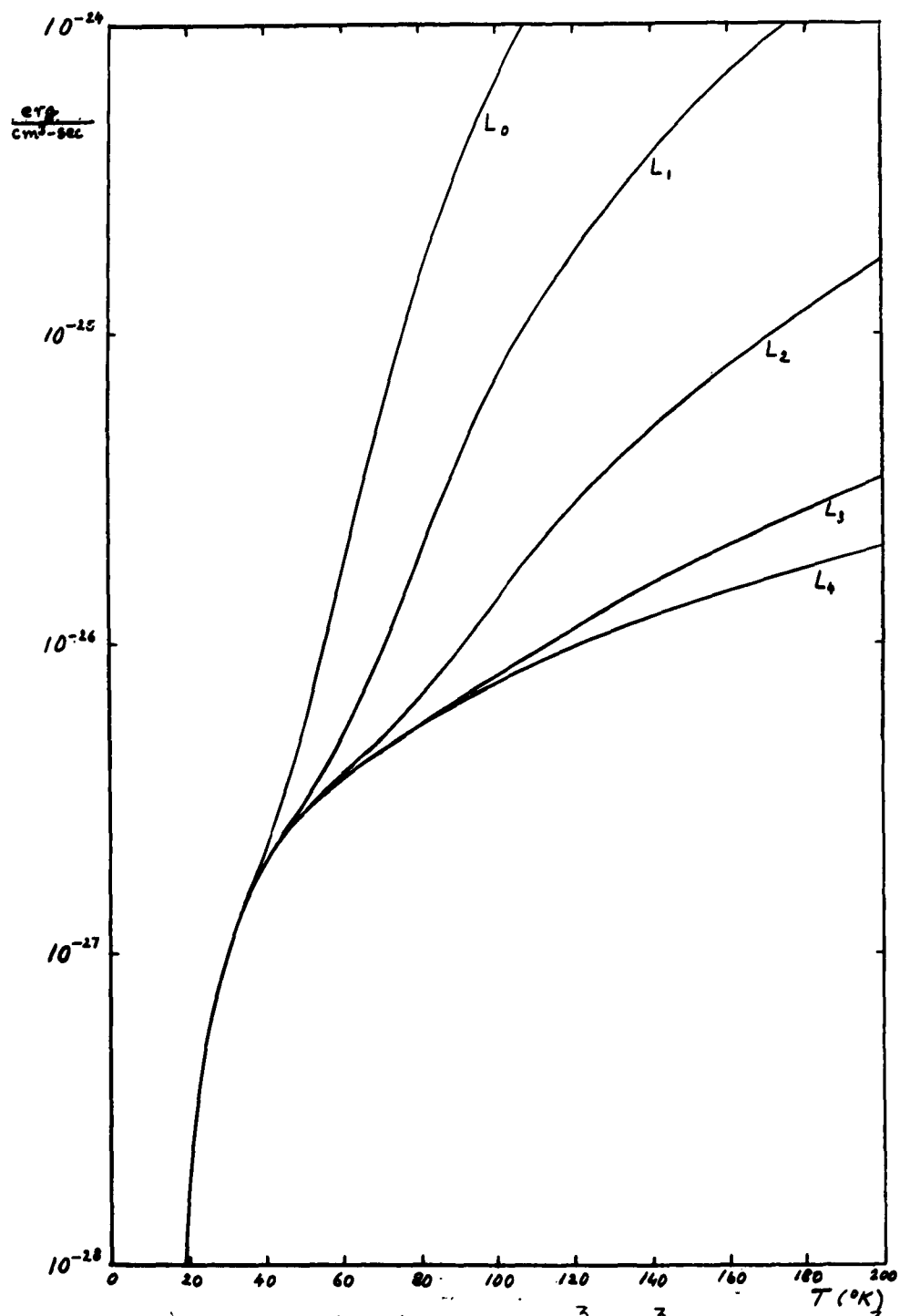
Fig. 33. $L_p(T)$ for $n_e = 2 \times 10^{-3}$ cm^{-3}, $n_H = 10$ cm^{-3}.

$$p = \log \frac{n_H}{n_{H_2}} \quad .$$
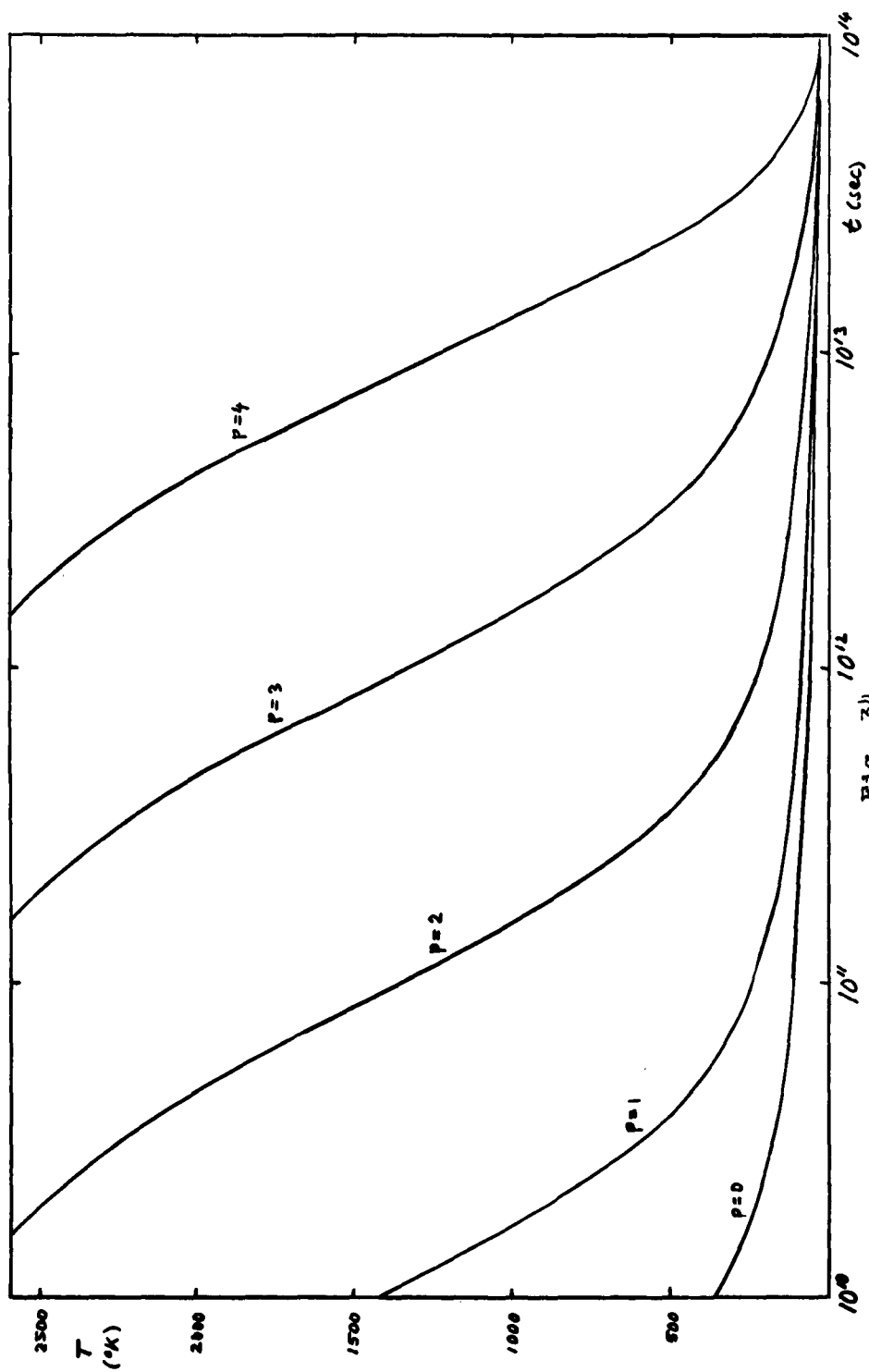
Fig. 34

Temperature as a function of time after heating for a cloud of total particle

density $n_o = 10$ cm^{-3}

collision frequency for the clouds. The factor e^{-Zt} is the probability of $\underline{not}$ colliding with another cloud (and being heated again) during a time t. The harmonic mean temperature is then

$$\overline{T} = (\int_{o}^{\infty} T^{-1} \, Z \, e^{-Zt} \, dt)^{-1} \quad . \tag{197}$$

This expression for $\overline{T}$ is different from that employed by Kahn and Seaton who used $\overline{T}' = (Z \int_{o}^{z^{-/}} T^{-1} \, dt)^{-1}$ which is the harmonic mean for an $\underline{individual}$ cloud and does not represent an average over many clouds as does (197). The relation (197) was first applied by Takayanagi and Nishimura (TN).

Since the clouds cool so quickly at high temperatures, the result $\overline{T}$ does not depend strongly on the value of T for t = 0. With T(t) calculated from the cooling equation (195), $\overline{T}$ can be determined by employing (197). This was done for several combinations of densities n_e and n_{H_2} by TN. Unfortunately, the resulting $\overline{T}$'s depend $\underline{strongly}$ on Z which is known only to order of magnitude. The following qualified conclusion can be made, however. $\underline{If}$ heating by suprathermal particles is negligible and cloud-cloud collisions are the major source of heating, and $\underline{if}$ Z ($\sim 10^{-14}$ sec^{-1}) is no larger than by a factor of about 3, then a harmonic mean temperature of 125°K would appear to rule out molecular densities larger than about 10^{-3} cm^{-3}. This figure was arrived at by noting that the curve with p = 4 in Fig. 34 has T $\approx$ 125°K for t $\approx \frac{1}{Z}$. As mentioned early in the

Introduction, there are conflicting results concerning the
21-cm determinations of H I cloud temperatures. While the
early investigators reported $T = 125^{\circ}K$, more recent work
indicates a value in the neighborhood of $60^{\circ}K$. It would
be desirable to remove this conflict by further observational
investigations. At present, the (indirect) evidence on
the basis of temperature considerations <u>for</u> or <u>against</u>
a large H_2 abundance must be regarded as inconclusive.

V. SUMMARY AND DISCUSSION

A. Comparison of Rate Constants

1. Formation of H_2

As mentioned previously in the summary in section IID, in a typical interstellar cloud of atomic hydrogen density $n_H = 10$ cm^{-3} and grain (mass) density $\rho_g = 10^{-25}$ gm/ cm^3 the recombination reaction on the surface of the interstellar grains is likely to be the most important mechanism for molecule formation. The range of grain temperatures where the recombination coefficient is close to unity is coincident with the expected range $5\text{-}20^\circ K$. It must be admitted, however, that if the physical properties of the grains differ appreciably from what is presently thought, this mechanism could become inoperative. If this is the case, the associative detachment reaction $H^- + H \longrightarrow H_2 + e$ is very likely to be the most important mechanism for molecule formation although it cannot produce a rate of molecule formation as large as that involving the grains. The state of affairs as to molecule formation might be represented as in Fig. 35 where the expected range for the rate $\dot{n}_{H_2}$ in a typical cloud is shown for the two most important mechanisms.

$$H^- + H \rightarrow H_2 + e$$

$$H + H\text{-}S \rightarrow H_2 + S$$

$$10^{-20} \qquad 10^{-19} \qquad 10^{-18} \qquad 10^{-17} \qquad 10^{-16} \qquad 10^{-15} \qquad 10^{-14}$$

$$\dot{n}_{H_2} \ (cm^{-3}sec^{-1})$$
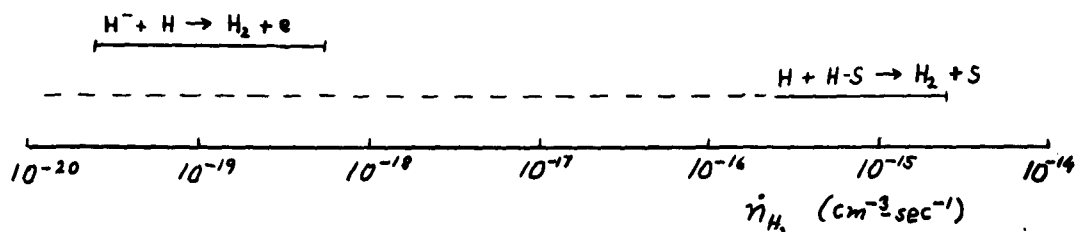
Fig. 35

Comparison of rates of formation of H_2 by the two most
important mechanisms. The dotted extension for the
surface recombination process indicates the possibility
that the mechanism may be inoperative.

We shall assume in the following sections that the
reaction on the grain surfaces is operative so that the rate
of formation is within the limits defined by the solid line
corresponding to $H + H\text{-}S \rightarrow H_2 + S$ in Fig. 35.

2. <u>Dissociation</u>

The four most important mechanisms for dissociation
of H_2 are: (i) dissociation thru the forbidden transition
$^1\sum_g \rightarrow {}^3\sum_u$, (ii) ionization (and subsequent dissociation)
by cosmic rays (or suprathermal particles), (iii) ionization
of the clouds thru random encounters with bright stars, and
(iv) direct dissociation in cloud-cloud collisions. The
rate constants in sec^{-1} associated with these processes
are represented in Fig. 36.
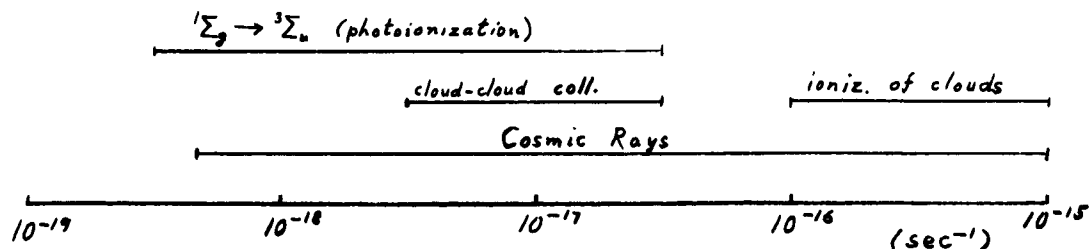
Fig. 36

Probable range of values of the rate constants for
dissociation of H_2 by various processes.

As Fig. 36 shows, the most important processes are the
ionization of the clouds by bright stars and (maybe)
dissociation by cosmic rays. If the cosmic rays are
important, it will be their low energy (suprathermal)
component that contributes. Because of our lack of knowledge
of these low energy cosmic rays we prefer to adopt the
cloud ionization process as the chief mechanism for limiting
the amount of H_2 that builds up in the interstellar clouds
and assume that the true cosmic ray flux does not correspond
to a rate constant as large as the upper limit exhibited in
Fig. 36. We shall, however, include the effects of cosmic
rays formally in some of our equations in the following
sections to show how their effects come in. In the end,
though, we discard the low energy cosmic ray (or suprathermal
particle) hypothesis since there is no compelling reason for
believing in their existence.

The overall view is then the following. In H I clouds molecule formation takes place steadily either thru surface recombination on the interstellar grains or by the slower process of associative detachment ($H^- + H \rightarrow H_2 + e$). At the same time the molecules are (slowly) dissociated by cosmic rays. When the clouds wander near hot stars, part or all of the cloud becomes ionized (and dissociated). As the cloud moves away from the star, electron-proton recombination takes place at a rapid rate, quickly producing a neutral cloud. We assume that the grain surface condition is reestablished in a time short compared to the time (10^8 yr) between ionizations of the cloud, so that molecules begin their gradual formation essentially immediately after the cloud has been ionized. The molecular concentration in individual H I clouds will then be different, depending on how recently the cloud has been ionized.

B. **Mean Galactic Abundance of Molecular Hydrogen**

    1. **Molecular buildup in an individual cloud - very dense regions**

        Consider a cloud of total heavy particle number density n_o with

$$n_o = n_1 + 2n_2 \quad , \tag{198}$$

n_1 being the atomic and n_2 the molecular density. In such a cloud the molecular concentration n_2 would be determined by the equation

$$\dot{n}_2 = \frac{1}{2}\gamma_g n_1 - \gamma_c n_2 \quad , \tag{199}$$

where the first term on the right corresponds to a formation rate and the second term to a dissociation rate (by cosmic rays). If formation on grains is effective, $\frac{1}{2}\gamma_g = \gamma b \rho_g$, γ being the recombination coefficient (see eq. 16). Eliminating n_1 in (199) by means of (198) we have

$$\dot{n}_2 + \gamma_{gc} n_2 = \frac{1}{2}\gamma_g n_0 \quad , \tag{200}$$

where

$$\gamma_{gc} = \gamma_g + \gamma_c \quad . \tag{201}$$

We shall assume n_0 and γ_g remain constant during the conversion to molecular form. Solving (200) for $n_2(t)$ with the condition $n_2(0) = 0$ (assuming the cloud was last ionized at $t = 0$) we have for the <u>fraction</u> of the hydrogen in molecular form:

$$f(t) = 2n_2(t)/n_0 = F(t)/(1 + \beta_{gc}) \quad , \tag{202}$$

where

$$F(t) = 1 - e^{-\gamma_{gc}t} \quad , \tag{203}$$

and

$$\beta_{gc} = \gamma_c/\gamma_g \quad . \tag{204}$$

For the case of a very dense cloud for which possibly $\gamma_{gc}t \gg 1$

$$f \longrightarrow (1 + \beta_{gc})^{-1} \quad . \tag{205}$$

This corresponds to the steady state condition resulting from an equilibrium between formation on grains and dissociation by cosmic rays. As stated previously, it is likely that $\beta_{gc} \ll 1$, so that in very dense clouds one can expect to find most of the gas in molecular form (if $\gamma_{gc}t \gtrsim 1$).

We shall be interested primarily in determining the mean fraction $\langle F \rangle$ of the hydrogen which is in molecular form in the spiral arms of the galaxy. Most of the H I clouds have densities of about 10 particles/cm^3 and in estimating $\langle F \rangle$ in the following section we assume that all the clouds have the same heavy particle density n_o. Moreover, we shall take $\beta_{gc} = 0$ although the treatment for non-zero β_{gc} is a straightforward extension.

2. Average over clouds

We shall see in this section that one can expect a molecular concentration in the spiral arms of our galaxy which is comparable to the atomic value and that the molecular hydrogen should be distributed spatially in the same manner as the atomic hydrogen.

(a) **Mean molecular abundance** - Consider a strip (actually a sheet) of width dz at a height z above the plane of the galaxy (see Fig. 37). In dz there are, say, $C(z)dz$ discrete clouds which contain $N_o(z)dz$ hydrogen atoms which may be free or part of a hydrogen molecule. The number of hydrogen molecules in dz is then $\langle F(z) \rangle N_o(z)dz/2$, $\langle F(z) \rangle$
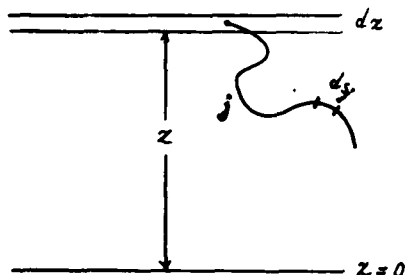
Fig. 37

Path of a cloud

being the fraction of the hydrogen which is in molecular form. We shall be concerned with the calculation of $\langle F(z) \rangle$.

For a cloud in dz arriving along path j (see Fig. 37) the probability that it was last ionized at a total linear distance along j between s_j and $s_j + ds_j$ is $\lambda_1^{-1}(s_j)$ exp $\left(- \int_0^{s_j} \lambda_1^{-1}(s_j')ds_j'\right)ds_j$, λ_1 being the mean free path for ionization. In travelling this distance s_j a fraction $F(s_j)$ of the hydrogen in the cloud will have become molecular, where

$$F(s_j) = 1 - e^{-\gamma_g t(s_j)} \quad , \tag{206}$$

with

$$t(s_j) = \int_0^{s_j} v^{-1}(s_j')\, ds_j' \quad . \tag{207}$$

If the probability of having arrived along j is W_j, the mean fraction in molecular form at z would be given by

$$\langle F(z) \rangle = \sum_j \left\{ \int_0^\infty ds\ \lambda_1^{-1}(s)\ \exp\left(-\int_0^s \lambda_1^{-1}(s')ds'\right) F(s) \right\}_j W_j, \tag{208}$$

with

$$\sum_j W_j \; = \; 1 \quad . \tag{209}$$

If the medium were uniform in density and there were no gravitational field, all paths would be equally probable. If, further, $\lambda_1(z)$ were independent of z and equal to a constant λ_1 we would have

$$\langle F \rangle \; \longrightarrow \; \int ds \; \lambda_1^{-1} \; e^{-s/\lambda_1} \; F(s) \quad . \tag{210}$$

For the case (I) $\lambda_1 \gg \lambda_c$ (λ_c = mean free path for cloud-cloud collisions) the cloud makes many collisions with other clouds between ionizations and

$$F_I(s) \; = \; 1 - e^{-\gamma_g s/\overline{v}} \quad , \tag{211}$$

where $\overline{v} = 2\eta$ is the mean cloud velocity (see Appendix B). We then have from (210) and (211):

$$\langle F_I \rangle \; = \; \frac{\mu}{\mu + 2} \quad , \tag{212}$$

with

$$\mu \; = \; \gamma_g \lambda_1/\eta \quad . \tag{213}$$

For the case (II) $\lambda_1 \ll \lambda_c$

$$F_{II}(s) \; = \; 1 - e^{-\gamma_g s/v} \quad , \tag{214}$$

and one should integrate over a distribution $f(v)$ of cloud velocities with

$$f(v) = \frac{v}{\eta^2} e^{-v/\eta} \quad .$$
(215)

We would then have

$$\langle F_{II} \rangle = \int_o^\infty ds \int_o^\infty dv \, \lambda_1^{-1} e^{-s/\lambda_1} f(v) F_{II}(s)$$
(216)

$$= \mu - \mu^2 e^\mu K(\mu) \quad ,$$
(217)

where

$$K(\mu) = \int_\mu^\infty y^{-1} e^{-y} dy \quad .$$
(218)

The two functions of μ, $\langle F_I \rangle$ and $\langle F_{II} \rangle$, are graphed in Fig. 38.
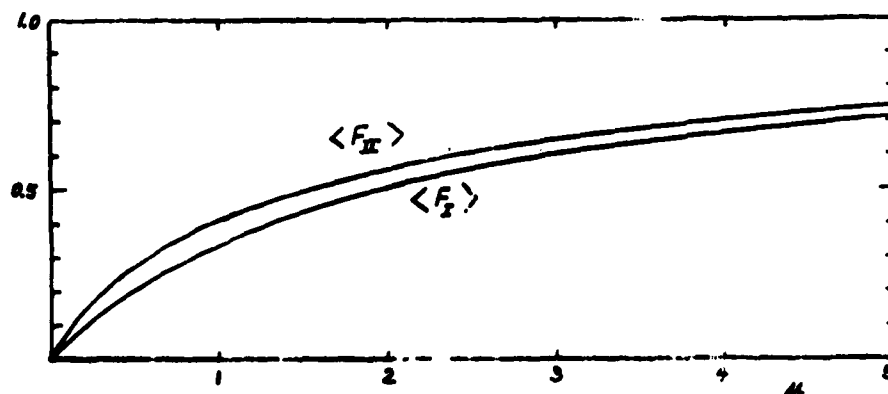
Fig. 38

Fraction in molecular form as a function of μ

The two cases I and II would correspond to the situations

I: $\quad \lambda_c \ll \lambda_1 \ll h_g, h_0$
(219I)

II: $\quad \lambda_1 \ll \lambda_c \ll h_g, h_0$
(219II)

h_g being the scale height (in z) of the galactic gas and h_0 the scale height of the O stars (which ionize the clouds). $\langle F_I \rangle$ and $\langle F_{II} \rangle$ would then be calculated from the <u>local</u> value of μ.

The actual conditions for our galaxy in the vicinity of the sun correspond to <u>neither</u> case I or II. In the galactic plane $\lambda_1 \approx 1$ kpc and $\lambda_c \approx 100$ pc while $h_g \approx 100$ pc and $h_0 \approx 50$ pc. The true situation approaches the completely <u>non-local</u> case in which between ionizations a cloud meanders thru essentially all values of z and makes many collisions with other clouds $(\lambda_1 \gg \lambda_c$, so that $t(s) \rightarrow s/\bar{v})$. In this case a cloud found at any value of z will have gone thru all z, and the fraction in molecular form $\langle F_o \rangle$ would be independent of z. To calculate $\langle F_o \rangle$ one need know only the probability of spending time at various values of z. Since $\langle F_o \rangle$ is independent of z this probability can be taken from the <u>observed</u> distribution of atomic hydrogen as determined by the 21-cm studies. Schmidt[56] gives the atomic distribution $a(z)$ with $a(0) = 1$ and this is exhibited in Fig. 39 below.

The normalized distribution is

$$A(z) = \frac{a(z)}{\int_{-\infty}^{\infty} a(z)\, dz} . \tag{220}$$

We would then have (see eq. 208)

$$\int_0^s \lambda_1^{-1}(s')\, ds' \rightarrow s \langle \lambda_1^{-1} \rangle , \tag{221}$$
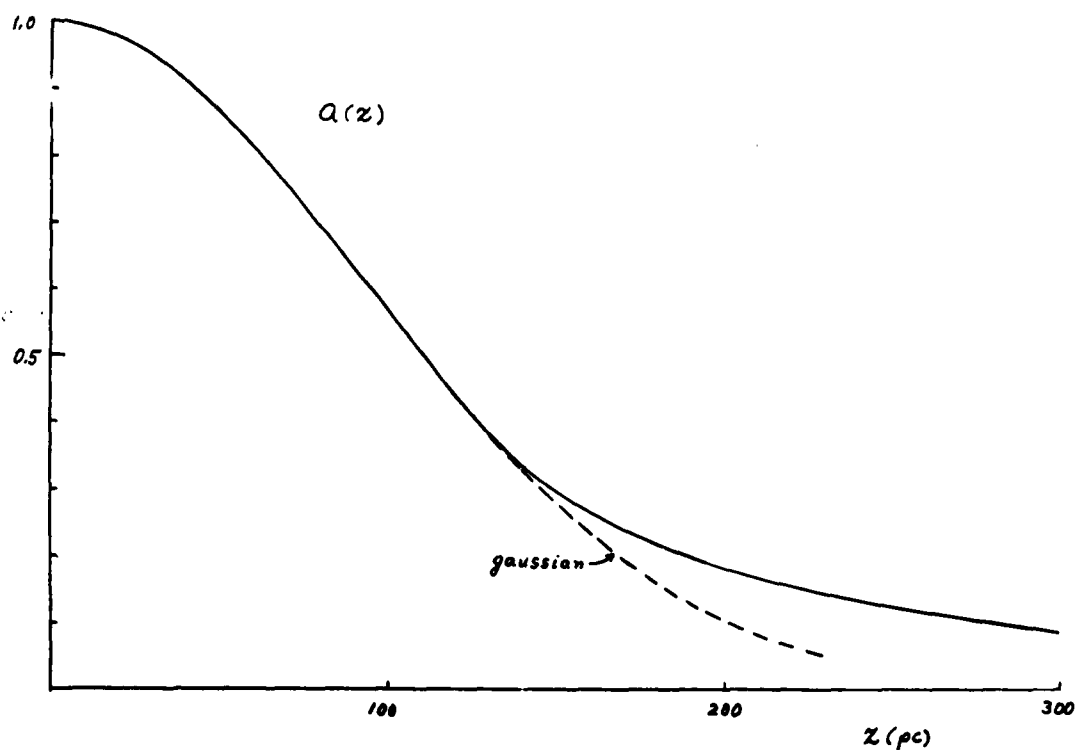
Fig. 39

Density of atomic hydrogen as a function of height above
the plane of the galaxy (after Schmidt). This dis-
tribution does not come from measurements of atomic
hydrogen densities in the solar neighborhood but is
thought to represent well the density distribution
throughout the spiral arms of the galaxy. A gaussian
distribution with the same half-width is also shown
in the figure.

with

$$\langle \lambda_1^{-1} \rangle = \int_{z_\infty}^{\infty} \lambda_1^{-1}(z) \, A(z) \, dz \quad .$$

(222)

The fraction $\langle F_o \rangle$ would be given by

$$\langle F_o \rangle \longrightarrow \int_o^\infty ds \int_{-\infty}^\infty dz \; \lambda_1^{-1}(z) \; A(z) \; e^{-s\langle \lambda_1^{-1}\rangle} F(s)$$

$$= \int_o^\infty ds \; \langle \lambda_1^{-1}\rangle \; e^{-s\langle \lambda_1^{-1}\rangle} F(s) \; = \frac{\mu}{\mu + 2} \; , \qquad (223)$$

where μ is now

$$\mu = \frac{\gamma_g}{\langle \lambda_1^{-1}\rangle \, \eta} \; . \qquad (224)$$

One should note that $\langle F_o(\mu)\rangle$ approaches 1 <u>slowly</u> (see Fig. 38, $\langle F_I \rangle$) so that if μ were large there would still be a considerable amount of atomic hydrogen on the average. For an individual cloud, however, $F(t)$ approaches 1 exponentially at large t.

According to eq. 192 and its associated discussion $\lambda_1^{-1} \propto \bar{n}_o^{-2/3} \, \phi$, where $\bar{n}_o$ is the mean total density and ϕ is the luminosity function. Since λ_1^{-1} is determined mainly by the O-B star component of the luminosity function, we should take the $\phi(z)$ for these stars in computing $\lambda_1^{-1}(z)$. For O (and also B) stars

$$\phi(z) = \phi(0) \; e^{-z^2/h_0^2} \; , \qquad (225)$$

where the scale height h_0 is related to the mean distance $\overline{|z|}$ from the galactic plane by

$$h_0 = \sqrt{\pi} \; \overline{|z|} \; , \qquad (226)$$

with $\overline{|z|}$ = 50 pc as given by Oort.[57] The gaussian distribution (225) can be expected to be quite accurate for the O

and B stars since it would result from the linearity in K_z, the gravitational acceleration in the z-direction. For the small z-values that the O and B stars have a linear z-dependence for K_z is a good approximation (see section B3 of this chapter). The distribution function for $\bar{n}_o$ is essentially the same as the distribution function a(z). Hence, we have

$$\lambda_1^{-1}(z) \; = \; \lambda_1^{-1}(0) \; e^{-z^2/h_0^2} \; a^{-2/3}(z) \quad , \qquad (227)$$

and

$$\langle \lambda_1^{-1} \rangle \; = \; \lambda_1^{-1}(0) \; \ell_o \quad , \qquad\qquad (228)$$

where

$$\ell_o \; = \; \int_{-\infty}^{\infty} e^{-z^2/h_0^2} \; a^{-2/3}(z) \; A(z) \; dz \quad . \quad (229)$$

By direct calculation one finds $\ell_o = 0.496$, so that the effective mean free path for ionization is roughly twice the value in the plane of the galaxy. If now we calculate μ from (224) with $\lambda_1^{-1}(0) = 0.800 \times 10^{-3}$ pc^{-1}, $\eta = 10$ km/sec, and γ_g calculated from $\gamma_g = 2b\rho_g\gamma$ with $b = 4.09 \times 10^9$ cm^3/sec· gm and $\rho_g = 10^{-25}$ gm/cm^3, we get $\mu = 6.7\gamma$. The value of the recombination coefficient γ is likely to be in the neighborhood of $\frac{1}{3}$, giving a value of μ of about 2. Considering the uncertainty in this and other parameters, perhaps the final estimate for μ should be written as

$$\mu \; = \; 2.0 \times 10^{\pm 1} \quad .$$

For the most likely value $\mu = 2$ we have for the fraction of the hydrogen in the spiral arms which is in molecular form:

$$\langle F_o \rangle = 1/2 \quad .$$

The values of $\langle F_o \rangle$ corresponding to $\mu = 0.2$ and $\mu = 20$ are 0.091 and 0.909 respectively.

We see that one can expect a molecular abundance comparable to the atomic concentration and that the molecular hydrogen should have approximately the same z-distribution as the atomic hydrogen. An estimate of the deviation of the molecular distribution $m(z)$ from the atomic distribution $a(z)$ will be made in part (b) of this section.

(b) <u>Distribution in z</u> - Here we shall perform a more accurate calculation or the fraction $\langle F \rangle$ of the hydrogen which is in molecular form and shall also calculate the expected distribution in z of the molecular hydrogen. We shall see that the molecular hydrogen should be distributed in almost the same manner as the atomic hydrogen as assumed in the elementary approach to the problem in part (a) of this section. The total variation in z of $\langle F \rangle$ amounts to only about 2%, while the correction to the absolute fraction is about 40%. The analysis in this section leading to these figures is quite lengthy and may be skipped by the reader interested only in the results.

The basic equation for $\langle F(z) \rangle$ can be derived from the following considerations. In dz let there be $N_0(z)dz$ hydrogen nuclei and $\langle F(z) \rangle \frac{N_0(z)}{2}dz$ molecules. The molecules are in dz because at some time (or linear distance) in the past a number of clouds containing $N_0(z')dz'$ hydrogen nuclei started out at a number of height intervals dz' and diffused along some path of length s to z. For clouds diffusing along such a path the probability that they were last ionized at a linear distance (backward in time) between s and s + ds is $\lambda_1^{-1}(s) \exp(- \int_0^s \lambda_1^{-1}(s')ds')$. In travelling a distance s a fraction $F(s) = 1 - e^{-ks}$ of the hydrogen in the cloud will have become molecular, with $k = \gamma_g/\bar{v} = \gamma_g/2\eta$. We denote by $W(z';z,s)dz$ the probability that a cloud starting out at z' will be within dz after travelling a total distance s (note that going backward along the path a distance s one arrives at z' so that $\lambda_1(s) = \lambda_1(z')$). Our basic equation is then

$$\langle F(z) \rangle \frac{N_0(z)}{2}dz = \int_0^\infty ds \int_{-\infty}^\infty dz \, \lambda_1^{-1}(z')$$

$$\exp(- \int_0^s \lambda_1^{-1}(s)ds) \, N_0(z') \frac{F(s)}{2} W(z';z,s)dz' \quad , \quad (230)$$

or more simply:

$$\langle F(z) \rangle = \int ds \int dz' \lambda_1^{-1}(z') \, e^{-\tau(s,z',z)} F(s) \bar{W}(z';z,s),$$

$$(231)$$

in which the factor $N_0(z')/N_0(z)$ has been incorporated into $W(z';z,s)$ to give $\overline{W}(z';z,s)$ and we have defined

$$\tau(s,z',z) \;=\; \int_0^s \lambda_1^{-1}(s')ds' \quad . \tag{232}$$

The basic equation (231) should now be compared with (223) which corresponds to the case where the diffusion rate is so large that the cloud meanders thru all z-values which are weighted according to $A(z')$. The probability function $\overline{W}(z';z,s)$ is extremely difficult to determine accurately since one must solve a diffusion problem in which the medium is not of uniform density and in which there is a gravitational field. However, we <u>do</u> know the limiting forms of $\overline{W}(z';z,s)$. For as the diffusion rate becomes very large, $\overline{W} \rightarrow A(z')$, and as it becomes very small (local phenomenon), $\overline{W} \longrightarrow \delta(z' - z)$. Now, one can easily solve the diffusion problem when the medium is uniform and there is no gravitational field. W is then the solution to the equation ($t = s/\overline{v}$)

$$\frac{\partial W}{\partial t} \;=\; D\,\frac{\partial^2 W}{\partial z'^2} \quad , \tag{233}$$

where the diffusion constant D is

$$D \;=\; \frac{1}{3}\,\lambda_c\overline{v} \quad , \tag{234}$$

and the initial condition for (233) is

$$W(z';z,t) \xrightarrow[t\to 0]{} \delta(z' - z), \tag{235}$$

the normalization being

$$\int_{-\infty}^{\infty} W(z';z,t)dz' = 1 \quad \text{(all t)} \quad . \tag{236}$$

The solution to (233) is well known to be (see also Appendix D)

$$W(z';z,t) = \frac{1}{(4\pi Dt)^{1/2}} e^{-(z'-z)^2/4Dt} \quad , \tag{237}$$

or in terms of s:

$$W(z';z,s) = \frac{1}{(\pi \Gamma s)^{1/2}} e^{-(z'-z)^2/\Gamma s} \quad , \tag{238}$$

where

$$\Gamma \equiv \frac{4}{3} \lambda_c \quad . \tag{239}$$

We shall take for $\overline{W}$:

$$\overline{W}(z';z,s) = \frac{1}{N(\overline{W})} A(z') e^{-(z'-z)^2/\Gamma s} \quad , \tag{240}$$

where

$$N(\overline{W}) = \int_{-\infty}^{\infty} \overline{W}(z';z,s)dz' \tag{241}$$

is the normalization factor. The ansatz (240) is certainly reasonable since, for example, the two limiting cases resulting from, say, $\Gamma \to 0, \infty$ are contained. We take for Γ the value corresponding to the harmonic mean of $\lambda_c(z)$. Since $\lambda_c(z) \propto a^{-1}(z)$, we have $\langle \lambda_c^{-1} \rangle = g \lambda_c^{-1}(0)$, with

$$g = \frac{\int a^2(z)dz}{\int a(z)dz} \quad . \tag{242}$$

Using Schmidt's $a(z)$ one obtains $g = 0.623_7$. Moreover, we take the model in which the clouds all have the same radius $r_c = 5$ pc and in which the clouds fill a fraction $f_c = 0.1$ of the interstellar space. Then

$$\digamma = \frac{16r_c}{9f_c g} \approx 140 \text{ pc} \quad . \tag{243}$$

The calculation of $\tau(s,z,z)$ is a much more difficult problem. τ is given by

$$\tau(s,z',z) = \int_0^s ds' \int_{-\infty}^\infty dz'' \; \lambda_1^{-1}(z'') \; \bar{w}(z'',s' \mid z',z,s) \tag{244}$$

where $\bar{w}$ is the probability of being within dz'' after diffusing a distance $s - s'$, <u>given</u> that the cloud started at z' at $s' = s$ and ended up $(s' = 0)$ at z. We employ the results of Appendix D and equations D10 with $t' = (s-s')/\bar{v}$ and $t - t' = s'/\bar{v}$ and make a second ansatz:

$$\bar{w}(z'',s' \mid z',z,s) = \frac{1}{N(\bar{w})} A(z'') \; e^{-(z''-z')^2/\alpha'^2} \times$$
$$e^{-(z'' - z)^2/\alpha^2} \quad . \tag{245}$$

Here the normalization is

$$N(\bar{w}) = \int_{-\infty}^\infty dz'' \bar{w}(z'',s' \mid z',z,s) \quad , \tag{246}$$

and we have defined

$$\alpha'^2 = \zeta(s - s'), \quad \alpha^2 = \zeta s' \quad . \quad (247)$$

We see that $\bar{w}$ has the correct limiting properties and that $\bar{w} \to \delta(z'' - z')$ as $s' \to 0$.

In the calculation of τ it is convenient to approximate the distribution $A(z)$ by a gaussian:

$$A(z) = \frac{1}{\sqrt{\pi}\, h_g} e^{-z^2/h_g^2} \quad (248)$$

This is actually quite a good approximation (see Fig. 39), especially for small z where $\lambda_1^{-1}(z)$ is peaked. We take h_g as the parameter which gives the same half width as Schmidt's distribution. It might be remarked here that one should really be taking the distribution function for the total gas density instead of the atomic distribution. However, as we shall see, the molecular distribution $m(z)$ is very close to the atomic distribution $a(z)$ so that $A(z)$ can also represent the total distribution well. We are, of course, now attempting to find the deviation of $m(z)$ from $a(z)$. With the approximation (248) we have, since $\lambda_1^{-1}(z) \propto \phi(z) \cdot A^{-2/3}(z)$ (see eq. 227),

$$\lambda_1^{-1}(z) = \lambda_1^{-1}(0)\, e^{-z^2/h_1^2} \quad , \quad (249)$$

where

$$1/h_1^2 = 1/h_0^2 - 2/3h_g^2 \quad . \quad (250)$$

With the help of these relations one easily calculates

$$N(\overline{w}) \;=\; \frac{\mathscr{S}_g}{h_g} \; e^{\mathscr{Z}_g^2/\mathscr{S}_g^2} \; e^{-z'^2/\alpha'^2} \; e^{-z^2/\alpha^2} \quad, \tag{251}$$

where

$$\mathscr{S}_g^{-2} \;=\; h_g^{-2} \;+\; \alpha'^{-2} \;+\; \alpha^{-2} \quad, \tag{252}$$

and

$$\mathscr{Z}_g/\mathscr{S}_g^2 \;=\; z'/\alpha'^2 \;+\; z/\alpha^2 \quad. \tag{253}$$

Carrying out the z'' integration in (244) we then obtain

$$\int_{\infty}^{\infty} dz'' \lambda_1^{-1}(z'') \; \overline{w} \;=\; \lambda_1^{-1}(0) \; \frac{\mathscr{S}_{g1}}{\mathscr{S}_g} \; e^{\mathscr{Z}_{g1}^2/\mathscr{S}_{g1}^2} \; e^{-\mathscr{Z}_g^2/\mathscr{S}_g^2} \quad, \tag{254}$$

with

$$\mathscr{S}_{g1}^{-2} \;=\; h_g^{-2} \;+\; h_1^{-2} \;+\; \alpha'^{-2} \;+\; \alpha^{-2}$$

$$\;=\; h_{g1}^{-2} \;+\; \alpha'^{-2} \;+\; \alpha^{-2} \tag{255}$$

and

$$\mathscr{Z}_{g1}/\mathscr{S}_{g1}^2 \;=\; z'/\alpha'^2 \;+\; z/\alpha^2 \quad. \tag{256}$$

Thus, we have for τ:

$$\tau(s,z',z) \;=\; \lambda_1^{-1}(0) \int_0^S G(s',z',z,s) \; ds' \quad, \tag{257}$$

with

$$G(s',z',z,s) = H(s',s) \; e^{-E(s',z',z,s)} \quad, \tag{258}$$

H and E being given by

$$H = \frac{\mathcal{Y}_{g1}}{\mathcal{Y}_g} = \frac{1/h_g^2 + 1/\mathcal{F}(s - s') + 1/\mathcal{F}s'}{1/h_{g1}^2 + 1/\mathcal{F}(s - s') + 1/\mathcal{F}s'} , \qquad (259)$$

and

$$E = \mathcal{Z}_g^2/\mathcal{Y}_g^2 - \mathcal{Z}_{g1}^2/\mathcal{Y}_{g1}^2 =$$

$$\left[\frac{z'}{\mathcal{F}(s - s')} + \frac{z}{\mathcal{F}s'} \right]^2 \left[\frac{1}{1/h_g^2 + 1/\mathcal{F}(s - s') + 1/\mathcal{F}s'} \right.$$

$$\left. - \frac{1}{1/h_{g1}^2 + 1/\mathcal{F}(s - s') + 1/\mathcal{F}s'} \right] . \qquad (260)$$

Now, for most of the range of integration over s', $H \approx h_{g1}/h_g$ and $E \sim (h_g/\mathcal{F}s')^2 h_g^2 \sim h_g^4/\mathcal{F}^2\lambda_1^2 \ll 1$ (since $z, z' \sim h_g \sim h_{g1}$ and $s' \sim \lambda_1$). However, as $s' \rightarrow 0$

$$E \rightarrow \frac{z^2}{h_1^2}(1 - \frac{\mathcal{F}s'h_1^2}{H_o^4} + \frac{z's'}{z(s - s')} + \frac{2s'}{h_1^2(s - s')}), \qquad (261)$$

where

$$H_o^{-4} = h_{g1}^{-4} - h_g^{-4} . \qquad (262)$$

For typical values of $z, z; s'$ the largest of the correction terms (1st order of s') to E is the first. Hence, for small s'

$$E \longrightarrow \frac{z^2}{h_1^2}(1 - \frac{\mathcal{F}h_1^2s'}{H_o^4}) \sim 1 \text{ for typical } z. \quad (263)$$

Similarly, at the other endpoint $s' \rightarrow s$

$$E \longrightarrow \frac{z^2}{h_1^2}(1 - \frac{\mathcal{F}h_1^2(s - s')}{H_o^4}) . \qquad (264)$$

The graph of E vs. s' is then of the form shown in Fig. 40 below.
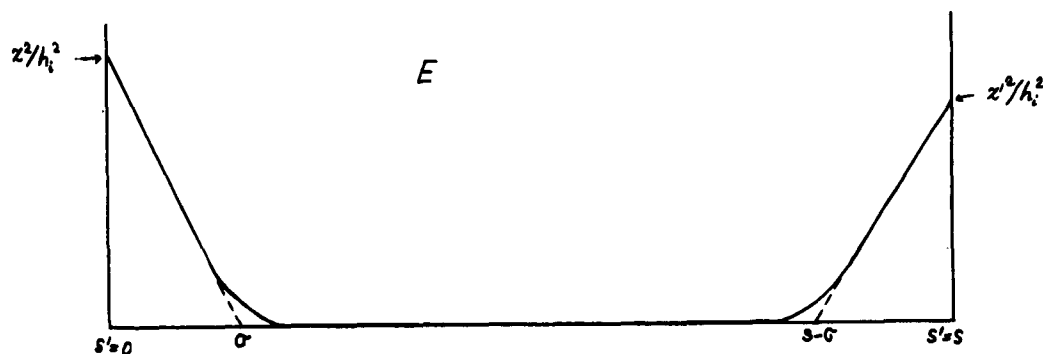
Fig. 40

Graph of E as a function of s'

$$\left(\sigma = H_o^4 / \xi \, h_1^2 \ll s \right)$$

One is thus led to make the following approximation:

$$\tau(s,z,z) = \tau_o(s,z) + \tau_o(s,z') \quad , \quad (265)$$

where

$$\tau_o(s,z) = \lambda_1^{-1}(0) \left\{ \int_0^\sigma + \int_\sigma^{s/2} \right\} ds' H(s',s) \, e^{-E(s',s,z)} \quad .$$

$$(266)$$

In the separate intervals we take $\left(\sigma = H_o^4 / \xi \, h_1^2 \right)$

$$0 < s' < \sigma : \quad H = 1 - \frac{\xi s'}{2h_1^2}$$

$$E = \frac{z^2}{h_1^2} \left(1 - \frac{s'}{\sigma} \right)$$

$$\sigma < s' < \frac{s}{2} \quad : \quad H = \frac{h_{g1}}{h_g} \left(1 + \frac{h_g^2 - h_{g1}^2}{2\mathcal{F}} \left(\frac{1}{s - s'} + \frac{1}{s'}\right)\right) \quad (267)$$

$$E = 0.$$

Evaluating the integrals we get $(\sigma \ll s)$

$$\tau_0(s,z) = \frac{s}{2\lambda_1'} - \frac{\sigma}{\lambda_1'} + \frac{h_g^2 - h_{g1}^2}{2\,\mathcal{F}\,\lambda_1'} \left(\ln\frac{s}{\sigma} - \frac{\sigma}{s}\right) + \lambda_1^{-1}(0)\sigma f(z) \quad ,$$

$$(268)$$

where

$$\lambda_1' \equiv \lambda_1(0) \frac{h_g}{h_{g1}} \quad , \qquad (269)$$

and the function $f(z)$ is

$$f(z) = \frac{1 - e^{-z^2/h_1^2}}{z^2/h_1^2} - \frac{1}{2z^2/h_1^2} \frac{H_0^4}{h_1^2}\left(1 - \frac{1 - e^{-z^2/h_1^2}}{z^2/h_1^2}\right) \quad .$$

$$(270)$$

As $z \to 0$

$$f(z) \to 1 - H_0^4/4h_1^4 - \tfrac{1}{2}(z/h_1)^2(1 - H_0^4/6h_1^4) + \tfrac{1}{6}(z/h_1)^4 \cdot$$

$$(1 - H_0^4/8h_1^4). \qquad (271)$$

Now, in (268) all terms except the first represent correction terms (c_1) and we should perhaps take the first term to be $\mathcal{K}s/2$ with $\mathcal{K} = \lambda_1^{-1}(0)\,\ell_0$ where ℓ_0 (eq. 228) is calculated with Schmidt's specific $A(z)$ (not the gaussian approximation). Hence we have

$$\tau = \mathcal{K}s + \sum_i c_1 \qquad (272)$$

and

$$e^{-\tau} = e^{-\varkappa s} \prod_i (1 - c_i) \approx e^{-\varkappa s}(1 - \sum_i c_i) \ . \quad (273)$$

The function $e^{-\tau}$ is to be substituted into (231) to be integrated over z and s. Since the weighting factor in the integration over z is peaked at $z = 0$, the expansion (271) which comes into $\tau_0(s,z')$ may be used with terms up to z^2. Making the substitution

$$f^*(z) = \frac{1 - H_0^4/2h_1^4 - f(z)}{1 - H_0^4/4h_1^4} \quad , \quad (274)$$

we get

$$\tau = \varkappa s - \frac{2\sigma}{\lambda_1'} + \frac{h_g^2 - h_{g1}^2}{\mathcal{F} \lambda_1'} (\ln \frac{s}{\sigma} - \frac{\sigma}{s})$$

$$- \lambda_1^{-1}(0) \sigma (2 - H_0^4/2h_1^4 - \frac{1}{2}(z/h_1)^2(1 - H_0^4/6h_1^4))$$

$$- \lambda_1^{-1}(0) \sigma (1 - H_0^4/4h_1^4) f^*(z) \quad , \quad (275)$$

the last term giving the z dependence.

Let us now return to $\bar{W}$ (eq. 240). Here one can expand the exponential and get, after evaluating $N(\bar{W})$:

$$\bar{W} = A(z') (1 - \frac{z'^2 - \overline{z^2}}{\mathcal{F} s}) \quad , \quad (276)$$

where we have dropped a linear term in z' since it will give nothing when integrated over z' in (231). Substituting the expressions for τ and $\bar{W}$ into (231) and evaluating the

integrals over z' by making a gaussian approximation to $A(z)$ in calculating the correction terms, we get for $\langle F(z) \rangle$:

$$\langle F(z) \rangle = (\langle F_o \rangle + C)(1 + \Delta f^*(z))$$ (277)

where

$$\langle F_o \rangle = \frac{k}{\varkappa + k} = \frac{\mu}{\mu + 2}$$ (278)

is the zero order term,

$$\Delta = \sigma \lambda_1^{-1}(0) (1 - H_o^4/4h_1^4)$$ (279)

gives the magnitude of the z-variation, and C is the correction term to the absolute fraction $\langle F_o \rangle$. C is given by

$$C = \lambda_1^{-1}(0) \int_0^\infty e^{-\varkappa s}(1 - e^{-ks})(\sum_i c_i)ds = \sum_{corr.,}$$ (280)

with

$$\sum_i c_i = \alpha/s - \beta - \gamma \ln \frac{s}{\sigma} ,$$

$$\alpha = \frac{1}{2\zeta}(h_g^2 - h_{g1}^3/h_g) + \frac{\sigma}{\zeta \lambda_1'} (h_g^2 - h_{g1}^2) ,$$

$$\beta = \lambda_1^{-1}(0) \sigma(2 - H_o^4/2h_1^4 - \frac{h_{g1}^3}{4h_g h_1^2}(1 - H_o^4/6h_1^4)) - 2\sigma/\lambda_1' ,$$

$$\gamma = \frac{h_g^2 - h_{g1}^2}{\zeta \lambda_1'} .$$ (281)

Evaluating the integrals in (280) we get ($\varkappa = \ell_o \lambda_1^{-1}(0)$)

$$C \;=\; \sum \text{corr.} \;=\; \alpha \lambda_1^{-1}(0) \ln \frac{k + \varkappa}{\varkappa} \;-\; \beta \ell_o^{-1} \frac{k}{k + \varkappa}$$

$$- \gamma \, \lambda_1^{-1}(0) \left(\frac{\ln\sigma(k + \varkappa)}{\varkappa + k} - \frac{\ln\sigma\varkappa}{\varkappa} \right) . \tag{282}$$

Inserting the numerical values $\alpha/\lambda_1(0) = 0.0376$, $\beta = 0.0122$, $\gamma = 0.0363$, and $\ell_o = 0.496$ we find for the most likely case $\varkappa = k$ $(\mu = 2)$:

$$\langle F_o \rangle = 0.50$$

$$C = -0.21,$$

while Δ is calculated to be (independent of k,)

$$\Delta = 0.024_5$$

We see that the correction to the absolute fraction F is sizeable ($\sim 40\%$) but that the term $1 + \Delta f^*(z)$ giving the z-dependence of $\langle F \rangle$ is fairly constant (total variation $\sim 2\%$). The relative deviation from the value of $\langle F \rangle$ at $z = 0$ is given by

$$\frac{\langle F(z) \rangle - \langle F(0) \rangle}{\langle F(0) \rangle} = \Delta f^*(z) \quad , \tag{283}$$

where the function $f^*(z)$ defined in (270) varies between 0 and 1. It is graphed below.

(c) <u>Critique</u> - Assuming that the basic microscopic physical processes have been treated correctly, the greatest uncertainty involved in the calculations just described lies in the validity of the model chosen for the interstellar gas.
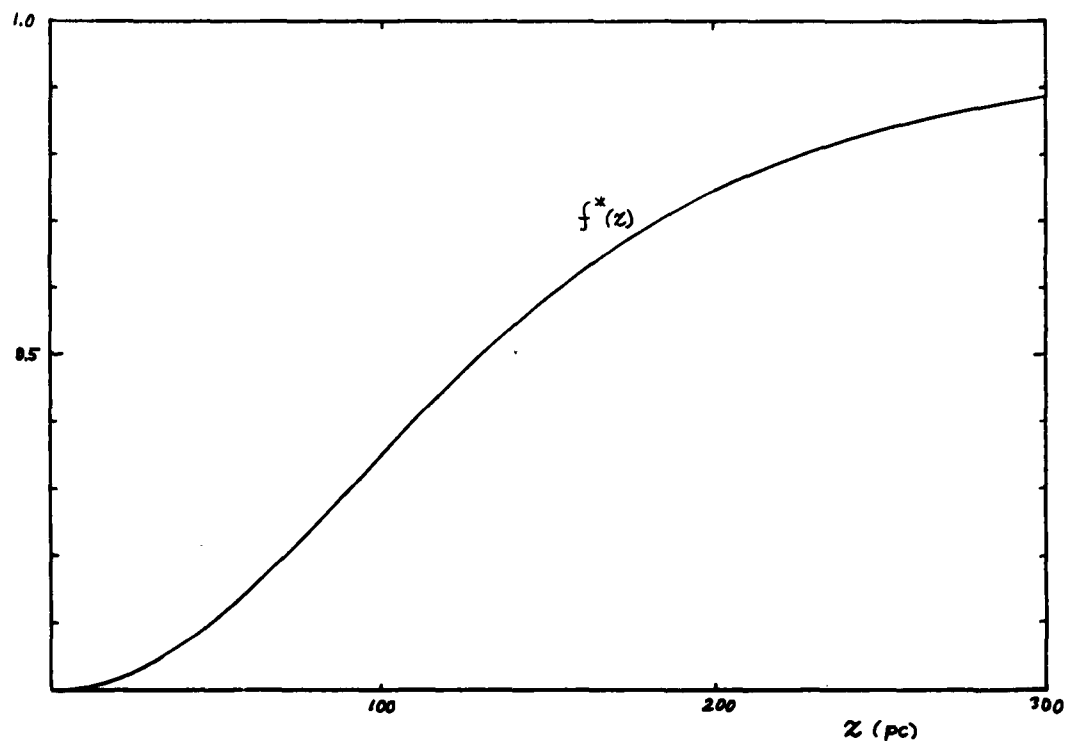
Fig. 41

Graph of $f^*(z)$

The cloud model has been widely used but has also received some criticism. It has been adopted in this work in order to treat the problem at hand analytically. Essentially, we have assumed that all the clouds have the same density and mass, since we have used a unique grain density ρ_g and a unique characteristic velocity η. It is known, however, that there is a range of cloud densities and masses, although the data is not sufficiently accurate to warrant a detailed

treatment which takes into account this fine structure in the model.

In considering the random motions of the clouds it has been assumed that the clouds retain their identity in making a number of collisions with other clouds. It may well be that the clouds are disrupted in cloud-cloud collisions; on the other hand, some clouds might join together in a collision. However, as long as the clouds are not disrupted completely, the results obtained will probably be valid. For example, if on collision a cloud breaks up into two smaller clouds, these clouds will undergo Brownian motion themselves and the general random motion of the gas will still be treated correctly. Actually, as Münch and Zirin have noted, there does seem to be some mechanism which prevents the disruption of the clouds. Perhaps the clouds have an internal magnetic field which confines the ions and neutral particles (by means of their interaction with the ions) to a certain volume. Alternatively, the clouds might be in pressure equilibrium with a hot, less dense inter-cloud medium and galactic halo. We have essentially taken the former view, since we have assumed that in the process of molecule formation in a cloud the total density $n_0 (=n_1 + 2n_2)$ remains constant. This leads to the result $F(s) = 1 - e^{-ks}$ for the fraction in molecular form as a function of s, the distance travelled since the last ionization. If the clouds are in pressure equilibrium, then it is more reasonable

to take $n_1 + n_2$ = constant during the gradual molecule formation. One can easily show that this leads to the following result for the fraction in molecular form as a function of s:

$$F'(s) = 2 \frac{1 - e^{-\bar{k}s/2}}{2 - e^{-\bar{k}s/2}} . \tag{284}$$

The mean fraction (averaged over clouds) then becomes (see eq. 223)

$$\langle F' \rangle = \int_0^\infty \varkappa \, e^{-\varkappa s} \, F'(s) \, ds$$

$$= 2 \nu \int_0^1 x^{\nu - 1} \frac{1 - x}{2 - x} \, dx = \langle F'(\mu) \rangle , \tag{285}$$

where $\nu = 2 \varkappa / k = 4/\mu$. The fraction $\langle F'(\mu) \rangle$ computed from (285) is shown below in Fig. 42. The function $\langle F(\mu) \rangle = \mu/(\mu + 2)$ is also shown and we see that there is little difference in the two functions. It is quite remarkable that, given the value of the dimensionless parameter μ, one calculates very nearly the same value for the fraction in molecular form by making different basic assumptions.

Finally, it should be remembered that we have taken the rate constant for formation on grains to remain constant during the conversion to molecular form. This assumes either of the following is true: (1) the characteristic time for grain formation is much longer than the molecular conversion time, or (2) the characteristic time for grain formation is much shorter than the molecular conversion time.
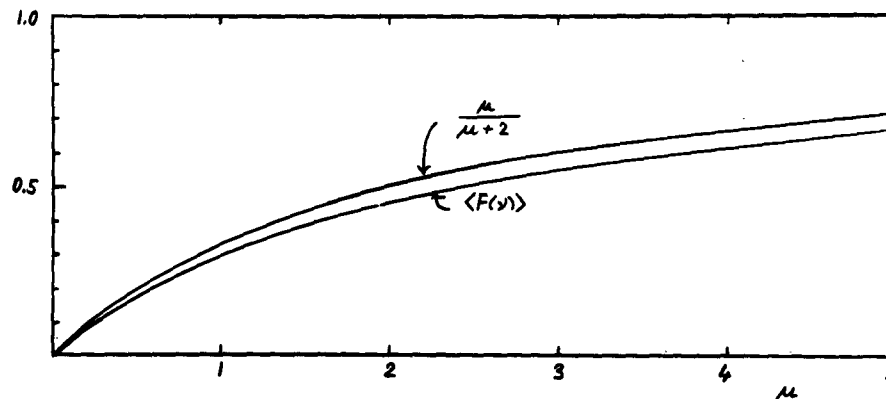
Fig. 42

Fraction in molecular form as a function of μ.

The case (2) would correspond to the situation where the grains are formed rapidly after being destroyed in cloud-cloud collisions or in close passages near bright stars. The observed grain density would then be interpreted either as the saturation value or as a steady state value, the steady state being established in a time short compared with the time for molecular formation.

(d) <u>Molecule/atom ratio between the spiral arms</u> - One might ask about the molecular concentration between the spiral arms of the galaxy where no atomic hydrogen is observed. We have essentially assumed an infinite plane of gas in considering the diffusion of clouds. Actually, the clouds are likely to diffuse $\sim \frac{1}{2}$ kpc in the plane of the spiral arms between ionizations and the absence of bright

stars between the arms leads one to expect a smaller

ionization rate there and a corresponding molecule/atom

ratio that is higher than in the spiral arms. There may be

such an effect although it is likely to be relatively small

in magnitude and of minor importance. For spiral galaxies

one generally observes an absence of dust between the arms

so that a high gas (atomic or molecular) abundance would be

unlikely since the gas tends to "drag along" the dust (and

vice-versa). Moreover, since we do not observe star

formation between the spiral arms, a high gas abundance would

be difficult to reconcile. It may be that the gas is con-

fined to the discrete spiral arms by either magnetic fields

or gravitational forces or both. In summary, while the

molecule/atom ratio may vary by, say, half an order of

magnitude in going from a spiral arm to the interarm region,

the absolute molecular concentration between the spiral arms

is likely to be small.

3. Dynamical astronomy's unobserved mass

About thirty years ago Oort made a study of the

motions of stars perpendicular to the galactic plane. From

the statistics of these motions in the z-direction he was

able to determine the mass density in the galactic plane.

This problem has been reinvestigated recently by Oort,[10]

Hill,[9] and others with the result that the density determined

in this manner is greater than previously thought. Of the

resulting mass density for the solar neighborhood about half

can be accounted for by the observed density of stars and gas. Oort has attributed the remaining "unobserved" mass to faint dwarf stars with $M_V > +15$. We shall try to see in this section whether one can account for this mass by assuming that it is due to molecular hydrogen.

The stellar motion studies essentially determine K_z, the acceleration in the z-direction. The total mass density is determined by Poisson's equation which becomes, in cylindrical coordinates with no Θ dependence,

$$\frac{\partial K_r}{\partial r} + \frac{K_r}{r} + \frac{\partial K_z}{\partial z} = -4\pi G \rho(r,z) \quad . \qquad (286)$$

By making use of Schmidt's model for the galaxy Oort has calculated the first two terms in (286) for the r-value corresponding to the sun. Oort also gives K_z as a function of z from his stellar dynamics studies. To calculate $\partial K_z / \partial_z$ (and $\rho(z)$) it is convenient to express Oort's K_z as a polynomial in z:

$$-K_z = k_1 |z| - k_2 |z|^2 \quad . \qquad (287)$$

By applying a least squares fit to Oort's data on K_z out to z = 300 pc one finds $k_1 = 8.90 \times 10^{-30}$ sec^{-2}, $k_2 = 1.014 \times 10^{-32}$ sec^{-2} pc^{-1}. We then have

$$\frac{\partial K_z}{\partial z} = -k_1 + 2k_2 |z| \quad , \qquad (288)$$

which when substituted into (286) allows one to compute $\rho(z)$ and the unobserved mass density $\rho(z) - \rho_{obs}(z)$. The results

are shown in Fig. 43. As seen from Fig. 43 the half width
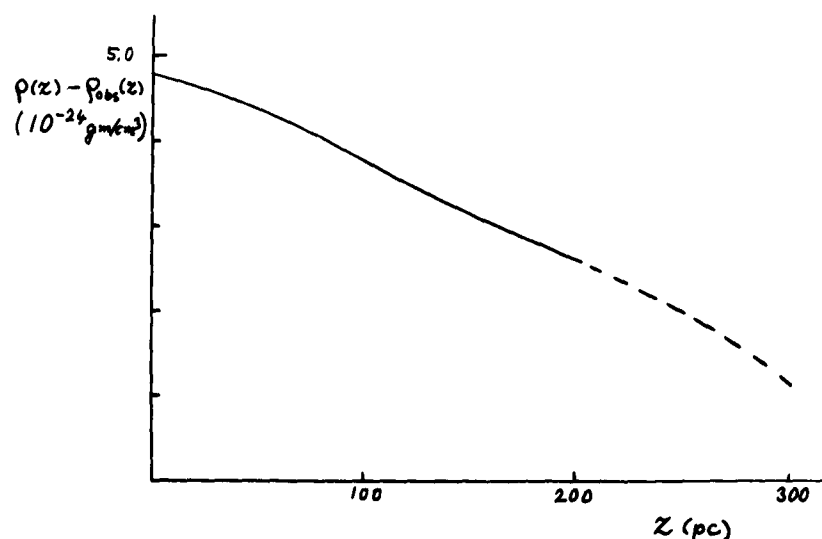
Fig. 43

Unobserved mass as a function of z.

of the distribution of unobserved mass is about 200 pc which is appreciably larger than the half width of the observed distribution of atomic hydrogen. Since we expect the molecular hydrogen to have essentially the same distribution as the atomic hydrogen, the results for the unobserved mass would seem to rule out H_2 as the major contributor. However, K_z was determined from the distribution of K giants which have a much larger spread in z than the interstellar gas. One would not be able to tell from the motion of a star at high z what the distribution of mass was at low z, for while this mass determines the acceleration of the star the same mass spread out over larger z-values would give almost the

same acceleration. For this reason the significance of the distribution exhibited in Fig. 43 should be weighed with care.

4. <u>The gravitational scale height of the galactic gas</u>

Assuming equipartition one can predict the characteristic height of the gas above the plane of the galaxy from a knowledge of the gravitational potential $V(z)$ and the velocity distribution $f(v)$ of the interstellar clouds. Conversely, given the z-distribution $n_o(z)$ of the gas and $f(v)$ one can calculate the gravitational potential function. The distribution of mass should be related to the potential function by an equation of the form

$$n_o(z) = e^{-mV(z)/kT} \quad , \tag{289}$$

where we have denoted the mass of the cloud by m and introduced a "temperature" for the cloud motions. The distribution $n_o(z)$ is normalized so that $n_o(0) = 1$ (also $V(0) = 0$). We assume equipartition in order to relate T to the mean squared velocity by means of the relationship $\frac{3}{2}kT = \frac{1}{2}m\overline{v^2}$, which allows one to rewrite (289) as

$$n_o(z) = e^{-3V(z)/\overline{v^2}} = e^{-V(z)/\overline{v_z^2}} \quad , \tag{290}$$

or equivalently:

$$V(z)/\overline{v_z^2} = - \ln n_o(z) \quad . \tag{291}$$

The total mass distribution $n_o(z)$ may be found from Schmidt's distribution $a(z)$ of atomic hydrogen and the results derived in section B2b of this chapter for the molecular distribution. The fraction of the hydrogen which is in molecular form was shown to have a slight z-dependence given by

$$\langle F(z) \rangle = \langle F(0) \rangle \; (1 + \Delta f^*(z)), \qquad (292)$$

The total density n_o is related to the atomic density n_1 by

$$n_o/n_1 = (2n_2 + n_1)/n_1 = (1 - \langle F(z) \rangle)^{-1} \qquad (293)$$

Because of the smallness $(\Delta \ll 1)$ of the deviation of the molecular distribution (and total distribution) from the atomic distribution we have, approximately,

$$\frac{n_o(z)}{a(z)} = 1 + \frac{\langle F(0) \rangle}{1 - \langle F(0) \rangle} \; \Delta f^*(z) \quad , \qquad (294)$$

and

$$\frac{V(z)}{\overline{v_z^2}} = - \ln n_o(z) \approx - \ln a(z) - \frac{\langle F(0) \rangle}{1 - \langle F(0) \rangle} \Delta f^*(z)$$

$$(295)$$

The second term on the right of (295) is actually quite small compared with $\ln a(z)$ and we have to a very good approximation:

$$V(z)/\overline{v_z^2} \approx - \ln a(z) \quad . \qquad (296)$$

This last relation readily allows the computation of the gravitational potential in units of $\overline{v_z^2}$ and hence the <u>shape</u>

of the potential function. This potential is to be compared
with Oort's function calculated from the statistics of star
densities. For the values of z that we shall be concerned
with, Oort's potential function can be well represented by
(see previous section)

$$V_s(z) = \frac{1}{2} k_1 |z|^2 - \frac{1}{3} k_2 |z|^3 , \qquad (297)$$

where the subscript s has been added to denote the fact that
this function is derived from observations of **stars**. As
shown in Appendix B, $\overline{v_z^2} = \overline{v^2}/3 = 2\eta^2$, so that we have

$$V_s(z)/\overline{v_z^2} = V_s(z)/2\eta^2 . \qquad (298)$$

The two potential functions, one computed from the distri-
bution of the gas and the other from the stars, are shown
in Fig. 44.

We see from Fig. 44 that the potential distribution
required to produce the observed gas distribution is much
steeper for small z than Oort's potential function as
determined from stellar motions. It is tempting to interpret
this steep potential well of -ln a(z) as a result of the
large self-gravitation of the gas as Gold[13] had done. The
potential due to the self-gravitation of the observed atomic
hydrogen cannot account for the deep well. We can easily
calculate the required mass density at z=0 needed to produce
the steep potential function of - ln a(z), since for small
z the gaussian distribution
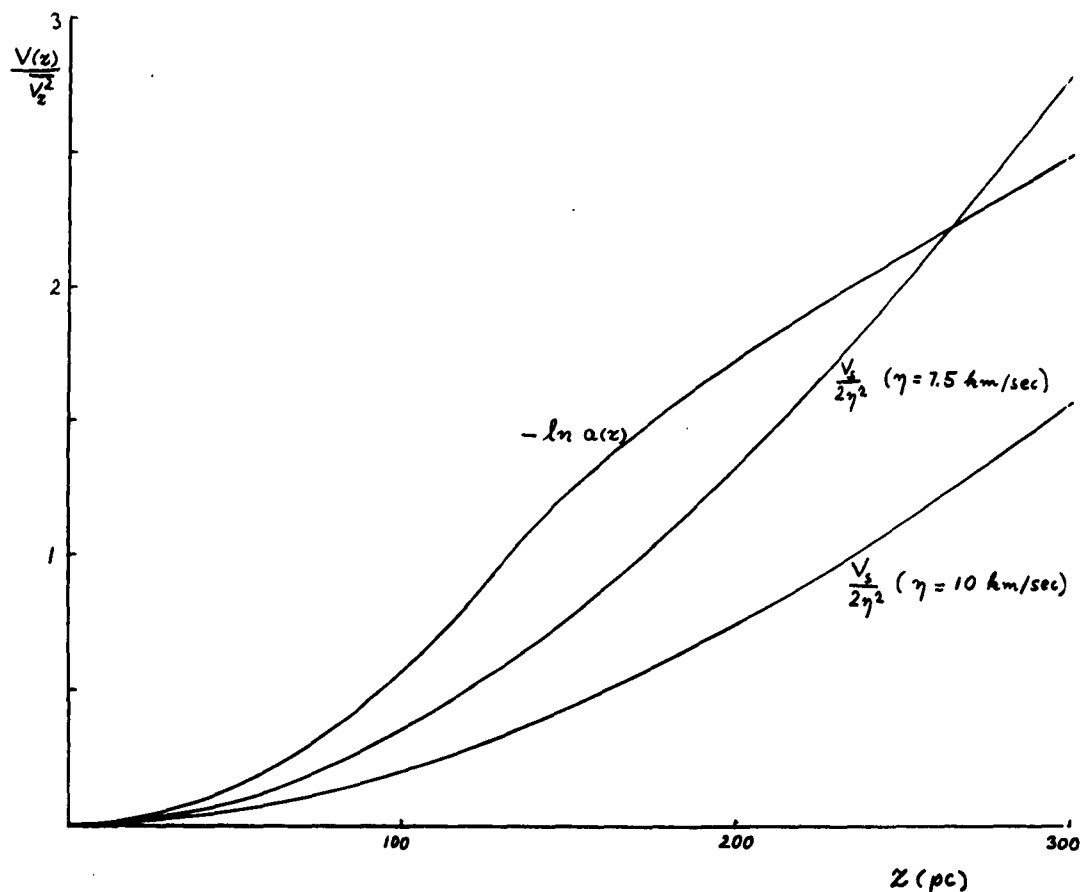
Fig. 44

Potential functions (in units of the mean squared
velocity of the clouds in the z-direction) as
determined by the observed distributions of gas
and stars.

$$a(z) \;=\; e^{-z^2/h_g^2} \tag{299}$$

is a very good approximation. Then for small z

$$V(z) \;=\; \overline{v_z^2} \; \frac{z^2}{h_g^2} \quad , \tag{300}$$

and Poisson's eq. (293) becomes

$$\frac{\partial K_r}{\partial r} \; + \; \frac{K_r}{r} \; - \; \frac{2\overline{v_z^2}}{h_g^2} \;\; = \;\; -4\pi G \; \rho(r,z) \quad . \qquad (301)$$

At $z = 0$ the first two terms on the left of (301) can be evaluated from the constants of galactic rotation to be 0.60×10^{-30} sec^{-2}. Substituting $h_g = 4.08 \times 10^{20}$ cm and $\overline{v_z^2} = 2\,\eta^2$ with $\eta = 7.5$ km/sec we get $\rho(0) = 15.4 \times 10^{-24}$ gm/cm^3; higher values of η would give even larger densities. Unfortunately, the characteristic velocity is poorly known, various authors have suggested values ranging from 5 km/sec to 12 km/sec (for example, the 21 cm investigations gave $\eta = 8.5$ km/sec). Observable stars and gas amount to about 5×10^{-24} gm/cm^3 so that in this analysis the majority of the mass density appears to be unaccounted for.

One can calculate the total mass density at various values of z in this manner. The result obtained is shown schematically in Fig. 45a. For comparison the mass density required to explain the observed stellar distribution is shown in Fig. 45b. The density needed to produce the observed distribution of gas is roughly constant and confined to within about 110 pc ($\equiv z_g$) of the galactic plane; beyond z_g the density needed is essentially zero. This results because the distribution $a(z)$ is essentially gaussian for $z < z_g$ and exponential for $z > z_g$. The characteristic height of 110 pc is just the half width of the observed distribution of atomic hydrogen (and presumably of molecular hydrogen) so that this
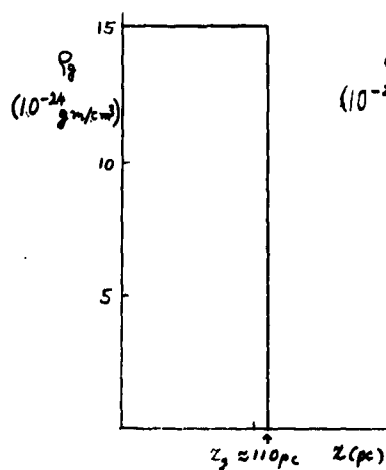
Fig. 45a.
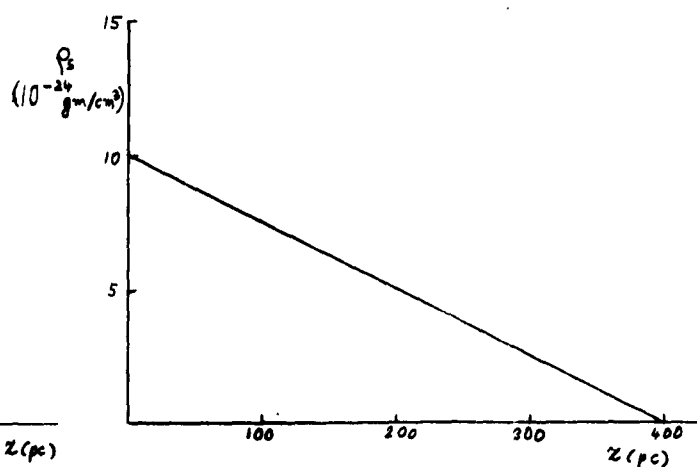
Fig. 45b.

$\rho(z)$ producing $V_g(z)$

$\rho(z)$ producing $V_s(z)$

result would suggest that the unobserved mass is molecular hydrogen.

As mentioned earlier, because of the large characteristic z-values of K giants ($|\bar{z}| \simeq 300$ pc) whose distribution gave the result in Fig. 45b, the statistics on the distribution of stars may not be good enough to resolve the width of a distribution as shown in Fig. 45a. The stellar motion studies would then essentially give $\int_0^z \rho(z')dz'$, a measure of the total amount of mass within z. For the distribution $\rho_g(z)$, $\int_0^{z > z_g} \rho_g(z')dz' \simeq 1.7 \times 10^{-21}$ gm-pc/cm^3. The distribution $\rho_s(z)$ integrated from 0 to 250 pc gives about the same "total mass", while $\rho_s(z)$ integrated from 0 to 400 pc gives about 2.0×10^{-21} gm-pc/cm^3.

This analysis has implicitly assumed that the galactic gas is isothermal and composed of clouds of identical mass. Both of these assumptions are objectionable (for example, that the cloud velocity distribution is non-maxwellian might indicate a distribution of cloud masses). However, if the interstellar gas is viewed as a highly turbulent medium instead of as a "particle" gas of discrete clouds, a baro-metric-type relation of the same form as (296) would relate the (mass) density and gravitational potential. In this case, the barometric equation results from considerations of (turbulent) pressure equilibrium (rather than thermal equilibrium) in which $\overline{v_z^2}$ is now interpreted as the mean squared systematic turbulent velocity in the z-direction. The correctness of the shape of the potential (Fig. 44) would still hinge on the constancy of $\overline{v_z^2}$ with z, however,

C. Outlook for Future Observations of Interstellar H_2

As we have shown, if the recombination reaction on the surface of the interstellar grains is effective, one can expect a molecular concentration in H I clouds comparable to the atomic value. Such a large amount of H_2 could easily be detected by the satellite-borne ultraviolet spectroscope designed by the group at the Princeton Observatory and scheduled for operation in 1966.

A number of people have considered the possibility of observing infrared radiation from interstellar H_2. One such experiment which has a good chance of succeeding is described in a paper[58] by M. Harwit and the author. The essential idea

is the following. In a region of high density surrounding
a bright star an appreciable fraction of the radiation from
the central star which is absorbed in the (electronic)
resonance lines of H_2 is converted into near infrared
vibration-rotation photons. For when the excited (by
resonance line absorption) molecule reverts to the ground
electronic state, it can end up in excited vibrational levels.
The vibrationally excited molecule then emits a series of
quadrupole infrared photons as it cascades to the ground
state. Certain dense regions, e.g. the Orion Nebula, should
then emit an amount of infrared radiation in the form of
vibration-rotation lines which, according to our estimates,
should be detectable. The radiation would be emitted from
the region surrounding the star where the resonance line is
absorbed. Even for a rather small molecular concentration
this region would correspond to a thin shell outside the
Strömgren sphere. Attempts to observe this radiation may be
made within the next year.

A very interesting suggestion regarding interstellar H_2
has been made recently by G. H. Herbig.[59] He observed that
the very broad interstellar absorption line at 4430 Å almost
coincides in wavelength with a transition between two excited
triplet states of H_2, the lower of which is metastable.
Herbig suggests that the 4430 Å line may correspond to an
absorption by hydrogen molecules on the surface of the inter-
stellar grains, the interactions with the solid accounting

for both the broadening and shift of the line. The problem
with this identification is that of populating the excited
triplet state so that the molecule can absorb at 4430 $\overset{o}{A}$.
Herbig has been unable to account for a mechanism which will
produce enough molecules in the excited triplet state to
explain the strength of the 4430 line. The opinion here is
that while the problems associated with identifying this
line with H_2 seem very great, attempts to explain the diffuse
interstellar lines as arising from atoms or molecules bound
to the interstellar grains may turn out to be very fruitful.

D. **Star Formation - Early Stellar Evolution**

There is a good deal of evidence that stars form out of
condensations of the interstellar gas and that star formation
is still taking place in the spiral arms of our galaxy. The
qualitative details of this condensation process are poorly
understood, however, and the general phenomenon of star
formation has remained one of the biggest unsolved problems
of modern astrophysics. Two principal difficulties are:
(1) how do the dilute gas clouds reach the stage where their
gravitational self energy allows them to contract against
the pressure from the kinetic energy (temperature) of their
constituent atoms and molecules, and (2) how is the initial
angular momentum of the gas cloud lost as the cloud contracts?
The answers to both of these questions are unknown although
there have been many suggestions. Several useful surveys of
the general problem may be found in the collection of prize

essays by Burbidge et al.[60]

We shall consider here only one particular phase of star formation, a phase which all stars are very likely to go thru, however. This is the very early stage of stellar evolution when the gas is still dilute, cool, gravitationally stable to fragmentation, and composed essentially of hydrogen molecules. This stage corresponds to the fairly dense protostar for which we shall assume a quasi-steady state exists in which the gravitational interactions are strong enough to establish a condition whereby the virial theorem is applicable. Moreover, we shall assume that there exists some efficient mechanism for the protostar to get rid of its angular momentum so that we shall not have to worry about rotation. It is quite certain that the gas is indeed in molecular form at this stage since, even if the grain recombination mechanism should fail, at the high densities involved other processes, especially associative detachment, will take place and insure complete formation of molecular hydrogen in a time shorter than the lifetime of this stage of evolution. Hydrogen molecules play a major role in the protostar development in this stage because they are very efficient at radiating away energy by de-excitation of rotational levels. The rate of radiation turns out to be proportional to $e^{-E_2/kT}$, where E_2 is the excitation energy of the $J = 2$ rotational level and T is the gas kinetic temperature. This strong dependence of the rate of radiation

on temperature tends to make the gas isothermal. With the help of the virial theorem, then, we can immediately write down the expression for the total energy of the gas mass:

$$\mathcal{E} = \frac{3\gamma - 4}{3(\gamma - 1)} \, \Omega \tag{302}$$

where γ is the ratio of specific heats for the gas and Ω is the total gravitational potential energy of the protostar. For a protostar of uniform density

$$\Omega = -\frac{3}{5} \frac{GM^2}{R} \, , \tag{303}$$

where M is its mass, and R its radius. For other mass distributions the numerical factor in the expression for Ω will be different but the dependence on M and R will be the same. From (302) and (303) we get a relation between $\mathcal{E}$ and R and so a relation between the contraction and energy loss rates. We neglect the variation of γ with R and get for the rate of energy loss from the gas:

$$\dot{\mathcal{E}} = \gamma \frac{\dot{R}}{R^2} \tag{304}$$

where

$$\gamma \equiv \frac{3\gamma - 4}{\gamma - 1} \frac{GM^2}{5} \, . \tag{305}$$

We see immediately that if the gas is to contract ($\dot{R} < 0$) by radiating energy ($\dot{\mathcal{E}} < 0$), γ must be less than 4/3.

We shall be concerned with protostars of temperatures such that $\Delta E / kT \ll 1$, ΔE being the excitation energy for

rotational levels of H_2. The gound state $(J = 0)$ is then
the most heavily populated. Moreover, ortho-para conversions
by collisional process are negligible because of the large
activation energy involved. The principal excitation is
then the population of the $J = 2$ state of para-hydrogen by
collisions with other hydrogen molecules. As Osterbrock[48]
has emphasized, the $J = 2$ state is more likely to be de-
excited to $J = 1$ and then to $J = 0$ (para $\rightarrow$ ortho $\rightarrow$ para)
by means of forbidden dipole radiation instead of falling
directly to the ground state in a quadrupole transition.
The population of the $J = 2$ state may be found from the
steady state equation (we neglect effects of downward
transitions from higher J states because of their high
excitation energy):

$$\dot{n}_{J=2} = n_{J=0} \, n \, \overline{v\sigma_{0\rightarrow2}} - n_{J=2} \, (A_2 + n \, \overline{v\sigma_{2\rightarrow0}}) = 0,$$

$$(306)$$

$$(n = n_{any \; J} \approx n_{J=0})$$

where the n's represent the number of molecules in the J
level per cm^3, A_2 is the de-excitation transition probability
(for $J = 2 \rightarrow J = 1$) per unit time, the σ's are the cross
sections for collisional excitation and de-excitation, and
v is the relative velocity. From detailed balance

$$\overline{v\sigma_{2\rightarrow0}} = \overline{v\sigma_{0\rightarrow2}} \, (g_0/g_2) \, e^{E_2/kT} \quad , \quad (307)$$

g_0 and g_2 being the degeneracies of the $J = 0$ and $J = 2$ states respectively. The de-excitation cross section $\sigma_{2 \to 0} \equiv \sigma_d$ has been measured indirectly and is approximately[49] 4.0×10^{-18} cm^2. The rate constant $\overline{v\sigma_{2 \to 0}}$ is then $\overline{v}\,\sigma_d$, where $\overline{v} = 4(kT/\pi M_{H_2})^{1/2}$ is the mean relative velocity of the hydrogen molecules. We have then for the population of the $J = 2$ level:

$$n_{J=2} = n\,(g_2/g_0)\,\frac{e^{-E_2/kT}}{1 + A_2/n\overline{v}\sigma_d} \quad . \tag{308}$$

Now, for the densities that we shall be concerned with the infrared radiation emitted in the de-excitation will not be absorbed or scattered appreciably by the grains in the protostar, especially if the grains are dielectric as is presently thought. Nor will the radiation be absorbed by hydrogen molecules or by molecules other than hydrogen. The small probability of the transition prevents its self absorption, especially since the bulk of the emitted radiation involves the transition $J = 2 \longrightarrow J = 1$ which is not a resonance transition. Molecules other than hydrogen cannot absorb the line since even if they happened to have strong infrared absorption lines at the right wavelength (a chance coincidence), the Doppler width of these lines would be much less than the corresponding width of the lines emitted by H_2 so that most of the H_2 emission line would escape without absorption. That the infrared opacity of

the grains is low is certainly true for the more massive
protostars for which the mean free path for the infrared
radiation is much less than the protostar radius in the
stage of evolution which we are interested in. It is true
with less certainty for masses of about $M_\odot$ due to our lack
of knowledge of the infrared absorption properties of the
grains. Because of this low opacity to the radiation the
energy loss from the protostar results from radiation from
the whole <u>volume</u> of the protostar instead of from a thin
surface layer and we have

$$\dot{\mathcal{E}} = - \frac{4\pi}{3} R^3 n_{J=2} E_2 A_2 = - M \frac{E_2 A_2}{M_{H_2}} \frac{n_{J=2}}{n} . \quad (309)$$

Substituting the expression for $n_{J=2}$ with the help of the
virial theorem again which gives the relation

$$kT = GMM_{H_2}/5R \quad (310)$$

between T and R, we have

$$\dot{\mathcal{E}} = - \eta \, e^{-\kappa R} , \quad (311)$$

with

$$\kappa = 5E_2/GMM_{H_2} , \quad (312)$$

$$\eta = \eta_e/(1 + q_e) , \quad (313)$$

$$\eta_e = M \frac{E_2 A_2}{M_{H_2}} \frac{g_2}{g_0} , \quad (314)$$

and

$$q_e = A_2/n\bar{v}\sigma_d$$

$$= \frac{A_2 M_{H_2}}{3\sigma_d} (5/G)^{1/2} (\pi/M)^{3/2} R^{7/2}. \quad (315)$$

q_e is a measure of the deviation from thermodynamic equilibrium (TE) in the rotational levels.

If $q_e \ll 1$ (small R), TE exists.

If $q_e \gg 1$ (large R), TE doesn't exist.

It turns out that for the values of R that we shall be particularly interested in TE exists.

The rate of contraction of the protostar can be calculated by combining (304) and (311) to give

$$\dot{R} = -\frac{\eta}{\zeta} R^2 e^{-\varkappa R} . \quad (316)$$

Because of the exponential dependence the contraction is slow at large R which corresponds to low temperature. However, the factor multiplying the exponential in (316) is so large that for $\varkappa R \approx 8$ the contraction rate approaches the contraction rate that the protostar would have if its mass elements were free falling from infinite R towards its center. This free fall or collapse rate is given by

$$\dot{R}_{ff} = -\zeta R^{-1/2} , \quad (317)$$

where

$$\zeta = (2GM)^{1/2} . \quad (318)$$

Thus the protostar contracts slowly at first but increases its rate rapidly as it contracts; finally at a critical radius R_c the contraction rate approaches the upper limit given by the free fall contraction value (see Fig. 46).
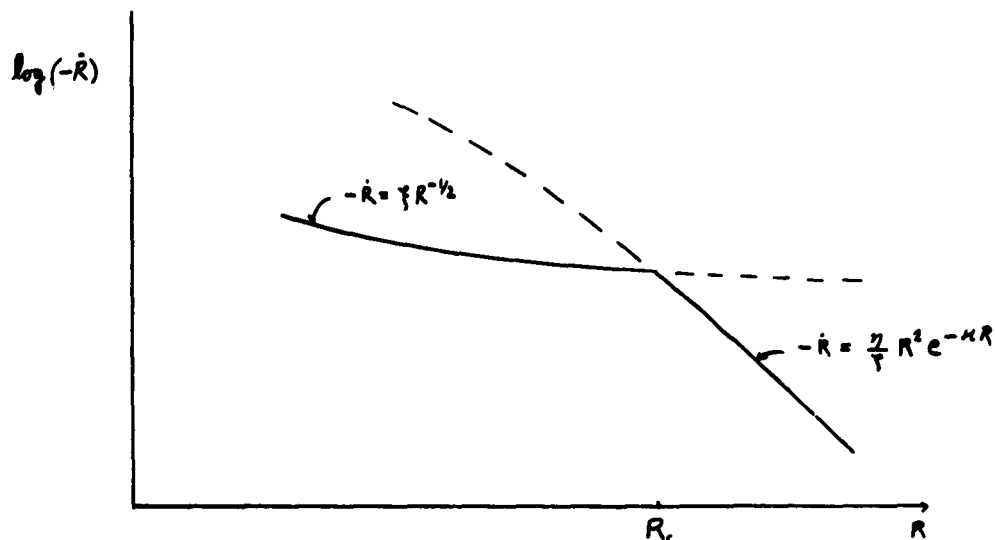
Fig. 46

Velocity of collapse as a function of R

The critical radius R_c is of interest and has been calculated for several different stellar masses. Using $\sigma_d =$ $4.0 \times 10^{-18} \text{ cm}^2$, $A_2 = 2 \times 10^{-9} \text{ sec}^{-1}$, $\gamma = 5/3$, and the other physical constants which are better known one finds the critical radii, temperatures, and densities given in Table 4 for stellar masses of 1, 3, 10, and 30 $M_\odot$. The calculated critical temperature T_c is more significant than R_c and n_c since it does not depend strongly on the density distribution assumed for the protostar; none of the critical

Table 4

M	R_c (cm)	T_c (°K)	n_c (cm^{-3})	t_{ff} (yr)
$M_\odot$	1.0×10^{16}	64	1.3×10^8	5.8×10^3
$3M_\odot$	3.6×10^{16}	54	9.5×10^6	2.2×10^4
$10M_\odot$	1.4×10^{17}	45	7.0×10^5	8.0×10^4
$30M_\odot$	4.7×10^{17}	41	4.2×10^4	3.3×10^5

quantities are strongly dependent on the physical parameters (such as A_2) which do not appear in the exponential factor in (316). The weak dependence on these parameters is a result of the steepness of $\dot{R}$ at the critical R. In the table we also give a rough estimate of the time scale for the collapse calculated from $t_{ff} = (G\rho_c)^{-1/2}$.

We see that due to the efficient radiative properties of H_2 the collapse phase begins at quite low temperatures. It is hard to say where the collapse will stop. Certainly all the H_2 will be dissociated before the end of the collapse. Cameron[61] has expressed the opinion that the collapse goes on thru the ionization of hydrogen and on thru the single and double ionization stages of He. The opacity of the material will then have increased so that radiation comes only from the surface layer and the protostar will begin the so-called Kelvin contraction phase.

It is natural to ask whether one could hope to find observational evidence that stars go thru the evolutionary

stage just described. If one could observe the infrared
(42.4μ) radiation coming from a small region of space where
there is a suspicion that a star is forming, the arguments
presented here could be considered verified with a high
probability. The maximum amount of this radiation emitted
per second by a protostar would be

$$|\dot{\mathcal{E}}| \leq \eta_e \cdot \tag{319}$$

If the protostar is at a distance R, the energy flux
received at the earth would be

$$|\dot{\mathcal{E}}|/\Delta A \leq \eta_e/4\pi R^2. \tag{320}$$

For a protostar of 30 $M_\odot$ at a distance R = 500 pc we get

$$|\dot{\mathcal{E}}|/\Delta A \sim 4 \times 10^{-14} \text{ watt/cm}^2.$$

The energy flux received per solid angle would, of course,
be much larger. It is quite possible that this radiation
could be observed when observations are made from satellites.
Of course, one would have to be fortunate enough to find a
protostar which is in the right stage where its rate of
emission is at maximum. Some of the so-called "globules"
seem to have the right size. Hopefully, such a series of
investigations can be carried out in a few years.

It is the opinion of the author that the collapse
phase is the only stage of stellar evolution in which
hydrogen molecules play a major role. How the gas
condenses to the early beginning of this stage remains a
mystery and it is not likely that molecules can point to
a way out of the difficulty.

APPENDIX A - PHOTODISSOCIATION AND PHOTOIONIZATION

1. ## Generalities about molecular structure and molecular processes

All approaches to molecular strcture are based on the realization that the electronic mass (m) is much smaller than the nuclear mass (M). Because of this mass difference, the electronic motion is thought to "follow" (to a certain extent) the nuclear motion, that is, the electrons are able to adjust themselves to the instantaneous internuclear distance. This is the physical basis for the so-called Born-Oppenheimer (B-O) approximation which we shall consider only for diatomic molecules. Denoting the electronic coordinates of the molecule by r and the relative nuclear coordinates by R , the B-O approximation consists in a separation of the total wave function for the molecule thusly (we neglect spin)

$$\psi(r, R) \simeq \psi_e(r; R) \psi_{v,r,e}(R) . \qquad (A1)$$

The electronic part contains the internuclear distance only as a parameter. One can easily show by simple order of magnitude arguments that this approach leads to the following gradation of energies for the molecule:

$$\text{Electronic energy}: \quad E_e \sim e^2/a_o \qquad \text{(A2)}$$

$$\text{Vibrational energy}: \quad E_v \sim \varkappa^2 \, E_e \qquad \text{(A3)}$$

$$\text{Rotational energy}: \quad E_r \sim \varkappa^4 \, E_e \qquad \text{(A4)}$$

where

$$\varkappa \;=\; (m/M)^{1/4} \qquad \text{(A5)}$$

To these relations we add two more which give the approximate spread of the wave functions for electronic and vibrational motion.

$$\Delta x_e \;\sim\; a_o \qquad \text{(A6)}$$

$$\Delta x_v \;\sim\; \varkappa \, \Delta x_e \qquad \text{(A7)}$$

It is really these last two relations which form the basis of the Franck-Condon principle.

In radiative processes, the cross section (for absorption) or the intensity (for emission) is proportional to the square of the matrix element of the electronic dipole operator between the initial and final electronic and vibrational states (we neglect rotation). The Franck-Condon approximation consists in a breaking down of this matrix element into a product of an electronic and a vibrational factor.

$$\langle e', v' \mid \mathbf{r} \mid e, v \rangle \;\approx\; \langle e'(R_o) \mid \mathbf{r} \mid e(R_o) \rangle \, \langle v' \mid v \rangle \qquad \text{(A8)}$$

The electronic matrix element is to be evaluated at the internuclear distance R_o where the vibrational overlap integral $\langle v' \mid v \rangle$ is a maximum. The cross section for a

photon absorption process, e.g., photodissociation or photoionization, is then given by

$$\sigma_{v'v} = \sigma_e \left| \langle v' | v \rangle \right|^2 \tag{A9}$$

where σ_e is the electronic factor. For photodissociation the vibrational state v' lies in the continuum and the vibrational wave function has to be normalized accordingly. We consider this in the next section.

2. Photodissociation

(a) Photodissociation to repulsive state - For ordinary atomic transitions the absorption coefficient $\mathcal{H}_\omega(\text{cm}^{-1})$ satisfies the relation

$$\int \mathcal{H}_\omega d_\omega = \frac{2\pi^2 e^2}{m c} \, n \, f \tag{A10}$$

where n is the density in cm^{-3} of the absorbing atom and f is the oscillator strength for the transition. The absorption coefficient $\mathcal{H}_\omega (= n \, \sigma_\omega)$ is proportional to the square of the matrix element of the electronic dipole operator. For a molecular transition, and in particular for one involving a dissociation, the cross section is proportional to the square of the vibrational overlap factor. With one of the vibrational states in the continuum we write the overlap integral as $\langle E | v \rangle$ where E stands for the relative kinetic energy of the dissociated atoms and v represents the initial (bound) vibrational state. We have then for the generalization of (A10) for molecular transitions

involving a dissociation

$$\mathcal{U}_\omega d_\omega = n \; \sigma_\omega \; d\omega = \frac{2\pi^2 e^2}{m \; c} \; n \; \overline{f}_e \; \left| \left\langle E \middle| v \right\rangle \right|^2 \; dN \;, \qquad \text{(A11)}$$

where dN is the number of vibrational continuum states in the energy interval $dE = \hbar \; d\omega$, and $\overline{f}_e$ is the oscillator strength evaluated at the equilibrium internuclear separation for the initial (ground) state. With a normalization length L for the coninuum state,

$$dN = \frac{L \; dp}{2\pi \hbar} = \frac{L}{4\pi} \sqrt{\frac{2\mu}{E}} \; d\omega \;, \qquad \text{(A12)}$$

μ being the reduced mass of the two atom system after dissociation. The cross section for photodissociation is then

$$\sigma_\omega = \frac{2\pi^2 e^2}{m \; c} \; \overline{f}_e \; \left| \left\langle E \middle| v \right\rangle \right|^2 \; \frac{L}{4\pi} \sqrt{\frac{2\mu}{E}} \;. \qquad \text{(A13)}$$

We now consider two different approximations for the continuum wave function ψ_E. Case I: ψ_E is a δ-function at the classical turning point (see Fig. A1 below).
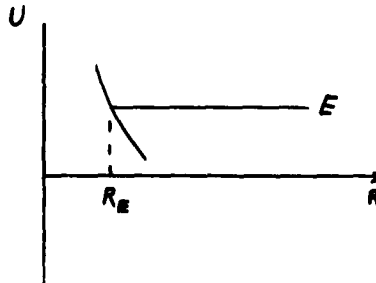
Fig. A1

Classical turning point for a repulsive potential

$$\psi_E^{(I)}(R) = C_E \, \delta(R - R_E) \quad . \qquad (A14)$$

We determine C_E from the normalization condition

$$\left|\langle E|v\rangle\right|^2 \, dN = 1 \quad , \qquad (A15)$$

which becomes

$$\int C_E^2 \, \psi_v^2(R_E) \, \frac{L}{4\pi} \, \sqrt{\frac{2\mu}{E}} \, d\omega = 1 \quad . \qquad (A16)$$

Changing the variable of integration to R_E by

$$d\omega \longrightarrow \left|\frac{\partial\omega}{\partial R_E}\right| dR_E \qquad (A17)$$

and taking the slowly varying factors out of the integral in (A16), we have

$$C_E^2 \, \frac{L}{4\pi} \, \sqrt{\frac{2\mu}{E}} \, \left|\frac{\partial\omega}{\partial R_E}\right| \int \psi_v^2(R_E) \, dR_E = 1 \quad . \qquad (A18)$$

Since ψ_v is normalized to unity we get for the relation which determines C_E :

$$C_E^2 \, \frac{L}{4\pi} \, \sqrt{\frac{2\mu}{E}} \, \left|\frac{\partial\omega}{\partial R_E}\right| = 1 \quad . \qquad (A19)$$

When C_E^2 from (A19) is substituted into the expression (A13) for the cross section, we have, finally,

$$\sigma_\omega = \frac{2\pi^2 e^2}{m\,c} \, \overline{f}_e \, \psi_v^2(R_E) \, \left(\left|\frac{\partial\omega}{\partial R_E}\right|\right)^{-1} \quad . \qquad (A20)$$

For a repulsive state the range of R_E covers the complete range of R and we have, again using the normalization condition for ψ_v,

$$\int \sigma_\omega d_\omega \;\; = \;\; \frac{2\pi^2 e^2}{m \, c} \;\; \overline{f}_e \;\; . \tag{A21}$$

While the expression (A20) is very easy to use, higher
accuracy would require a more realistic treatment of the
continuum wave function. The following case can be
considered as an improvement over (A14).

Case II: ψ_E is a WKB wave function.

Away from the classical turning point, the WKB ψ_E is[62]

$$\psi_E^{(II)}(R) \;\; = \;\; \frac{C}{\sqrt{p(R)}} \;\; \sin \left(\frac{1}{\hbar} \int_{R_E}^{R} p(R') \, dR' + \frac{1}{4}\pi \right). \tag{A22}$$

To determine the normalization constant C we make use of
the asymptotic behavior of ψ_E which is

$$\psi_E^{(II)}(R) \longrightarrow A \sin (kR + \delta) \quad , \tag{A23}$$

where

$$k = p_E/\hbar, \;\; p_E = p(R = \infty) \cong p \quad . \tag{A24}$$

From the normalization condition

$$\int_0^L \psi_E^2 \; dR = 1 \tag{A25}$$

we get

$$A = (2/L)^{1/2} \quad . \tag{A26}$$

Comparing (A23) with (A22), we determine C to be

$$C = (2p/L)^{1/2} \quad , \tag{A27}$$

so that the normalized WKB wave function away from the turning point is

$$\psi_E^{(II)}(R) = \sqrt{\frac{2p}{L\, p(R)}} \; \sin\left(\frac{1}{\hbar}\int_{R_E}^{R} p(R')\, dR' + \frac{1}{4}\pi\right) .$$

(A28)

We match this wave function to a wave function around the turning point which is an Airy function. This procedure is described in the book[62] of Landau and Lifshitz. The result is that the continuum wave function for **all** R is given by

$$\psi_E = (2p/L)^{1/2}\, u_E , $$

(A29)

where

$$u_E = \begin{cases} (2\mu F\, \hbar)^{-1/6} \; \blacklozenge(-\zeta) & \text{near turning pt.} \\[2mm] (p(R))^{-1/2} \; \sin\left(\frac{1}{\hbar}\int_{R_E}^{R} p(R')\, dR' + \frac{1}{4}\pi\right) & \text{away from turning pt.} \end{cases}$$

(A30)

Here, $\blacklozenge$ is the Airy function

$$\blacklozenge(\zeta) = \pi^{-1/2} \int_0^{\infty} \cos\left(\frac{1}{3}u^3 + u\zeta\right) du, $$

(A31)

with

$$\zeta = (R + E/F)(2\mu F/\hbar^2)^{1/3} , $$

(A32)

$$F = -\left(\frac{\partial U}{\partial R}\right)_{R_E} . $$

(A33)

With the wave function given by (A30), the normalization condition (A15) becomes

$$\left|\langle E|v\rangle\right|^2 dN = \left|\langle u_E|v\rangle\right|^2 \frac{\mu}{\pi}\, d\omega , $$

(A34)

so that (A11) gives for the cross section

$$\sigma_\omega = \frac{2\pi\, e^2 \mu}{m\,c}\ \bar{f}_e\ \left|\left\langle u_E | v \right\rangle\right|^2 \quad . \qquad (A35)$$

(b) <u>Photodissociation to attractive states</u> - The two expressions for the photodissociation cross section which were derived in the previous section are also applicable when the upper electronic state in the dissociation process is an attractive state. For attractive states, however, (A20) is less accurate, since the errors involved in the approximation of a δ-function wave function no longer have a way of cancelling as they do when the upper state is repulsive. Nevertheless, (A20) <u>is</u> useful in deciding which electronic states contribute to the photodissociation process. For a more accurate calculation of the contribution of these states to the cross section it is advisable to then employ the relation (A35).

We shall consider the case where the potential curve for the upper state can be approximated by a Morse potential (see Fig. A2 below)
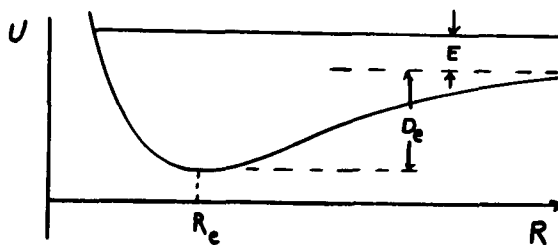
Fig. A2

Classical turning point for an attractive potential

$$U_e(R) = D_e (1 - e^{-\beta(R - R_e)})^2 . \qquad (A36)$$

The momentum $p(R)$ in (A30) would then be given by

$$p(R) = \left[2\mu \left\{ E + D_e - D_e(1 - \alpha'e^{-\beta R})^2 \right\} \right]^{1/2} \qquad (A37)$$

where

$$\alpha' = e^{\beta R_e} . \qquad (A38)$$

Making the substitutions

$$\gamma = 1 - \alpha'e^{-\beta R} , \qquad (A39)$$

$$k^2 = D_e/(E + D_e) , \qquad (A40)$$

and

$$y = k\gamma = y(R) , \qquad (A41)$$

we have

$$p(R) = (2\mu(E + D_e))^{1/2} (1 - y^2)^{1/2} . \qquad (A42)$$

The WKB wave function u_E becomes, since

$$dy = k\, d\gamma = k\alpha'\beta\, e^{-\beta R}\, dR = \beta(k - y)\, dR , \qquad (A43)$$

$$u_E = \left[2\mu(E + D_e)(1 - y^2(R)) \right]^{-1/4} \sin\left\{ \frac{1}{\hbar} \int_{-1}^{y(R)} \right.$$

$$\left. (2\mu(E + D_e))^{1/2} \frac{(1 - y^2)^{1/2}}{\beta(k - y')}\, dy' + \frac{1}{4}\pi \right\} . \qquad (A44)$$

To evaluate the integral in the argument of the sine we let

$$k = 1 - \epsilon , \qquad (A45)$$

where

$$\epsilon = 1 - (D_e/(E + D_e))^{1/2} \approx E/2D_e \quad . \qquad (A46)$$

Then,

$$k - y' = (1 - y')(1 - \zeta) \quad , \qquad (A47)$$

where

$$\zeta \equiv \frac{\epsilon}{(1 - y')} \quad . \qquad (A48)$$

The function to be integrated in (A44) becomes

$$f(y') = \frac{(1 - y'^2)^{1/2}}{k - y'} = \frac{1 + y'}{1 - y'} \frac{1}{1 - \zeta}$$

$$= \sqrt{\frac{1 + y'}{1 - y'}} \sum_{n=0}^{\infty} \zeta^n \quad . \qquad (A49)$$

Making the further substitution $y = \cos 2\theta$, $f(y)$ becomes

$$f(y) = \sum_{n=0}^{\infty} \frac{\epsilon^n}{2^{n-2}} f_n(y) \quad , \qquad (A50)$$

with

$$f_n(y) = \int_{\frac{1}{2}\cos^{-1}y}^{\pi/2} \frac{\cos^2\theta}{\sin^{2n}\theta} \, d\theta \quad . \qquad (A51)$$

The integrals $f_n(y)$ are easily evaluated. The first few
are enumerated below.

$$f_0(y) = \frac{1}{4}(-\cos^{-1}y - (1 - y^2)^{1/2} + \pi)$$

$$f_1(y) = Y + \frac{1}{2}\cos^{-1}y - \frac{1}{2}\pi, \quad Y = \sqrt{\frac{1+y}{1-y}}$$

$$f_2(y) = Y^3/3 \tag{A52}$$

$$f_3(y) = Y^3(Y^2 + 1/3)/5$$

$$\cdot \qquad \cdot$$
$$\cdot \qquad \cdot$$
$$\cdot \qquad \cdot$$

Hence, we obtain for the WKB wave function with a Morse potential:

$$u_E = 2\mu(E + D_e)(1 - y^2)^{-1/4} \sin\left\{ \frac{(2\mu(E + D_e))^{1/2}}{\beta\hbar} \right.$$

$$\left. \sum_{n=0}^{\infty} \frac{\epsilon^n}{2^{n-2}} f_n(y) + \frac{1}{4}\pi \right\} . \tag{A53}$$

These methods can be applied to the problem of the photodissociation of the hydrogen molecule. The edge for photodissociation of H_2 thru allowed transitions is at 14.5 eV corresponding to a dissociation in which one of the hydrogen atoms goes off in an excited state with $n = 2$. The sharpness of the edge can only mean that the upper state involved in the dissociation is an attractive state. Two attractive states which, on separation of the nuclei, result in one H-atom in the ground state and the other in the first excited state and which have large oscillator strengths for

transitions from the ground state are well known. They are the B $(^1\Sigma_u^+)$ and the C $(^1\Pi_u)$ states which give rise on absorption from the ground state X $(^1\Sigma_g^+)$, to the Lyman and Werner bands of the molecule. To decide which of these states is likely to contribute to photodissociation, (A20) was employed with the result that the X $\longrightarrow$ B transition can definitely be ruled out because of the very small vibrational overlap. The X $\longrightarrow$ C contribution is not negligible however. Herzberg and Monfils[63] have expressed this opinion after investigating the rotational structure of the dissociation edge. Employing (A35) with a WKB wave function calculated from (A53) matched to an Airy function at the classical turning point, one obtains a value $0.8_5 \times 10^{-18}$ cm^2 for the X $\longrightarrow$ C contribution to the photo-dissociation cross section at the edge. A harmonic oscilla-tor wave function (gaussian) was used for the ground vibrational state and an oscillator strength of 0.6 was taken for $\overline{f}_e$. This semi-emperical value was arrived at in the following manner. The "experimental" f-value from dispersion data[64] of 0.84 has been taken to be due to the sum of the transitions X $\longrightarrow$ B and X $\longrightarrow$ C. Since the f-value for the former transition has been calculated[55] to be 0.27, the difference between 0.84 and 0.27 can be taken (if no other transitions contribute) to be due to X $\longrightarrow$ C. Because of the uncertainty of the data, a value of 0.6 was adopted for the f-value for X $\longrightarrow$ C. The calculated cross section

of $0.8_5 \times 10^{-18}$ cm^2 seems too small by about an order of

magnitude when compared with the rough experimental data[36]

for the cross section at the edge. Thus, these calculations

would seem to rule out both the B and C states as the most

important upper state in the photodissociation. Perhaps

the recently discovered B' state mentioned by Herzberg and

Monfils may be the chief contributor to the cross section.

At present, little data exists for this state.

3. Photoionization

The cross section for the process

$$\gamma + H_2 \longrightarrow H_2^+ + e \tag{A54}$$
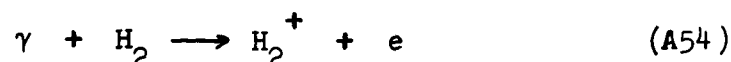
has an edge at about 15.4 eV corresponding to a transition

between the ground vibrational states of H_2 and H_2^+. The

cross section for photoionization in which the transition

is from a vibrational state v_o of H_2 to a vibrational state

v_1 of H_2^+ can be written, with the help of the Franck-

Condon principle, as

$$\sigma_{v_1 v_o}(\omega) = \sigma_e(\omega_v) \left| \langle v_1 | v_o \rangle \right|^2 \tag{A55}$$

where

$$\omega_v = \omega - \Delta\omega_v \tag{A56}$$

and $\sigma_e(\omega_v)$ results from the electronic part of the matrix

element for the transition and would be calculated for the

equilibrium internuclear separation of H_2. For practical

purposes $\sigma_e(\omega)$ can be taken from experiment to be of the

form[35]

$$\sigma_e(\omega) \approx B/\omega \qquad\qquad (A57)$$

with $B \approx 0.17_6$ cm^2 sec^{-1}, giving a threshold value of the electronic part of the cross section of $\sigma_e(\omega_0) = 7.5 \times 10^{-18}$ cm^2. The total cross section for transitions from the ground state $v_0 = 0$ to all vibrational states v_1 consistent with energy conservation is then

$$\sigma(\omega) = \sum_{v_1} \sigma_{ov_1}(\omega) = \sum_{v_1} \sigma_e(\omega_v) \left| \langle v_0 | 0 \rangle \right|^2. \qquad (A58)$$

If we approximate the vibrational states of H_2 and H_2^+ to harmonic oscillator states, the factors $\left| \langle v_1 | 0 \rangle \right|^2$ may be calculated readily, and ω_v is simply $\omega - v_1 \omega_{v_1}$ where ω_{v_1} is the fundamental vibrational frequency of H_2^+. The results of the calculation are shown in Fig. A3 below. The low value of the cross section just to the right of the edge results from the small value of the vibrational overlap factor $\left| \langle 0 | 0 \rangle \right|^2$. The general shape of the edge appears to be in agreement with the rough experimental curve sketched by Lee and Weissler.[36]

It is interesting to note that both the magnitude and frequency dependence of the electronic part of the (experimental) photoionization cross section of H_2 are very similar to that of He as calculated by Huang.[65] This agreement is probably not accidental. The equilibrium internuclear distance for H_2 is rather small (0.74 $\overset{\circ}{A}$) and
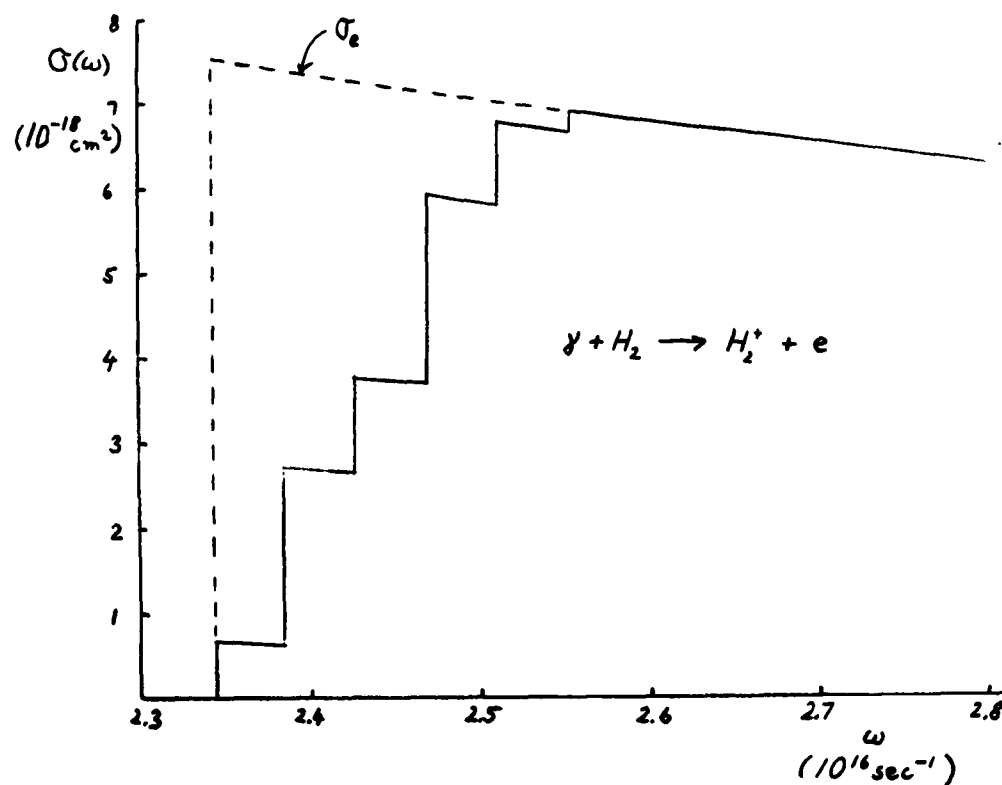
Fig. A3

Photoionization edge of H_2

the electronic structure of the molecule can be expected to resemble that of He which is the "united atom" corresponding to H_2. Moreoever, at the internuclear distance of 0.74Å, the H_2^+ molecule should be similar to He^+.

The one dimensional (radial) distribution of cloud velocities is known from interstellar absorption studies to be of the form

$$f_{v_r} = \frac{1}{2\eta} e^{-|v_r|/\eta} \quad , \tag{B1}$$

with $\eta \simeq 10$ km/sec. The distribution function f_v for the absolute velocity v is easily found if the assumption is made that the distribution is isotropic. In this case the probability of a velocity vector being in $\Delta\Theta$ is $\frac{1}{2} \sin \Theta \, \Delta\Theta$ (see Fig. B1 below).
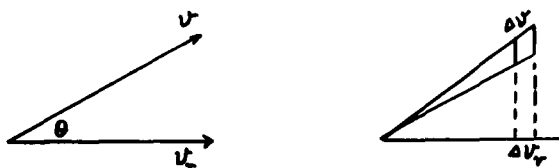
Fig. B1
Velocity Vectors

The number of radial velocity vectors between v_r and $v_r + dv_r$ is then

$$dN_{v_r} = f_{v_r} \, dv_r = \frac{1}{2} \int_{0}^{\pi/2} f_v(v) \sin \Theta \, d\Theta \, dv. \tag{B2}$$

$$(v_r = v \cos \Theta)$$

205.

This integral denotes a summation over angles such that $v \cdot \cos \Theta = v_r$ (v_r is fixed in the integration). From the geometry we can write $dv = dv_r / \cos \Theta$, giving an integral equation for the desired function f_v:

$$f_{v_r}(v_r) = \frac{1}{2} \int_0^{\pi/2} f_v(v_r / \cos \Theta) \, \tan \Theta \, d\Theta$$

$$= \frac{1}{2} \int_{v_r}^{\infty} f_v(y) \, \frac{dy}{y} \, . \qquad (B3)$$

The solution to this equation is

$$f_v(v_r) = -2 \, v_r \, \frac{\partial f_{v_r}}{\partial v_r} \, . \qquad (B4)$$

With $f_{v_r} = \frac{1}{2\eta} \, e^{-|v_r|/\eta}$, we get for f_v:

$$f_v(v) = \frac{v}{\eta^2} \, e^{-v/\eta} \, . \qquad (B5)$$

This distribution gives an average velocity

$$\bar{v} = \int_0^{\infty} v \, f_v(v) \, dv = 2\eta \, , \qquad (B6)$$

and a mean squared velocity

$$\overline{v^2} = 6 \, \eta^2 \, . \qquad (B7)$$

More generally,

$$\overline{v^n} = \Gamma(n + 2) \, \eta^n \, . \qquad (B8)$$

APPENDIX C - STRÖMGREN SPHERES

1. Solution of the ionization equation

The basic equation for Strömgren sphere calculations is the integro-differential equation (168). In this appendix we shall outline methods for the solution of this equation for the case $\overline{v} = 0$, that is, the static case. The same methods can be extended to cases when $\overline{v} \neq 0$ although more tedious calculations are required. With $\overline{v} = 0$, (168) becomes

$$n_o \, x^2 \, \overline{\sigma_p' v} = (1 - x) \, \frac{R^2}{4r^2} \int_{\omega_t}^{\infty} J_\omega \sigma_\omega \, e^{-\tau_\omega(r)} d\omega \qquad (C1)$$

where

$$\tau_\omega(r) = \sigma_\omega n_o \int_o^r (1 - x(r')) \, dr' \quad . \qquad (C2)$$

Once $\tau_\omega(r)$ is determined, the integral in (C1) can be evaluated and the equation can be solved for x, the solution being

$$x = -b + (b^2 + 2b)^{1/2} \quad , \qquad (C3)$$

where $(\alpha_o = \hbar/kT_o)$

$$b = \frac{1}{8r^2} \left(\frac{R}{\pi c}\right)^2 \frac{\sigma_t \, \omega_t^3}{n_o \, \overline{\sigma_p' v}} \int_{\omega_t}^{\infty} \frac{1}{\omega} \, e^{-\alpha_o \omega - \tau_\omega(r)} \, d\omega. \qquad (C4)$$

The following expansions of (C3) are useful:

$$x = 1 - 1/2b + 1/2b^2 - 5/8b^3 + \ldots \quad b \gg 1 \qquad (C5)$$

$$x = (2b)^{1/2} (1 - (b/2)^{1/2} + b/4 - b^2/32 + \ldots) \quad b \ll 1.$$

$$\text{(C6)}$$

The motivation for the methods developed here for the solution to (C1) comes from the fact that the contributions to τ_ω from various elements of the gas are additive. We write τ_ω as

$$\tau_\omega(r) = \frac{\beta(r)}{\omega^3} = \frac{\sigma_t \omega_t^3 n_o}{\omega^3} \, t(r) \quad , \qquad \text{(C7)}$$

where

$$t(r) = \int_0^r (1 - x(r')) \, dr' \quad . \qquad \text{(C8)}$$

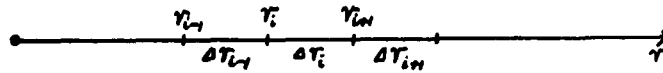The distance r to the central star can be broken up as shown in Fig. C1.

Fig. C1
Intervals of r

The value of $t(r)$ at r_1 can be approximated by the sum

$$t_1 = \sum_{j=1}^{i-1} (1 - x(r_j)) \, \Delta r_j \quad , \qquad \text{(C9)}$$

and the value of $t(r)$ at r_{i+1} by

$$t_{i+1} = t_i + (1 - x(r_i)) \, \Delta r_i \quad . \qquad \text{(C10)}$$

The general procedure for solving (C1) should now be evident. After t_1 has been determined, we calculate $\tau_\omega(r_1)$, $b(r_1)$, and $x(r_1)$. With this $x(r_1)$, we calculate t_{i+1} by (C10), and so on. The principal mathematical problem is the evaluation of the integral in (C4), namely

$$I(\beta) \;=\; \int_{\omega_t}^{\infty} \frac{1}{\omega}\, e^{-\alpha_0 \omega \,-\, \beta/\omega^3}\, d\omega \quad . \qquad (C11)$$

Close to the star the degree of ionization is high $(x \to 1)$ and so the optical thickness τ_ω is small. This suggests an iteration procedure for the solution to (C1). With $\tau_\omega = 0$, we have from (C4)

$$b_0(r) \;=\; \frac{1}{8r^2}\, \left(\frac{R}{\pi c}\right)^2 \frac{\sigma_t \omega_t^3}{n_0\, \sigma_p' v}\, K(\alpha_0 \omega_t) \quad , \qquad (C12)$$

where

$$K(\alpha_0 \omega_t) \;=\; \int_{\alpha_0 \omega_t}^{\infty} \frac{e^{-u}}{u}\, du. \qquad (C13)$$

With this b_0 we can calculate $1 - x \simeq 1/2b_0$ from (C5) and substitute it into the expression (C2) for τ_ω giving

$$\tau_\omega \;=\; \sigma_\omega n_0 \int_0^r \frac{dr'}{2b_0(r')} \;=\; \frac{1}{3}\, \sigma_\omega n_0\, a\, r^3 \;, \qquad (C14)$$

where

$$a \;=\; 4\left(\frac{\pi c}{R}\right)^3 \frac{n_0\, \overline{\sigma_p' v}}{\sigma_t\, \omega_t^3\, K(\alpha_t \omega_t)} \quad . \qquad (C15)$$

We then substitute the expression for τ_ω from (C14) into (C4), making the approximation $e^{-\tau_\omega} \simeq 1 - \tau_\omega$. Evaluating

the integrals, we get

$$b(r) = b_o(r) (1 - Br) ,$$
<div align="right">(C16)</div>

where

$$B = \frac{n_o \sigma_t}{6 b_o} \frac{K_4(\alpha_o \omega_t)}{K(\alpha_o \omega_t)} .$$
<div align="right">(C17)</div>

Here the K's are the generalized exponential integrals defined in the appendix of Unsöld's book.[66] They have the following properties:

$$K_n(x) = \int_1^\infty \frac{e^{-xw}}{w^n} \, dw = x^{n-1} \int_x^\infty \frac{e^{-u}}{u^n} \, du,$$
<div align="right">(C18)</div>

$$K_1(x) \equiv K(x) ,$$
<div align="right">(C19)</div>

$$(n - 1) K_n(x) = e^{-x} - x \, K_{n-1}(x)$$
<div align="right">(C20)</div>

Using the recursion relation (C20), the generalized integrals for higher indices n can be calculated from K(x) which is tabulated.[67]

The iteration solution (C16) provides the simplest method for calculating x(r) and is valid roughly for $r < r_s/2$. For larger values of r the optical thickness τ is no longer small and the iteration procedure breaks down. However, at this point we can evaluate the integral $I(\beta)$ by expanding $e^{-\beta/\omega^3}$ in a power series. When this is done, $I(\beta)$ becomes

$$I(\beta) = \sum_{n=0}^{\infty} \left(\frac{-\beta}{\omega_t^2}\right)^n \frac{K_{3n+1}(\alpha_0 \omega_t)}{n!} \quad . \tag{C21}$$

This expansion can be used to calculate $b(r_1)$, $x(r_1)$, etc. Fortunately, the argument of the K-functions does not contain β so that they need be calculated only once for the given value of T_0.

Eventually, when β becomes large, the expansion (C21) will converge slowly and become impractical. At this point, however, we can obtain an asymptotic expression for $I(\beta)$ since the main contribution to the integral will come from a region where both $\alpha_0 \omega$ and β/ω^3 are large (see Fig. C2 below.
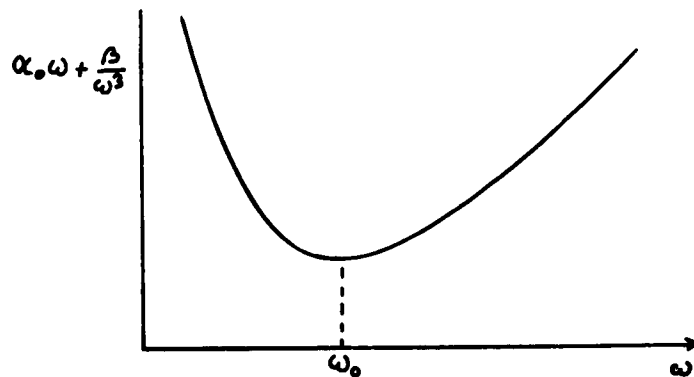
Fig. C2

Graph of exponent in photoionization rate

Expanding the exponential $g(\omega) = \alpha_0 \omega + \dfrac{\beta}{\omega^3}$ around the minimum ω_0, we can obtain an approximate expression for the integral $I(\beta)$. The result is

$$I(\beta) = \sqrt{\pi/6\gamma} \; e^{-4\gamma} \quad , \qquad\qquad (C22)$$

where

$$\gamma = (\alpha_0/3)^{3/4} \beta^{1/4} \quad . \qquad\qquad (C23)$$

These methods were used to calculate $x(r)$ for a region of density $n_0 = 10 \text{ cm}^{-3}$ surrounding a main sequence B2 star ($T_0 = 20,000^{\circ}\text{K}$). In this calculation a radius $R = 2.15 \times 10^{11}$ cm was taken for the star (from Table 1.2 of Schwarzschild's book[51]). The results are shown in Fig. C3.

Fig. 3C

Ionization as a function of distance from a main sequence B2 star ($T_0 = 20,000^{\circ}$K0 for a density $n_0 = 10$ cm-3.

2. Molecular effects - the "A-shell"

We conclude this appendix by considering the problem
of determining, in the static case, the regions of ioniza-
tion and dissociation of a hydrogen gas surrounding a hot
star. The shell of atomic hydrogen which is surrounded by
H_2 will be referred to as the A-shell. By the static case
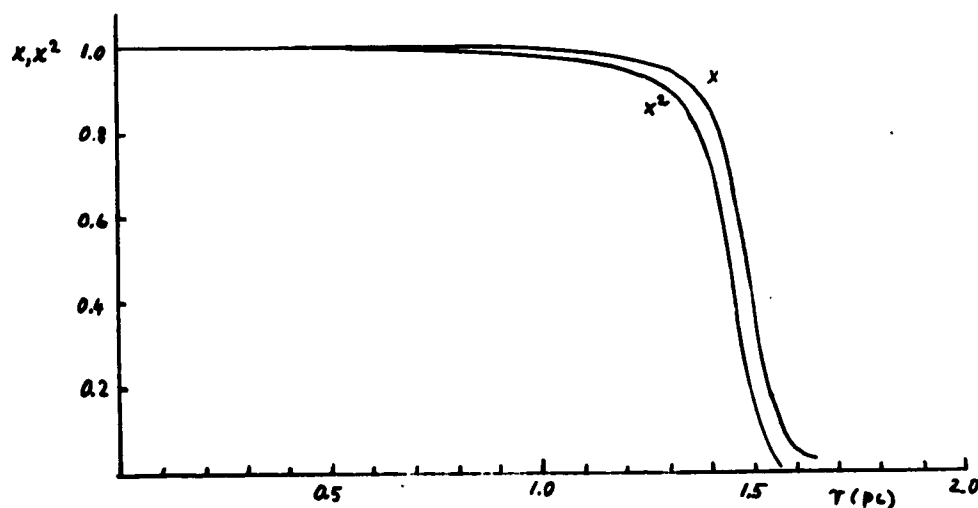we mean the state which would result after an infinitely
long time. Thus, even though the relaxation time for
formation of H_2 is very long, we assume the gas to be
undisturbed for a sufficiently long time for an equilibrium
situation to exist. We consider the medium to have a
constant "heavy particle density" $n_o = 2n_{H_2} + n_H + n_p$ and
shall ignore the pressure differences set up by the
differences in density and temperature. Moreover, we shall
assume from the beginning that the molecular region is
sufficiently separated from the ionization region so that
when regarding molecular processes we shall have to deal
only with the region of neutral hydrogen (the results will
be seen to be consistent with this assumption). For the
neutral region we take $T = 100^\circ K$ and for the ionized region
$T_e = 10^{4\circ}K$. The problem we are considering is unrealistic
in the sense that it neglects the effects of pressure
differences, but some of the qualitative results may be of
some value. A realistic situation to which the results
would be applicable, however, is that of a cloud of
completely associated molecular hydrogen moving past a

bright star. The region coming <u>toward</u> the star, that is,
the ionization and dissociation fronts, would be described
in a manner similar to the static case since here the
dynamical motions would not have set in as yet.

The processes which determine the equilibrium concen-
trations are:

$$H + \gamma \rightleftharpoons p + e \qquad\qquad (C24)$$

$$H_2 + \gamma \rightarrow H + H \qquad\qquad (C25)$$

$$H_2 + \gamma \rightarrow H_2^+ + e \qquad\qquad (C26)$$

$$H_2^+ + \gamma \rightleftharpoons H + p \qquad\qquad (C27)$$

$$H_2^+ + e \rightarrow H_2 + \gamma \qquad\qquad (C28)$$

$$H_2^+ + e \rightarrow H + H \qquad\qquad (C29)$$

$$H + S\text{-}H \rightarrow H_2 + S \qquad\qquad (C30)$$

the last process representing association on grains. We
assume (C29) to be much faster than (C27) and (C28) so that
any H_2^+ formed quickly becomes H + H and the reactions to
be considered are essentially

$$(i) \quad H + \gamma \rightleftharpoons p + e$$

$$(ii) \quad H_2 + \gamma \rightarrow H + H$$

$$(iii) \quad H + S\text{-}H \rightarrow H_2 + S$$
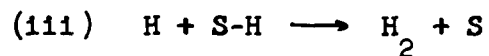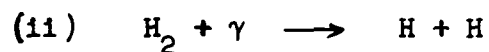
The equilibrium concentrations will be determined from the
steady state relations

$$n_H \, \tau_{\gamma_1}^{-1} = k \, n_e^2 \tag{C31}$$

$$n_{H_2} \, \tau_{\gamma_2}^{-1} = n_H \, b \, \rho_g \tag{C32}$$

and the condition of constant density

$$n_o = 2 \, n_{H_2} + n_H + n_e \quad . \tag{C33}$$

Here, $k = \overline{\sigma_p' v}$, and $\tau_{\gamma_2}^{-1}$ is the sum of the rate constants for photodissociation and photoionization $(\tau_{\gamma_2 d}^{-1} + \tau_{\gamma_2 i}^{-1})$.

The last three equations are to be solved for n_{H_2}, n_H, and n_e.

Combining (C32) and (C33), we have

$$n_e = n_o - y \, n_H \quad , \tag{C34}$$

where

$$y = 1 + \frac{2b \, \rho_g}{\tau_{\gamma_2}^{-1}} \tag{C35}$$

Substituting (C34) into (C31), we get an equation for n_H:

$$n_H^2 - 2\left(\frac{n_o}{y} + \frac{\tau_{\gamma_1}^{-1}}{2ky^2}\right)n_H + \frac{n_o^2}{y^2} = 0 \quad , \tag{C36}$$

which has the solution

$$n_H = \frac{n_o}{y} + \frac{\tau_{\gamma_1}^{-1}}{2ky^2} - \sqrt{\left(\frac{n_o}{y} + \frac{\tau_{\gamma_1}^{-1}}{2ky^2}\right)^2 - \frac{n_o^2}{y^2}} \tag{C37}$$

The molecular and electronic densities are then found from:

$$n_{H_2} = \frac{b \, \rho_g}{\tau_{\gamma_2}^{-1}} \, n_H \; ; \tag{C38}$$

$$n_e = n_o - y \, n_H \quad . \qquad\qquad (C39)$$

For $\dfrac{n_o}{y} \gg \dfrac{\tau_{\gamma_1}^{-1}}{2ky^2}$,

$$n_H \simeq \frac{n_o}{y} \; , \; n_e \simeq \left(n_H \, \frac{\tau_{\gamma_1}^{-1}}{k}\right)^{1/2} \qquad\qquad (C40)$$

The rate constant for photodissociation or photo-ionization of species k (H_2 or H) is given by

$$\tau_{\gamma k}^{-1} = \left(\frac{R}{2\pi c}\right)^2 \frac{1}{r^2} \int \sigma_k(\omega) \, \omega^2 \, e^{-\alpha_o \omega \, - \, \tau_\omega} \, d\omega. \qquad (C41)$$

When absorption is by several different kinds of particles

$$\tau_\omega = \sum_j \sigma_j(\omega) \, t_j \quad , \qquad\qquad (C42)$$

$$t_j = \int n_j \, dr \quad . \qquad\qquad (C43)$$

The cross section $\sigma_j(\omega)$ is usually of the form

$$\sigma_j(\omega) = \beta_{oj} \left(\frac{\omega t_1}{\omega}\right)^{m_j} \quad . \qquad\qquad (C44)$$

For large optical thicknesses most of the integral in (C41) comes from the region of ω where $f(\omega) = \alpha_o \omega + \tau_\omega$ is a minimum. Expanding $f(\omega)$ around this frequency ω_o, we have

$$f(\omega) = f(\omega_o) + \frac{(\omega - \omega_o)^2}{2} \, f''(\omega_o) + \ldots \quad , \qquad (C45)$$

where ω_o is found from

$$\alpha_o - \sum_j \beta_{oj} m_j \; \frac{\omega_{t_j}^{m_j}}{\omega_o^{m_j+1}} \; t_j \;=\; 0 \qquad\qquad (C46)$$

and

$$f''(\omega_o) \;=\; \sum_j \beta_{oj} \; m_j \,(m_j+1) \; \frac{\omega_{t_j}^{m_j}}{\omega_o^{m_j+2}} \; t_j \qquad (C47)$$

The asymptotic formula for $\tau_{\gamma h}^{-1}$ is then

$$\tau_{\gamma k}^{-1} \;\simeq\; \left(\frac{R}{2\pi c}\right)^2 \frac{\sigma_k(\omega_o)}{r^2} \sqrt{\frac{2\pi}{f''(\omega_o)}} \; e^{-f(\omega_o)} \quad . \qquad (C48)$$

We consider the specific situation of a region of density $n_o = 10 \text{ cm}^{-3}$ surrounding a B2 star. The effects of molecules are negligible if $y - 1 = \dfrac{2b\,\rho_g}{\tau_{\gamma_2}^{-1}} \ll 1$. It turns out that molecules become important only when the region becomes almost completely neutral. Hence, the ionization results may be taken over from the previous calculations which produced Fig. C3. Moreover, the asymptotic formula (C48) will be valid when considering the H-H_2 regions. For the cross section for molecular dissociation and ionization we take $\sigma_2 = B/\omega$ which is the emperical ionization expression (see Appendix A). The approximation of considering only the ionization process is valid since the optical thickness τ is so large that ω_o in (C48) lies in the region beyond that where dissociative effects are appreciable. For the numerical calculations we

take b ρ_g = 4 x 10^{-16} sec^{-1}, k = $\overline{\sigma_p' v}$ = 2.73 x 10^{-13} cm^3 sec^{-1}. The results of the calculations are presented in Fig. C4.

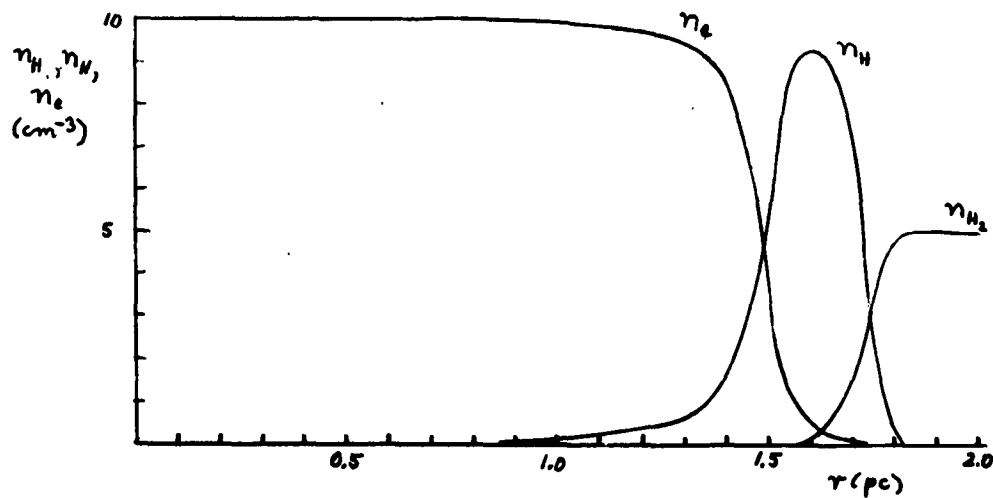Fig. C4

Particle densities as a function of distance from a B2 star with a surrounding medium of density $n_o = 2n_{H_2} + n_H + n_e = 10$ cm^{-3}.

Only a thin shell of atomic hydrogen separates the ionized from the molecular region. It is emphasized again that this situation does not represent that of a typical interstellar cloud.

APPENDIX D - A PROBLEM IN BROWNIAN MOTION

In this appendix we shall derive a probability function associated with a special problem in Brownian motion. The motion may be of an individual molecule, a macroscopic particle immersed in a fluid, or, in the special case we are considering, an interstellar cloud undergoing collisions with other clouds. It is desired to find the probability function $w(z'',t'|z',z,t)$, where $w(z'',t'|z',z,t)dz''$ is the probability that a "particle" was within dz'' after undergoing Brownian motion for a time t', given that it started out at z' at $t' = 0$ and ended up at z after a time $t > t'$. Thus, we fix the z-values of the endpoints for the motion and the total time that the particle has traveled, and ask for the probability function for z'' at the intermediate time t'. This problem can be solved easily by considering the associated discrete random walk problem and then making the transition to the continuum case. We shall use methods similar to those employed, for example, in the review article by Chandrasekhar.[68]

Consider the random walk process in which a particle takes N steps $(1,2,\ldots,j,\ldots,N)$ of length ℓ and of equal probability $(=\frac{1}{2})$ to the left or right along the z'' axis (see Fig. D1) which is divided into elements denoted by integers $(\ldots,1,2,\ldots,i,\ldots,n,\ldots)$.
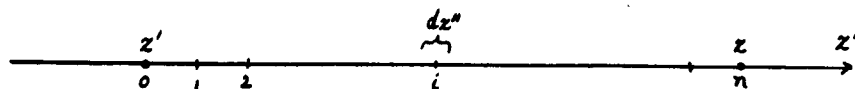
219.

Fig. D1

Discrete and continuous z"

It is desired to find the probability $W(i,j|n,N)$ that the jth step puts the particle at i, _given_ that the Nth step puts it at n. This probability function is given by

$$W(i,j|n,N) \;=\; \frac{W(i,j;n,N)}{W(n,N)} \tag{D1}$$

where $W(i,j;n,N)$ is the probability that the jth step puts it at i _and_ the nth step puts it at N, and $W(n,N)$ is the probability that the Nth step puts it at n (with no special specifications on the intermediate jumps). Now,

$$W(n,N) \;=\; \frac{N!}{\left(\frac{N+n}{2}\right)! \; \left(\frac{N-n}{2}\right)!} \left(\tfrac{1}{2}\right)^{N} , \tag{D2}$$

the combinatorial factor being the number of ways of taking $(N+n)/2$ steps to the right and $(N-n)/2$ to the left. The probability function $W(i,j;n,N)$ is the product of the probability of getting to i in j steps and the probability of then getting to n in the remaining $N-j$ steps. Thus, we have

$$W(i,j|n,N) \; =$$

$$\frac{\dfrac{j!}{(\frac{j+1}{2})!\,(\frac{j-1}{2})}\,(\tfrac{1}{2})^{j}\;\dfrac{(N-j)!}{(\frac{N-j+n-1}{2})!\,(\frac{N-j-n+1}{2})}\,(\tfrac{1}{2})^{N-j}}{\dfrac{N!}{(\frac{N+n}{2})!\;(\frac{N-n}{2})!}\,(\tfrac{1}{2})^{N}} \tag{D3}$$

We take the case $N \gg n$, $j \gg i$, $N - j \gg n - i$ and make use of Stirling's approximation:

$$\ln x! \approx (x + \tfrac{1}{2})\ln x - x + \tfrac{1}{2}\ln 2\pi , \tag{D4}$$

and also

$$\ln(1 \pm y) \approx \pm y - y^{2}/2 . \tag{D5}$$

With the approximations (D4) and (D5) an expression like

$$w = \frac{A!}{(\frac{A+a}{2})!\;(\frac{A-a}{2})!} \qquad (A \gg a) \tag{D6}$$

can be approximated by

$$\ln w \approx -\tfrac{1}{2}\ln A = (A + 1)\ln 2 - a^{2}/2A - \tfrac{1}{2}\ln 2. \tag{D7}$$

In this manner we calculate $W(i,j,n,N)$ to be

$$W(i,j|n,N) \; =$$

$$\frac{2}{(2\pi \frac{j(N-j)}{N})^{1/2}} \; \frac{e^{-i^{2}/2j}\; e^{-(n-i)^{2}/2(N-j)}}{e^{-n^{2}/2N}} . \tag{D8}$$

We now make the transition to the continuum. Since $z'' = z' + i\ell$, $z = z' + n\ell$ we make the replacement $i = (z'' - z')/\ell$, $n - i = (z - z'')/\ell$. Now, if j is odd (even), i must be odd (even) so that the number of allowable points i within $\Delta z''$ if j is <u>fixed</u> is $\Delta z''/2\ell$. Thus we have

$$W(i,j|n,N)\,\frac{\Delta z''}{2\ell} = w(z'',j|n,N)\,\Delta z'', \qquad (D9)$$

$w(z'',j|n,N)$ being the continuum distribution function. If the particle makes r displacements per unit time we can replace j and N by rt' and rt respectively. We also define $D \equiv \frac{1}{2}r\ell^2$ and get finally:

$$w(z'',j|n,N)dz'' = w(z'',t'|z',z,t)dz'' =$$

$$\frac{1}{\sqrt{4\pi Dt'\,\frac{(t-t')}{t}}}\;\frac{e^{-(z''-z')^2/4Dt'}\;e^{-(z''-z)^2/4D(t-t')}}{e^{-(z-z')^2/4Dt}}\;dz'' \;.$$

$$(D10)$$

We note that as $t' \to 0$, $w \to \delta(z''-z)$ and, as $t' \to t$, $w \to \delta(z'' - z)$ and, moreover, that

$$w \xrightarrow[t \to \infty]{} (4\pi Dt)^{-1/2}\,e^{-(z''-z')^2/4Dt'} \;. \qquad (D11)$$

When the second point is fixed in the infinite future, the resulting formula reduces to the familiar expression for diffusion from a single fixed point when the endpoint is <u>not</u> fixed.

REFERENCES

1. L. Spitzer Jr., Ap. J., 120, 1 (1954).

2. H. C. van de Hulst, C. A. Muller, and J. H. Oort,
   B.A.N. 12, 117 (1954) (No. 452).

3. B. G. Clark, V. Radhakrishnan and R. W. Wilson, Ap. J.
   135, 151 (1962).

4. I. S. Shklovsky, Cosmic Radio Waves, Cambridge,
   Harvard U. Press, 1960.

5. L. Spitzer Jr. and J. B. Rogerson, Mém. Soc. Roy. Sci.
   Liège (5) 4, 86 (1961).

6. reference 2, p. 131.

7. A. E. Lilley, Ap. J. 121, 559 (1955).

8. D. S. Heeschen, Ap. J. 121, 569 (1955).

9. E. R. Hill, B.A.N. 15, 1 (1959) (No. 494).

10. J. H. Oort, B.A.N. 15, 45 (1959) (No. 494)

11. J. H. Oort, Cambridge Symposium on Gas Dynamics of
    Cosmic Clouds (1953), New York, Interscience, 1955,
    p. 20.

12. B. J. Bok, Paris Symposium on Radio Astronomy IAU/URSI
    (1958), Stanford U. Press, 1959, p. 430

13. T. Gold, Mém. Soc. Roy. Sci. Liège (5) 4, 476 (1961).

14. F. D. Kahn, reference 11, p. 60.

15. H. A. Bethe and E. E. Salpeter, Quantum Mechanics of
    One and Two Electron Atoms, New York, Academic Press,
    1957, p. 250.

16. L. Spitzer Jr., Ap. J. 109, 337 (1949).

17. W. H. McCrea and D. McNally, M.N. 121, 238 (1960).

18. J. H. Oort and H. C. van de Hulst, B.A.N. $\underline{10}$, 187 (1946).

19. J. H. deBoer and J. van Steenis, Proc. Kon. Ned. Ak. v. Wet. $\underline{55B}$, 572 (1952).

20. S. Glasstone, K. J. Laidler, and H. Eyring, Theory of Rate Processes, New York, McGraw-Hill, 1941

21. W. Feller, Introduction to Probability Theory and Its Applications, New York, Wiley, 1950, p. 327.

22. K. E. Shuler and K. J. Laidler, J. Chem. Phys. $\underline{17}$, 1212 (1949).

23. R. T. Brackmann and W. L. Fite, J. Chem. Phys. $\underline{34}$, 1572 (1961).

24. H. C. van de Hulst, Rech. Astr. Obs. Utrecht $\underline{11}$, part 2 (1949).

25. C. A. Coulson, Valence, Oxford, Clarendon Press, 1953.

26. F. Seitz, Modern Theory of Solids, New York, McGraw-Hill, 1940, p. 50.

27. J. O. Hirschfelder, C. F. Curtiss, and R. B. Bird, Molecular Theory of Gases and Liquids, New York, Wiley, 1954.

28. L. Landau, Phys. Z. Sowjet. $\underline{8}$, 489 (1935).

29. Data from Landolt-Börnstein, Zahlenwerte und Funktionen etc., 6. Aufl. Bd. 1, Teil 3, p. 509, Berlin, Springer-Verlag, 1951.

30. D. McNally, M. N. $\underline{124}$, 155 (1962).

31. H. Lambrecht, Mém. Soc. Roy. Sci. Liège (4) $\underline{15}$, 562 (1955).

32. D. R. Bates and L. Spitzer Jr., Ap. J. $\underline{113}$, 441 (1951).

33. G. Herzberg, Mém. Soc. Roy. Sci. Liège (4) $\underline{15}$, 291 (1955).

34. D. R. Bates, Phys. Rev. $\underline{78}$, 492 (1950).

35. D. R. Bates, M. N. $\underline{111}$, 303 (1951).

36. P. Lee and G. Weissler, Ap. J. $\underline{115}$, 570 (1952), see also Encyclopedia of Physics (Handbuch der Physik) XXI - Gas Discharges I, Berlin, Springer-Verlag, 1956, p. 328.

37. M. R. C. McDowell, Observatory $\underline{81}$, 240 (1961).

38. F. D. Kahn, Mém. Soc. Roy. Sci. Liège (4) $\underline{15}$, 393 (1955).

39. Reference 15, p. 181

40. S. F. Singer, Prog. El. Part. and Cos. Ray Phys. IV, 203 (1958).

41. E. Fermi, Phys. Rev. $\underline{75}$, 1169 (1949).

42. S. Hayakawa and K. Kitao, Prog. Theor. Phys. $\underline{16}$, 132 (1958).

43. V. L. Ginzburg, Prog. El. Part. and Cos. Ray Phys. IV, 339 (1958).

44. N. F. Mott and H. S. W. Massey, Theory of Atomic Collisions, 2nd ed., Oxford, Clarendon Press, 1949.

45. S. Hayakawa, S. Nishimura, and K. Takayanagi, Publ. A. S. Japan $\underline{13}$, 184 (1961).

46. M. J. Seaton, Ann. d'Ap. $\underline{18}$, 188 (1955).

47. K. Takayanagi and S. Nishimura, Publ. A.S. Japan $\underline{12}$, 77 (1960).

48. D. E. Osterbrock, Ap. J. $\underline{136}$, 359 (1962).

49. L. Spitzer Jr., Ap. J. $\underline{107}$, 6 (1948).

50. L. H. Aller, Astrophysics II, New York, Ronald Press, 1954, p. 258, eq. 29

51. M. Schwarzschild, Structure and Evolution of the Stars, Princeton, Princeton U. Press, 1958.

52. C. B. Haselgrove and F. Hoyle, M.N. $\underline{119}$, 112 (1959); see also F. Hoyle, M. N. $\underline{120}$, 22 (1960).

53. G. P. Kuiper, Ap. J. 88, 429 (1938).

54. A. Sandage, Ap. J. 125, 422 (1957).

55. H. C. van de Hulst, I. A. U. Symposium No. 4, Cambridge U. Press, 1957, p. 3.

56. M. Schmidt, B. A. N. 13, 247 (1956) (No. 475).

57. J. H. Oort, Stellar Populations, New York, Interscience, 1958, p. 415.

58. R. J. Gould and M. Harwit, Ap. J. 137, (1963) (to be published).

59. G. H. Herbig, preprint, 1962.

60. G. R. Burbidge et al, Die Entstehung von Sternen, Berlin, Springer-Verlag, 1960.

61. A. G. W. Cameron, Icarus 1, 13 (1962).

62. L. Landau and E. Lifshitz, Quantum Mechanics, Non-Relativistic Theory, Reading, Mass., Addison-Wesley, 1958.

63. G. Herzberg and A. Monfils, J. Mol. Spectroscopy 5, 482 (1960).

64. R. S. Mulliken and C. Riecke, Rep. Prog. Phys. 8, 231 (1941).

65. S. Huang, Ap. J. 108, 354 (1948).

66. A. Unsöld, Physik der Sternatmosphären, 2. Aufl., Berlin, Springer, 1955.

67. Jahnke-Emde-Lösche, Tables of Higher Functions, New York, McGraw-Hill, 1960.

68. S. Chandrasekhar, Rev. Mod. Phys. 15, 1 (1943).